

**DISEASE PROGRESSION AND
THERAPY-INDUCED CHANGES IN
METASTATIC COLORECTAL CANCER**

Jennifer M.J. Jongen

Disease Progression and Therapy-Induced Changes in Metastatic Colorectal Cancer

Jennifer M.J. Jongen

Disease Progression and Therapy-Induced Changes in Metastatic Colorectal Cancer

PhD thesis, Utrecht University, The Netherlands

© Jennifer Maria Jacoba Jongen, 2019

ISBN: 978-94-6332-449-6

All rights reserved. No part of this thesis may be reproduced or transmitted in any form or by any means without prior written permission from the author. The copyright of the papers that have been published or have been accepted for publication, have been transferred to the respective journals.

The research described in this thesis was supported by a Dutch Cancer Society research grant (grant no. UU2013–5865).

Printing of this thesis was financially supported by: The studies described in this thesis were supported by the Dutch Cancer Society [grant nr UU 2013-5865]. This thesis was accomplished with financial support from the Dutch Cancer Society, ChipSoft, UMCU Cancer Center, and Ipsen Farmaceutica B.V.

Lay-out and design
Printed by

Loes Kema
GVO drukkers & vormgevers B.V, Ede, the Netherlands

Disease Progression and Therapy-Induced Changes in Metastatic Colorectal Cancer

Ziekteprogressie en therapie-geïnduceerde veranderingen
in gemetastaseerd colorectaal kanker

(met een samenvatting in het Nederlands)

Proefschrift

ter verkrijging van de graad van doctor aan de Universiteit Utrecht
op gezag van de rector magnificus, prof.dr. H.R.B.M. Kummeling,
ingevolge het besluit van het college voor promoties
in het openbaar te verdedigen op donderdag 28 maart 2019
des middags te 6.00uur

door

Jennifer Maria Jacoba Jongen

geboren op 16 november 1986
te Loon op Zand

Promotoren:

Prof. dr. I.H.M Borel Rinkes

Prof. dr. O. Kranenburg

Table of Contents

Chapter 1	General introduction and thesis outline	7
PART I - Surgery in metastatic Colorectal Cancer		
Chapter 2	Surgery-induced tumour growth in (metastatic) colorectal cancer <i>Surgical Oncology</i> . 2017 Dec;26(4):535-543	17
Chapter 3	Downregulation of DNA repair proteins and increased DNA damage in hypoxic Aldefluor ^{bright} colon cancer cells is a therapeutically exploitable vulnerability <i>Oncotarget</i> . 2017 Sep 21;8(49):86296-86311	43
Chapter 4	Increased levels of oxidative damage in liver metastases compared with corresponding primary colorectal tumors: association with molecular subtype and prior treatment <i>American Journal of Pathology</i> . 2018 Oct;188(10):2369-2377	75
PART II - Radioembolization in metastatic Colorectal Cancer		
Chapter 5	Progressive disease after treatment with radioembolization in patients with metastatic colorectal cancer is most often due to new lesions <i>submitted - Journal of Vascular and Interventional Radiology</i>	101
Chapter 6	Anatomic versus metabolic tumor response assessment after radioembolization treatment. <i>Journal of Vascular and Interventional Radiology</i> . 2018 Feb;29(2):244253.e2	117
PART III - Discussion and Summary		
Chapter 7	General discussion and future perspectives	139
Chapter 8	Summary – Nederlandse samenvatting	149
PART IV - Appendices		
	Review committee	163
	Authors and affiliations	164
	List of publications	167
	Acknowledgements – Dankwoord	169
	Curriculum vitae auctoris	173

The background of the page is a light teal color. It is decorated with several abstract, hand-drawn circular shapes in a darker teal and a light orange color. These shapes are scattered across the page, some overlapping, and they vary in size and complexity, resembling stylized cells or organic forms. The text is centered on the page.

CHAPTER 1

General Introduction and Thesis Outline

In PART I of this thesis, the putative effects of surgery on colorectal cancer are investigated.

Colorectal cancer (CRC) is the third most common cancer worldwide and a major cause of cancer-related mortality with about 700,000 deaths annually worldwide [1]. The prognosis of patients with CRC is mostly determined by the presence of distant metastases, mainly in the liver. Approximately 45% of CRC patients eventually develop metastases, while ~15-20% presents with metastases at the time of primary diagnosis (synchronous metastases) [2]. If left untreated, median survival of patients with colorectal liver metastases (CRLM) is <1 year [3] and 5-year survival is only ~13% [4,5]. This makes CRC or metastatic CRC (mCRC) one of the most lethal diseases worldwide. Surgery is currently the golden standard, however, already about 100 years ago papers described how surgical manipulation might on the other hand also promote tumour outgrowth and metastasis formation [6]. Nonetheless, this is controversial since especially clinical evidence is lacking. In this respect, **chapter 2** reviews our current understanding of how, if at all, surgical resection of primary tumors and liver metastases might accelerate outgrowth of remaining/residing micrometastases in patients with mCRC based on the available (preclinical and clinical) data.

While metastases determine prognosis to a large extent, traditional staging of CRC is the basis for assessing prognosis and guiding treatment decisions [7,8], especially in earlier stages of the disease. A drawback of this classification system is that patients with the same CRC stage still may have different outcomes, leading to over-treatment, or unsuccessful treatment in many cases. For instance, patients with high-risk stage II and stage III CRC are – in principle – eligible for adjuvant chemotherapy. However, approximately 50% of these patients would not have developed distant metastases without treatment, and are thus over-treated. In addition, approximately 35% of the patients develop metastases despite treatment (inadequate treatment), leaving an estimated ~15% of all high-risk stage II and stage III patients actually benefitting from the treatment. A new classification system was introduced in 2015 based on an understanding of the pathways that drive metastasis and recurrence. RNA-based tumor classification has identified 4 distinct Consensus Molecular Subtypes (CMS1-4). CMS1 mostly consists of tumors with microsatellite instability (MSI), caused by a deficient mismatch repair system. CMS2 is the 'canonical' epithelial subtype with activation of WNT and MYC signaling pathways. CMS3 is characterized by high expression of genes regulating metabolic pathways and is enriched in tumors with activating mutations in the KRAS oncogene. CMS4 is characterized by atypical expression of genes reflecting a mesenchymal and a stem cell-like phenotype and has the highest propensity to form metastases [9]. Based on this classification, subtype specific features with potential diagnostic information can be selected. These features can be used to discriminate between subtypes and select patients for subtype-specific forms of treatment. In case of the poor prognosis CMS4 subtype, stroma and necrosis are thought to be of predictive value.

Despite adequate patient-selection and margin-free resection, recurrences develop in more than half of the patients operated [10]. Hence, it is essential to develop alternative/additional therapeutic strategies. These should be based on a thorough understanding of the pathways that drive metastasis and recurrence. One of the features of the poor prognosis CMS4 subtype is the presence of hypoxia. **Chapter 3** focusses on the combination of an increased proportion of cancer stem cells (CSCs) with the suppression of DNA repair pathways occurring as a consequence of hypoxia. CSCs have a high regenerative and tumorigenic potential and are generally intrinsically or indirectly resistant to chemotherapy [11,12]. Hypoxia is also known to decrease some of the DNA repair pathways [13], hypothetically resulting in less DNA repair capacity after treatment with DNA damaging agents. We assess the effect of hypoxia on DNA damage and DNA repair pathways and evaluate how hypoxia-activated prodrugs (HAPs) such as the topoisomerase-II inhibitor Tirapazamine (TPZ) can be used to target hypoxic tumor tissue, especially in CSCs.

Apart from hypoxia, CSCs and DNA damage, also oxidative signaling has been associated with the recently identified molecular subtypes in CRC [9]. This links the expression of increased oxidative signaling signatures to the poor prognosis CMS4 subtype [14]. An imbalance between the production of reactive oxygen species (ROS) and their neutralization by antioxidants results in oxidative stress in the tumor. Moderately increased levels of ROS stimulate tumorigenesis by acting as secondary messengers in tumor-promoting signaling pathways [15]. Interestingly, high levels of oxidative stress are measured in metastasizing tumor cells. Increased oxidized stress can be formed during metastatic outgrowth, following chemotherapy, or as a consequence of aggressive tumor biology. In **chapter 4** we describe how increased oxidative stress could actually create a therapeutically exploitable vulnerability.

First of all, the just described neoadjuvant or perioperative therapies together with the improved effectiveness of neoadjuvant chemotherapeutic regimens increased the number of patients eligible for resection. Secondly, if eligible for surgery, outcomes are better due to advances in surgical techniques [16-18]. Nevertheless, only 20-30% of patients with liver metastases are potential candidates for resection [19,20]. Until now, liver resection remains the only treatment with curative intent for patients with colorectal liver metastases. If not eligible for surgery, systemic therapy is the therapy of choice. With the newest chemotherapeutic combinations, median overall survival is 12.1-13.5 months if chemotherapy is given as second-line therapy [21] and 7.1-8.8 months for third and/or fourth-line therapy [22,23]. Various alternative, liver directed treatment options have been pursued, including radioembolization (RE), radio frequent ablation (RFA) and high intensity focused ultrasound (HIFU). While RFA in selected cases may approach the results of radical surgery, this is -again- only feasible in a small subset of patients, leaving a large population of patients with refractory CRLM confined to the liver. For these patients, the promising novel alternative treatment strategy radioembolization (RE) might present an interesting option.

In PART II of this thesis the role of radioembolization in metastatic colorectal cancer is investigated.

As RE is now increasingly applied in unresectable chemorefractory CRLM, it is important to critically reflect on both patient selection and evaluation of the treatment effect. In radioembolization, microspheres (± 30 μm) are loaded with the radioactive isotope yttrium-90 (^{90}Y) or holmium-166 (^{166}Ho) and injected intra-arterially via a branch of the hepatic artery supplying the tumor [24]. The injected microspheres embolize the microvasculature surrounding the tumour and emit high-energy beta radiation. The remainder of the liver is largely spared since healthy liver tissue is mainly supplied by the portal vein [25,26]. Patients that could participate in the trials had unresectable, chemorefractory, liver-dominant metastases.

Tumor response to treatment is generally measured by the Response Evaluation Criteria in Solid Tumors (RECIST) system [27]. RECIST identifies patients with progressive disease by either growth of the intrahepatic lesions, growth of the extrahepatic lesions, the development of new lesions (either intra- or extrahepatic) or a combination of these factors. However, the results of most RE clinical studies in stage IV extensive (liver) disease are modest [21,28].

RE in the second-line setting (after 1 line of failed chemotherapy) had a median survival of 13.2 months, 9.1 months as third-line treatment and 8.1 months as fourth-line treatment. As previously described, for chemotherapy treated patients, this is 12.1-13.5 as second-line therapy and 7.1-8.8 months for third and/or fourth-line therapy [21]. Whether progressive patients after RE show progression based on growth of intrahepatic lesions, growth of extrahepatic lesions, new lesions or a combination of those is currently underexposed. Therefore, in **chapter 5**, an inventory of the mode of progression in mCRC patients after RE was made. Based on this data, patient selection might be optimized, i.e. more precisely delineated.

The widely adopted and accepted RECIST system is based on changes in one-dimensional tumor diameter on cross-sectional imaging and patient prognosis [29]. It is, however, questionable whether RECIST is applicable for other therapies, since treatment response may not primarily be characterized by tumor shrinkage. Metabolic tumor response on ^{18}F -fluorodeoxyglucose positron emission tomography/computed tomography (^{18}F -FDG-PET/CT) might offer a solution [30]. The applicability of this method after RE in patients with CRLM by comparison with one-dimensional size-based response assessment on MRI is assessed in **chapter 6**.

References

1. Ferlay, et al. Cancer incidence and mortality worldwide: wources, methods, and major patterns in GLOBOCAN 2012. *Int. J. Cancer*, 2015. 136 (5):p E359-86.
2. Siegel R, Desantis C, Jemal A. Colorectal cancer statistics, 2014. *CA Cancer J Clin* 2014; 64: 104-117
3. Hackl C, Neumann P, Gerken M, Loss M, Klinkhammer-Schalke M, Schlitt HJ. Treatment of colorectal liver metastases in Germany: a ten-year population-based analysis of 5772 cases of primary colorectal adenocarcinoma. *BMC Cancer* 2014;14:810
4. Torre, L.A., et al., Global cancer statistics, 2012. *CA Cancer J Clin*, 2015. 65(2): p. 87-108
5. Siegel, R.L., K.D. Miller, and A. Jemal, Cancer statistics, 2016. *CA Cancer J Clin*, 2016. 66(1): p. 7-30
6. Clunet J. Recherches expérimentales sur les tumeurs malignes. Steinheil, Paris. 1910; Marie PC, J. . Fréquences des métastases viscérales chez les souris cancéreuses après ablation chirurgicale de leur tumeur. *Bull Assoc Franc L'Étude Cancér.* 1910;3:19-23
7. [Guideline] NCCN Clinical Practice Guidelines in Oncology: Colon Cancer. National Comprehensive Cancer Network. Available at http://www.nccn.org/professionals/physician_gls/pdf/colon.pdf. Version 2.2017 — March 13, 2017; Accessed: January 9, 2018
8. American Joint Committee on Cancer. Colon and Rectum. Amin MB, Edge S, Greene F, Byrd DR, Brookland RK, et al, eds. *AJCC Cancer Staging Manual*. 8th ed. New York, NY: Springer; 2016
9. Guinney J, Dienstmann R, Wang X, de Reynies A, Schlicker A, Soneson C, Marisa L, Roepman P, Nyamundanda G, Angelino P, Bot BM, Morris JS, Simon IM, et al. The consensus molecular subtypes of colorectal cancer. *Nat Med*. 2015; 21: 1350-6. doi: 10.1038/nm.3967
10. Abdalla EK, Vauthey JN, Ellis LM, Ellis V, Pollock R, Broglio KR, Hess K, Curley SA. Recurrence and outcomes following hepatic resection, radiofrequency ablation, and combined resection/ablation for colorectal liver metastases. *Ann Surg*. 2004; 239: 818-25; discussion 25-7
11. O'Brien CA, Pollett A, Gallinger S, Dick JE. A human colon cancer cell capable of initiating tumour growth in immunodeficient mice. *Nature*. 2007; 445: 106-10
12. Pang R, Law WL, Chu AC, Poon JT, Lam CS, Chow AK, Ng L, Cheung LW, Lan XR, Lan HY, Tan VP, Yau TC, Poon RT, et al. A subpopulation of CD26+ cancer stem cells with metastatic capacity in human colorectal cancer. *Cell Stem Cell*. 2010; 6: 603-15
13. Bristow RC, Hill RP. Hypoxia and metabolism. Hypoxia, DNA repair and genetic instability. *Nat Rev Cancer*. 2008; 8: 180-92. doi: 10.1038/nrc2344
14. Emmink BL, Laoukili J, Kipp AP, et al. GPx2 suppression of H₂O₂ stress links the formation of differentiated tumor mass to metastatic capacity in colorectal cancer. *Cancer Res* 2014; 74: 6717-6730
15. Qing G, Simon MC. Hypoxia inducible factor-2alpha: a critical mediator of aggressive tumor phenotypes. *Curr Opin Genet Dev*. 2009; 19: 60-6

16. Shindoh J, Tzeng C-WD, Aloia TA, Curley SA, Zimmitti G, Wei SH, et al. Portal vein embolization improves rate of resection of extensive colorectal liver metastases without worsening survival. *Br J Surg* 2013;100:1777–83
17. Lam VWT, Spiro C, Laurence JM, Johnston E, Hollands MJ, Pleass HCC, et al. A systematic review of clinical response and survival outcomes of downsizing systemic chemotherapy and rescue liver surgery in patients with initially unresectable colorectal liver metastases. *Ann Surg Oncol* 2012;19:1292–301
18. Wicherts DA, de Haas RJ, Andreani P, Sotirov D, Salloum C, Castaing D, et al. Impact of portal vein embolization on long-term survival of patients with primarily unresectable colorectal liver metastases. *Br J Surg* 2010;97:240–50
19. Kopetz S, Chang GJ, Overman MJ, Eng C, Sargent DJ, Larson DW, et al. Improved survival in metastatic colorectal cancer is associated with adoption of hepatic resection and improved chemotherapy. *J Clin Oncol* 2009;27:3677–83
20. Manfredi S, Lepage C, Hatem C, Coatmeur O, Faivre J, Bouvier A-M. Epidemiology and management of liver metastases from colorectal cancer. *Ann Surg* 2006;244:254–9
21. Kennedy, A., et al., Updated survival outcomes and analysis of long-term survivors from the MORE study on safety and efficacy of radioembolization in patients with unresectable colorectal cancer liver metastases. *J Gastrointest Oncol*, 2017. 8(4): p. 614-624
22. Mayer RJ, et al., Randomized trial of TAS-102 for refractory metastatic colorectal cancer. *N Engl J Med*. 2015 May 14;372(20):1909-19
23. Grothey A, et al. Regorafenib monotherapy for previously treated metastatic colorectal cancer (CORRECT): an international, multicentre, randomised, placebo-controlled, phase 3 trial. *Lancet*. 2013 Jan 26;381(9863):303-12
24. Smits, M.L., et al., Intra-arterial radioembolization of breast cancer liver metastases: a structured review. *Eur J Pharmacol*, 2013. 709(1-3): p. 37-42
25. Bierman, H.R., et al., Studies on the blood supply of tumors in man. III. Vascular patterns of the liver by hepatic arteriography in vivo. *J Natl Cancer Inst*, 1951. 12(1): p. 107-31
26. Breedis, C. and G. Young, The blood supply of neoplasms in the liver. *Am J Pathol*, 1954. 30(5): p. 969-77
27. Eisenhauer, E.A., et al., New response evaluation criteria in solid tumours: revised RECIST guideline (version 1.1). *Eur J Cancer*, 2009. 45(2): p. 228-47
28. Martin, L.K., et al., Yttrium-90 radioembolization as salvage therapy for colorectal cancer with liver metastases. *Clin Colorectal Cancer*, 2012. 11(3): p. 195-9; Sofocleous, C.T., et al., Radioembolization as a Salvage Therapy for Heavily Pretreated Patients With Colorectal Cancer Liver Metastases: Factors That Affect Outcomes. *Clin Colorectal Cancer*, 2015. 14(4): p. 296-305
29. Buysse M, Thirion P, Carlson RW, Burzykowski T, Molenberghs G, Piedbois P. Relation between tumour response to first-line chemotherapy and survival in advanced colorectal cancer: a meta-analysis. *Meta-Analysis Group in Cancer. Lancet (London, England)*. 2000;356(9227):373-8

30. Fendler WP, Philippe Tiega DB, Ilhan H, Paprottka PM, Heinemann V, Jakobs TF, et al. Validation of several SUV-based parameters derived from ^{18}F -FDG PET for prediction of survival after SIRT of hepatic metastases from colorectal cancer. *Journal of nuclear medicine: official publication, Society of Nuclear Medicine*. 2013;54(8):1202-8



PART I

Surgery in metastatic Colorectal Cancer



CHAPTER 2

Surgery-induced tumour growth
in (metastatic) colorectal cancer

J.M.J. Jongen
K.M. Govaert
O. Kranenburg
I.H.M. Borel Rinkes

Abstract

Metastatic colorectal cancer (mCRC) is a devastating disease causing 700,000 deaths annually worldwide. Metastases most frequently develop in the liver. Partial hepatectomy has dramatically improved clinical outcome and is the only curative treatment option for eligible patients with mCRC. Pre-clinical studies have shown that surgical procedures can have tumour-promoting local 'side-effects' such as hypoxia and inflammation, thereby altering the behaviour of residual tumour cells. In addition, systemically released factors following (colon or liver) surgery can act as a wakeup-call for dormant tumour cells in distant organs and/or help establish a pre-metastatic niche. Tumour handling during resection may also increase the number of circulating tumour cells. Despite the overwhelming amount of pre-clinical data demonstrating the pro-tumourigenic side effects of surgery, clinical evidence is scarce. Indications for hepatic surgery are rapidly increasing due to a rise in the incidence of mCRC and a trend towards more aggressive surgical treatment. Therefore, it is increasingly important to understand the principles of surgery-induced tumour growth, in order to devise perioperative or adjuvant strategies to further enhance long-term tumour control. In the current study we review the evidence for surgery-stimulated tumour growth and suggest strategies to assess the clinical relevance of such findings.

Keywords

Colorectal cancer; Surgery; Liver metastasis; Preclinical; Clinical; Tumour growth

Highlights

- Experimental surgical procedures for the removal of primary or metastatic colorectal tumours have local and systemic effects on disease progression.
- These procedures include primary tumour resection, partial liver resection, local tissue ablation, vascular clamping protocols, portal vein embolization and transcatheter arterial embolization.
- In preclinical model systems surgery creates a pro-tumourigenic microenvironment which is characterized by hypoxia and inflammation and installs an aggressive tumour cell phenotype.
- Surgery causes shedding of tumour cells into the circulation and promotes the release of soluble factors that affect multiple steps of the metastatic cascade.
- Despite the vast amount of preclinical studies documenting these phenomena, evidence from clinical studies is limited.
- The advent of novel technologies, such as improved imaging, will help assessing the clinical relevance of the observed phenomena.



Introduction

Surgery has been a treatment modality for tumours in the abdomen since the early 19th century[1]. The concept of metastatic spread was introduced in 1829 by Récamier [2]. A few years later, in 1835, John Hunter advocated the surgical removal of primary tumours and metastases whenever possible[3]. It took another 43 years before the first colon tumour was surgically removed by von Volkmann in 1878[4], and more than a century before the first liver metastasis was surgically removed by Lortat-Jacob in 1952[5].

The fields of cancer surgery and basic cancer research have evolved in parallel. Virchow noted around 1860 that all cells, including malignant cells, arise from other cells and observed a close correlation between inflammation and cancer[6]. Around the same time tumour cells were found in the bloodstream of cancer patients at autopsy and were recognized to be potential seeds for metastases[7]. In 1899 Paget hypothesized that such cells may need a specialized environment in order to grow out and that this would make some organs more metastasis-prone than others[8]. Strikingly, these topics are still very relevant today and are actively being researched worldwide.

Surgery became a curative treatment modality for cancer patients following the development of anaesthetics (1847)[9], antiseptic surgical techniques (1867)[10], antibiotics (1929)[11] and blood transfusions (1930)[12]. As a result, survival has dramatically improved over the years. In addition, a large number of chemotherapeutic and targeted anti-cancer drugs have become available, which in some cases, have had spectacular effects on (progression-free) survival. In metastatic colorectal cancer (mCRC), systemic combination therapy has increased median overall survival from 5-6 months (best-supportive care) to approximately 2 years with the most effective regimens[13]. However, in the vast majority of cases, systemic treatment alone is not curative and surgery, whenever possible, remains the only chance for cure.

Despite the overwhelming impact of oncological surgery on patient survival, it was noted already in the early twentieth century that surgical manipulation might also promote tumour outgrowth and metastasis formation[14-16]. Liver surgery has been particularly linked to accelerated outgrowth of microscopic tumour deposits residing in the liver remnant (see Supplemental Table 1 for an overview of translational experiments regarding surgery induced tumour growth confined to the liver). However, the concept of surgery-induced tumour growth is largely built on results from preclinical studies; clinical data to support this are scarce. With the increasing incidence of mCRC and a trend towards more aggressive surgical treatment it is becoming more important than ever to understand the principles and clinical relevance of surgery-induced tumour growth. In this review we discuss our current understanding of how surgical resection of primary tumours and liver metastases might accelerate tumour growth in patients with mCRC based on the available (preclinical and clinical) data. For the scope of the article, we focus on the direct effects of surgery itself on tumour growth and leave other known or presumed factors, such as anaesthetics, medication, and comorbidities, undiscussed. We

ascertain a gap between preclinical and clinical data and describe how new modalities and strategies might bridge this gap.

Pre-clinical evidence

Local and systemic changes by surgery

Surgery and circulating tumour cells

A report from 1914 described that chemically damaged peritoneum harboured metastases from subcutaneously injected tumour cells while non damaged peritoneum did not[17]. Others found that surgically damaged peritoneum by scalpel blade, laser and electrocautery led to local tumour formation in 28%, 50% and 82% of the cases respectively, following intravenous injection of cancer cells[18]. Also, massage of subcutaneous tumours resulted in increased circulation of tumour cells and metastasis formation in the majority of the cell lines studied[19], despite the fact that the vast majority of these cells dies during dissemination and only a fraction of surviving cells has the capacity to form metastases[20]. In short, surgical handling promotes cancer cell shedding via manipulation of the tumour, and surgical trauma acts as a preferred site for metastases formation.

Hypoxia

Surgery, by definition, creates tissue damage and disruption of the (micro)vascular system. This leads to hypoxia, which is essential for initiating wound repair through a cascade of interconnected processes including inflammation, angiogenesis, vasculogenesis, fibroplasia and reepithelialization[21]. In tumours, hypoxia is common and chronic[22] and can be aggravated by external factors such as surgery. Interestingly, the local effects of surgery-induced tumour growth are found within the surgery-induced hypoxic tissues, potentially containing residual tumour cells[23-25]. Exposure of these tumour cells to hypoxia increases the cancer stem cell (CSC) subpopulation accompanied by an increase in tumour- and metastasis-initiating potential[26]. *In vitro*, hypoxia alone is sufficient to promote an invasive CSC-like phenotype in human colon cancer cells[23, 27], believed to be associated with disease progression[28]. For a more detailed overview regarding the effect of surgery on the CSCs niche, we refer to a recent review[29].

Immune system and inflammation

Selective immune-repression or stimulation has also been proposed as a major factor in surgery-stimulated tumour growth. Several pre-clinical studies have shown that cells of both the adaptive and the innate immune system (T cells and natural killer (NK) cells, respectively) normally actively suppress tumour progression and metastasis formation[30]. NK cell function is impaired due to peri-tumoural (fibrin and platelet) clot formation during the postoperative hypercoagulable state, resulting in increased pulmonary metastasis formation in mice[31]. Also, increased metastasis formation is seen in tumour bearing NK-deficient mice after the injection of dysfunctional NK cells



derived from surgically stressed mice compared to mice that received normal functioning NK cells[32]. Moreover, a recent report demonstrated that the transient, but profound suppression of tumour-associated antigen-specific CD8⁺ T-cell immunity following major surgery promotes the development of cancer metastases and local recurrence in a mouse model[33]. Surgery can also stimulate the tumour-suppressive effects of the immune system. For example, local tumour destruction by radiofrequency ablation (RFA) leads to the release of a bulk of tumour antigens, which initiates a T cell-mediated anti-tumour immune response[34-36]. Following complete thermal destruction of liver tumours, expression of CD8 and B7-2 was enhanced in the invasive front of a second, distant, non-treated tumour, resulting in a T-cell driven anti-tumour response[35]. Blocking the inhibitory receptor cytotoxic T-lymphocyte-associated antigen 4 enhanced the anti-tumour immunity in RFA treated mice[34]. Exploiting this anti-tumour immune reaction following RFA via co-administration of a vaccine resulted in complete elimination of distant non-RFA treated metastases and improved survival[36, 37].

Angiogenesis and tumour dormancy

The surgical removal of a primary tumour influences the systemic levels of many bioactive substances. Folkman and colleagues have demonstrated that primary tumours produce anti-angiogenic factors that actively suppress the outgrowth of distant metastases[38]. Surgical removal of the primary tumour also removes these factors. In addition, the surgical procedure itself leads to a strong increase in the levels of circulating pro-angiogenic growth factors, including vascular endothelial growth factor (VEGF) and stromal-derived factor 1 (SDF1). The post-surgical increase in VEGF production is also capable of activating distant tumour cells from dormancy[39-41]. There are at least two reasons why these latent micro-metastases initially do not grow out. First, they are unable to initiate an angiogenic program, which limits their expansion[39, 42]. Surgery can initiate this angiogenic program by the aforementioned upregulation of VEGF[40], whereupon tumours will grow out[43]. Second, the immune system is known to be able to favour either tumour growth or tumour suppression. Where dormant cells are thought to have reached an equilibrium, surgery can tip this balance towards tumour growth via the immune system[44]. Repeated laparotomy in rats several months after intravenous injection of tumour cells, resulted in 90-100% metastasis, initiated from dormant tumour cells, compared to 0% in non-surgery exposed controls[45, 46].

Growth factors

Another key element in surgery-induced tumour growth involves liver regeneration following partial (major) hepatectomy, as this is characterized by the release of various factors that were subsequently shown to accelerate tumour growth *in vitro*[47, 48], including transforming growth factor- β (TGF- β), transforming growth factor- α (TGF- α) and basic fibroblast growth factor (bFGF)[49]. Interestingly, TGF- β has tumour suppressive effects in normal and pre-malignant cells, but has little effect on colon cancer cells due to frequent inactivation of this pathway, specifically in colon cancer[50]. However, high TGF- β levels activate gene programs in a wide range of tumour-associated

stromal cell types resulting in tumour and metastases initiation via pro-metastatic cytokine such as Interleukin-11 (IL11). Tumour cell lines with TGF- β producing stromal cells injected in the cecum of mice promoted distant liver and lung metastases while control cell lines did not[51]. This establishes a pro-metastatic signalling loop involving the reciprocal influence of tumour and stromal cells. Surgery-induced increase of TGF- β levels could therefore play a role in tumour progression.

Oncological effects of liver interventions

Liver resection

Partial hepatectomy has been an established technique since the 1950s[5]. At that time Paschke already noted that a 2/3 hepatectomy in rats resulted in a significant increase in growth of present subcutaneous tumours[52]. This observation has been confirmed by several other groups (Supplemental Table 1). More than 20 studies have been published focussing on metastasis formation or tumour growth following hepatectomy in murine models. Most groups injected tumour cells intravenously via the portal vein either prior to, or following, hepatectomy and noted a significant increase in metastasis formation. Likewise, a significant increase in tumour volume was seen in two studies in rats in which tumour cells were injected in the remnant liver concomitant with the partial hepatectomy. Additionally, one study in which pieces of two xenotransplanted human tumours were placed intrahepatically in nude mice, showed a significant 8- to 13-fold increase in tumour load following 30% hepatectomy[53].

Radiofrequency ablation

RFA, microwave or laser-based therapies cause local destruction of tumour tissue by the generation of heat. Mounting preclinical evidence indicates that locally recurring tumours following these ablative techniques, display a more aggressive growth pattern than before the ablation[24, 54, 55]. The outgrowth of micro-metastases in the periphery of the ablated lesion was four-fold higher than the outgrowth of micro metastases in non-ablated control liver tissue[24]; this was accompanied by high levels of hypoxia inducible factor (HIF)-1 and HIF-2, as a read out of hypoxia. Destabilisation of HIF-1 and HIF-2 resulted in a 40% decrease of accelerated tumour growth[24]. Increased levels of growth factors such as VEGF[54], FGF[54, 55] and TGF- β [55] as possible contributors to the observed induced tumour growth were also found post-ablation.

Liver vessel clamping

Vascular clamping induces hepatic ischemia-reperfusion and has been shown to promote outgrowth of intrahepatic micro-metastases[56, 57]. Murine liver lobes which were clamped for 45 minutes, 5 days after intrasplenic injection of C26 cells showed a 5- to 6-fold increase in metastasis formation compared to non-clamped (control) lobes[57]. In another study, 2 liver lobes of rats were clamped for 30 minutes followed by intraportal injection of hepatoma cells, which resulted in an 8-fold increase in tumour load compared to the non-clamped lobe[56].

Selective portal vein embolization

Selective portal vein embolization (PVE) causes atrophy of the embolized liver lobe accompanied by hypertrophy of the contralateral lobe and is used to stimulate liver regeneration in patients with otherwise marginal post-operative remnant liver tissue[58]. A study in a rodent hepatocellular carcinoma (HCC) model showed a significant increase in tumour growth rate if the rabbits were subjected to PVE 14 days after subcapsular implantation of VX2 tumour fragments in the cranial liver lobe, compared to laparotomy alone (control)[59]. Limitation of this study is the difficulty in judging computed tomography (CT) based volumes; total tumour volumes are small and baseline volumes display great variability.

Transcatheter arterial embolization

Transcatheter arterial embolization (TAE) techniques include embolization with spheres only, spheres loaded with chemotherapeutic agents (chemoembolization; TACE) or with radioactive spheres (radioembolization; TARE)[60]. A critical issue is that, by obstructing the microvasculature, by definition TAE techniques induce ischemia and hypoxia in the treated liver segments[61, 62] with a subsequent upregulation of VEGF[63]. A preclinical study in hepatoma-harboring rats showed a 70% increase ($p=0.03$) of lung metastases following TACE treatment. Immunohistochemistry of the treated tumours revealed an upregulation of HIF-1 α expression and induction of epithelial to mesenchymal transition (EMT), characterized by the loss of E-cadherin and upregulation of N-cadherin and vimentin[64].

Clinical evidence

Despite the vast amount of pre-clinical data on accelerated outgrowth of colorectal (micro)metastases following surgical removal or other oncological interventions, this is not matched by robust clinical evidence [65-67]. Following surgery for primary colon cancer, local recurrence is observed in 5-24% of the patients depending on the stage of the disease[68]. If an incomplete resection has been performed[69], if positive lymph nodes nearby are not resected[70] or if the resected tumour may have been part of a larger pre-malignant epithelial field[71], the remaining cells can grow out or progress towards malignancy under the influence of the surgical wound. This local recurrence rate can be enhanced following anastomotic leakage[72].

One randomized trial by Lacy *et al* comparing laparoscopic with open colectomy for colon cancer found fewer metastatic events in the former approach and proposed that minor surgical damage would indeed result in less tumour growth[73]. However, this trial was criticized by several groups. Loco-regional relapse rate in the conventional group was significantly higher than expected, the number of radical resections (R0/R1) was not addressed and especially chemotherapy was not reported adequately and not equally distributed between the groups[74-77]. Moreover, similar studies in rectal and

colon cancer patients did not show any differences in recurrence and survival rates[78, 79]. Nonetheless, Lacy *et al* updated their study with a median follow up of 95 months showing a trend towards lower tumour recurrence (18% vs 28%, $p=0.07$) and lower cancer related mortality (16% vs 27%, $p=0.07$) in the laparoscopic group compared to the open colectomy group. Also, the survival curves showed a significantly higher probability of cancer-related survival ($p=0.02$) for the laparoscopy group and multivariate analysis confirmed the procedure itself ($P=0.03$) to be an independent predictor of cancer-related survival[80]. They explained these findings by the preserved cellular immunity, attenuated stress and inflammatory response, minimal tumour handling, and lower complication rate in patients treated with laparoscopy-assisted colectomy. More studies will be needed to clarify the existing contradictions.

Local and systemic changes by surgery

Surgery and circulating tumour cells

Following both palpation and biopsy of tumours, the number of circulating tumour cells rise in respectively 25% and 40% of patients[81]. Clinical evidence also exists for circulating tumour cells resulting from manipulation during surgery of colorectal tumours[82] and during resection of liver metastases[83]. Several studies have linked circulating tumour cells to worse prognosis in CRC patients[84, 85]. Two meta-analyses have demonstrated an association between the presence of circulating tumour cells and poor prognosis in CRC: Patients in whom circulating tumour cells were detectable had a ~2.5-fold increased chance of disease progression and death[86, 87]. Sub-analyses revealed an even higher hazard ratio for circulating tumour cells in intra- and post-operative samples compared to pre-operative samples[87]. Interestingly, only high levels of circulating tumour cells expressing the CSC marker CD133 were correlated with relapse, while circulating non-CSC were not[88].

Hypoxia

Inadequate angiogenesis, as well as surgery or other interventions, can cause tumour cells to become hypoxic. Hypoxic tumour cells behave more aggressively, have a higher propensity to develop metastases[89, 90] and are accompanied by an upregulation of the transcription factor HIF. Indeed, HIF-expression has been found to be associated with poorer prognosis in many cancer types[91]. It is also an independent risk factor for recurrence after curative resection of colorectal liver metastases[92]. Hence, the search for drugs that interfere with this pathway has been intensified[93].

Immune system and inflammation

Circumstantial clinical evidence indicates that an impaired function of immune cells affects tumour cell behaviour. Immune-suppressed liver-transplant recipients have an increased relative risk of 1.8 (95% CI 1.1–2.9) to develop CRC compared to non-transplanted immune-competent subjects[94]. The ensuing cancers all demonstrated lymphatic and vascular invasion, and nodal involvement in 80%, compared to 64%[95] and <50%[96] respectively, in non-transplanted CRC patients. Post-transplant CRC may therefore be

more aggressive than conventional CRC[97]. In addition, the function of circulating NK cells, as part of the innate immune system, is impaired after surgery in cancer patients[32, 98]. Earlier work has associated impaired NK cell function with poor prognosis[99]. More recently, 2 patients reportedly received a vaccine to activate NK cells prior to surgery after blood was drawn at multiple postoperative time points. Adding this postoperative blood *in vitro* to a tumour cell line led to improved tumour-directed NK cell toxicity[32]. High levels of activated T cells (part of the adaptive immune system) in primary colorectal tumours are associated with a markedly lower incidence of metastasis formation[100, 101]. Analysis of resected colorectal liver metastases revealed that an abundance of T cells was correlated with improved survival[102, 103]. Surgery decreases post-operative T cell levels[104-106]. Although no direct clinical evidence exists, this could weaken the T cell protective effect on cancer progression. Taken together, these findings suggest a role of both the innate, and adaptive immune system on (liver) metastasis formation and survival.

Angiogenesis and tumour dormancy

Plasma levels of VEGF increase following major abdominal surgery[107]. Clinical evidence for the pro-tumourigenic effects of surgery-induced angiogenesis was provided in a study showing that removal of primary colorectal tumours results in increased vascular density, increased proliferation and decreased apoptosis in synchronous liver metastases. These observations were associated with accelerated metastatic outgrowth[108], implying that inhibiting post-surgical angiogenesis might be beneficial. Several large clinical studies have shown that the addition of the angiogenesis inhibitor Bevacizumab to the standard regimen of chemotherapy prolongs disease-free and overall survival in patients with mCRC[109-111]. Strikingly, the advantage of Bevacizumab was restricted to those patients who had already undergone surgery for their primary tumour[112]. This provides clinical evidence for the concept that removal of the primary tumour leads to VEGF-mediated support of distant metastases. Surprisingly, addition of Bevacizumab to *adjuvant* chemotherapy for stage II/III patients (i.e., without distant metastases at diagnosis) appears to have no survival benefit[113]. It is currently unknown why VEGF-targeting is beneficial in the treatment of advanced but not early stage CRC. An important question is whether addition of anti-VEGF therapy to adjuvant chemotherapy following surgical removal of liver metastases could prevent recurrence and improve patient survival. Unfortunately, a clinical phase III study that was designed to answer this question was closed prematurely due to slow patient accrual[114].

Circulating tumour cells can give rise to distant undetectable tumour cell deposits. These deposits can subsequently shed circulating tumour cells over time, which would explain circulating tumour cells in otherwise disease-free breast cancer patients up to 22 years following mastectomy. As circulating tumour cells are unable to survive such a long period, these cells must be shed from clinically undetectable “dormant” tumour cell deposits[115]. Another observation underpinning the existence of tumour dormancy comes from autopsy studies on victims of fatal accidents, where many

clinically unpresented or unknown tumours were encountered. It has been shown that 20% of females have breast malignancies[116], 35.6% of patients have occult papillary thyroid cancer[117], while prostate cancer rates range from 3.6% to 33.3%, depending on age[118]. An accident or trauma may be sufficient to activate such dormant tumour cells into growth and expansion to clinically manifest disease states[42].

Growth factors

Other growth factors than VEGF have been suggested to play a role in post-surgery tumour growth as well. Following liver resection, high levels of hepatocyte growth factor (HGF) and TGF- β have been reported[119]. In resected tissue specimens of colorectal liver metastases, high c-Met expression and high levels of its ligand HGF, were correlated to early recurrence after hepatectomy and poorer prognosis[120]. In addition, high levels of circulating TGF- β mark metastasis-prone colon tumours[121]. Targeted therapeutics have been developed against many of these ligand/receptor systems, providing multiple opportunities for adjuvant therapy following surgery. An extensive overview of targeting surgery-induced growth factor signalling is provided elsewhere[122].

Oncological effects of liver interventions

Liver resection

As stated above, formal proof for hepatectomy-induced outgrowth of liver (micro) metastases in cancer patients is lacking. The only indication suggestive of this phenomenon is that tumour progression after the first resection during a scheduled two-stage liver resection is the major reason for not performing the second resection. In two studies, 11 and 23% of the total cohort of patients with colorectal liver metastases were initially unresectable and underwent a two-stage procedure. Of these, 24 and 31% respectively did not reach the planned second hepatectomy[123, 124]. This suggests that hepatectomy may stimulate the outgrowth of liver (micro)metastases. By contrast, a study in which proliferation markers were compared in tumours resected at first- and second stage hepatectomy did not show any differences[125]. However, these patients had received preoperative chemotherapy, complicating the interpretation of the results.

An interesting development is the 'liver first' approach in treating resectable synchronous colorectal liver metastases. Classically, the primary tumour would be resected first followed by resection of the liver metastases. However, since many patients experienced progressive metastatic tumour growth, the 'liver-first' approach to the surgical treatment of mCRC was prompted[126, 127]. For rectal cancer patients this has the advantage of additional time for chemo-radiotherapy before final rectal surgery, which, in case of a complete response, might even obviate the need for surgery[128]. Performing liver surgery prior to chemotherapy circumvents chemotherapy-associated parenchymal damage as well as the problem of localizing lesions that have shown (near) complete responses. A meta-analysis comparing colon-first, simultaneous, and liver-first surgical approaches revealed no superiority of any of the three[129]. However, no randomized clinical trials have been conducted that adequately compare the different surgical

approaches. Therefore, the current standard of care remains removal of the primary tumour first, reserving both simultaneous resections and the liver-first approach to expert centres and/or clinical trials.

Radiofrequency ablation

Following RFA, local recurrence rates remain a matter of concern, ranging from 3-60% between studies[130]. Risk factors include the size, number and location of tumours, proximity to major vessels, experience of the physician and the approach used to perform RFA (open, laparoscopic, or percutaneous)[131]. Although preclinical evidence indicates that the locally recurring tumours display a more aggressive growth pattern than before ablation, this is difficult to prove in patients as normally no tissue is collected for examination after ablation. Also, the ablated necrotic area hampers proper identification of local recurrence. Nonetheless, several case reports describe a more aggressive growth pattern of recurrent disease following RFA in patients[132-134].

Liver vessel clamping

During resection, blood loss is minimized by clamping the blood vessels to the liver or liver segment, an approach that was first described by Pringle[135] and is since commonly referred to as the 'Pringle manoeuvre'. Vascular clamping is also used during RFA of tumour lesions adjacent to large blood vessels, since the blood stream in such vessels acts as a 'heat sink' thus reducing the ablative effect[136]. However, vascular clamping during liver surgery also causes ischemia of the clamped liver segment(s) followed by a reperfusion phase upon de-clamping. Apart from re-oxygenation, reperfusion leads to a burst of reactive oxygen and nitrogen species, causing tissue damage. We have previously provided clinical evidence that prolonged vascular clamping during oncological liver surgery is associated with accelerated tumour recurrence[137], but this could not be confirmed by others[138-140]. Nevertheless, to reduce tissue damage following (oncological) liver surgery, intermittent rather than continuous clamping protocols are now common practice as they were shown to minimize ischemia/reperfusion damage[141].

Selective portal vein embolization

Several studies have associated PVE prior to liver resection with tumour growth stimulation[142-145]. While aiming at inducing contralateral regeneration, PVE may also enhance tumour growth in the non-embolized parts of the liver[146]. Factors that may play a role are altered hepatic blood flow and changes in cytokines and growth factors promoting local (and distant) tumour growth. However, most clinical studies involve small numbers of patients, precluding a definitive assessment of the effect of PVE on tumour progression[147]. A retrospective case-control study reported that PVE was not associated with altered long-term outcome in patients with mCRC[148], but this has yet to be established[149, 150]. Concurrent treatment of chemotherapy and PVE significantly delayed tumour progression and improved long-term survival. PVE without chemotherapy resulted in 8% tumour growth, while combining PVE with chemotherapy

resulted in 13% tumour reduction ($p < 0.001$), suggesting a tumour growth enhancing effect of PVE. Five year survival for PVE without chemotherapy was 24%, PVE with chemotherapy showed a 5-year survival of 49% ($P = 0.006$) [151].

Transcatheter arterial embolization

The effect of TAE techniques on tumour growth has so far not been studied in clinical trials. Nonetheless there are some concerns regarding pro-tumourigenic effects of the procedure, since increased VEGF levels are observed following TACE of HCC [152] and VEGF levels were highest in the non-responders and correlated with worse prognosis [153]. Moreover, increased HIF-1 levels are observed in immunostained tissue that was resected $26 (\pm 14.5)$ days after TACE [154]. Also, post TACE livers showed a higher level of inflammatory injury [155]. Taken together, this creates a pro-tumourigenic niche for residual tumour cells in patients treated with TACE preoperatively. These findings might explain the observed higher recurrence rates in patients treated with TACE prior to liver surgery, compared to patient treated with surgery alone [154]. An overview of the surgical procedures for mCRC and their effects on post-surgery tumour recurrence is provided in Supplemental Table 2.

The gap between bench and clinic

In short, there is ample preclinical evidence supporting the notion of surgery-induced tumour growth in (m)CRC, but clinical evidence is scarce. One possible explanation could be that animal models insufficiently mimic the clinical situation [156]. First, most cell lines used in murine models are the product of *in vitro* tissue culture selection and may not adequately reflect the original human (or murine) tumours they were derived from. Culturing cells *in vitro* induces mutations and structural genomic changes and influences gene expression patterns. Second, most models use heterotopic tumour cell injections rather than spontaneous liver metastasis formation from an orthotopic site (e.g. caecum) (Supplemental Table 1). Third, experimental set-ups are usually designed to gain maximal effects, which may not reflect the clinical reality. An example is the liver clamping method in mice, which leads to an extent of tissue damage that is likely to be more severe than that induced by non-extreme liver surgery in cancer patients [57]. Fourth, experiments with human tumour cell lines are mostly carried out in immunocompromised mouse strains [23] in which immune-mediated effects of surgery on tumour growth cannot be studied. Fifth, there is a difference in the set-up of animal experiments versus clinical studies. Where animal studies make use of early stage disease models, end-stage disease patients are most commonly included in clinical trials. Sixth, the poor reproducibility of preclinical findings could contribute to the scarcity of clinical evidence. Attempts to reproduce published experimental studies were successful in only 11-25% of the cases [157, 158]. This has been proposed to contribute to the high failure rate of phase 2 clinical trials [159].

Despite all these limitations, translational studies in animal models are still indispensable[160]. However, other methodologies and novel technologies are critical to overcome the gap between pre-clinical data and clinical outcomes.

Bridging the gap

Improved imaging modalities and a more extensive use of patient-derived material, in combination with the recently developed three-dimensional 'organoid' culture systems, may aid in overcoming the gap between experimental studies and clinical proof and relevance.

Much may be expected from new imaging techniques that allow visualization of relevant biological processes and phenomena, and permit functional, rather than anatomical interpretation. For example, advances are made in specifically visualizing tumour hypoxia with positron emission tomography (PET) in combination with tracers, e.g. nitroimidazole analogues (^{18}F -FMISO, ^{18}F -FAZA, ^{18}F -FETNIM, ^{18}F -HX4, ^{18}F -FRP-170) or Cu diacetyl-bis(N^4 -methylthiosemicarbazone) (ATSM) ligands[161].

Magnetic resonance imaging (MRI), contrast-enhanced color duplex sonography or near-infrared spectroscopy are other non-invasive techniques used to identify pre- and post-surgery hypoxia levels in patients[162, 163]. In addition, ultrasonography, MRI and CT may be used to visualize angiogenesis in tumours in a morphologic, functional or molecular way[164]. Still in its infancy, single circulating tumour cells (including dormant tumour cells) can be visualized and tracked *in vivo* in the murine brain[165]. The discovery and development of fluorescence-labeled markers for human tumour cells could transpose this model to the clinic. Indeed, the technology of intra-operative fluorescence imaging to detect occult micro-metastases is now starting to be implemented in several surgical oncological settings. This is a powerful tool to trace dormant and/or microscopic tumour residue. Another application involves real time imaging of the tumour- or surgery-induced immune response. Alpacaca-derived antibody fragments can be visualized acting towards specific parts of the immune system, e.g. major histocompatibility complex (MHC) class II and CD11b products. These are both recruited to the interface of normal and tumour tissue[166].

Eventually, such non-invasive "bio-imaging" may direct and individualize treatment regimes. For instance, local (hypoxia-activated pro)drug releasing millirods, beads or nanoparticles can be dosed and embolize surrounding vessels, or can be placed in the RFA needle tract to help prevent or delay local recurrence. Post-surgery imaging could identify one or more factors known to play a role in (surgery stimulated) tumour growth in individual patients. Consequently, individual treatment plans can be made by targeting these identified factors at the right moment and location.

Bio-optical imaging is becoming increasingly important during surgery. Optical imaging with near infrared fluorescence can be used as a navigator during oncological surgical procedures to delineate normal from tumour tissue[167]. This might be of special interest in combination with tumour, or even tumour edge, specific fluorescent nanobodies[168]. An application might lie in detection and resection of previously invisible tumour cell deposits, e.g. peritoneal deposits from CRC or ovarian cancer during cytoreductive surgery and hypothermic intraperitoneal chemotherapy (HIPEC).

Another avenue in attempting to better connect the lab with the clinic involves the systemic and sustained collection and storage of tissue samples of patients before, during and after treatment. Not only will tissue samples be necessary for deoxyribonucleic acid (DNA)-analysis and immunohistochemistry. Samples of tissue taken during or directly following treatment (e.g. radio-embolization) will allow us to study structural changes in gene and transcriptome and proteome expression resulting from that treatment, both in tumour and host-organ tissues[169]. Previous clinical trials in which post-RFA liver lesions were resected to confirm necrotic lesions and adequate ablation[170, 171] are nowadays unrealistic. RFA is proven to be safe and efficient for patients with unresectable colorectal liver metastases and post-RFA resection for scientific purposes would pose unnecessary additional risks for these patients. Nonetheless, a recent trial studying TACE before surgery in HCC patients[154, 155] could provide the tissue needed for such analyses. In this sense, two stage liver resection can also be used to evaluate post-surgical environmental changes over a longer period of time[125]. Furthermore, tumour biopsies can be taken at diagnostic colonoscopy and compared with the resection specimen of the surgically removed primary tumour. With biopsies taken over time following a treatment, biological changes within the tumour tissue can be assessed. Next-generation DNA and ribonucleic acid (RNA) sequencing may display treatment-induced genetic changes in the obtained tissue[172]. Our group recently launched the first of such “proof of biological concept”-trials (www.clinicaltrials.gov/NCT02685046).

Furthermore, storage of tissue and blood in biobanks is pivotal in this regard. Precise collection of clinical data, appropriate ethical systems to obtain informed consent, standardized methods to collect and preserve tissue samples, improved infrastructure to minimize pick-up times and an enhanced system for database management; these factors all contribute to the indisputably valuable place of systematic clinical biobanking for clinical research and will definitively have a great impact on future research[173]. Ideally, a biobank should contain both paired samples of primary tumours with their local and/or distant recurrences and corresponding blood samples[174]. By centralizing such biobanks within hospitals, multidisciplinary collection of samples will make analysis of tumour tissue possible over time. Here, we emphasize the importance of obtaining samples during and after treatment as well. As such, tumour tissue prior to chemo- and/or radiotherapy (samples taken at colonoscopy) can be compared with tissue after neoadjuvant treatment, following resection of the primary tumour, and eventually following liver metastases (should they arise).

Cancer research still relies heavily on culturing of patient-derived tumour tissue. Designing systems and techniques to enhance the representativity of cultured material is crucial to help bridge the gap between lab and clinic. The three-dimensional culture systems, such as the before mentioned organoids (originally established by Sato and colleagues from normal tissue[175]), are an excellent example of this endeavor. Recently, it was shown in pancreatic cancer that tissue from biopsies is sufficient to establish organoids that accurately mimic the human disease[176]. Organoids consist of different tumour cell populations with distinct characteristics, making it possible to investigate the interactions between different subsets of tumour cells within tumours[177, 178]. Furthermore, organoids may facilitate high-throughput *in vitro* testing of (novel) compounds or combinations thereof[179], and the assessment of treatment- and/or surgery-induced biological changes by comparing pre- with post-interventional tumour derived organoids.

Another approach lies in the upcoming use of technology in medicine. Organs-on-chips, or even “human-on-chips”, is a next generation tool recapitulating the complex organ cellular properties and interactions[180-182]. They enable high-resolution, real-time imaging and *in vitro* analysis of biochemical, genetic and metabolic activities of living (tumour) cells in a functional tissue and organ context. The power of these microsystems is the ability to design synthetic culture systems in which many different parameters such as oxygen gradients, cytokine levels or activation of immunological components, can be varied while maintaining high resolution imaging[182]. Following changes of certain conditions as seen after surgery, continuous imaging of different (though connected) microfluidic cell chambers, interactions between primary and metastasized colorectal tumour cells can be visualized. It will allow to evaluate the impact of novel anti-cancer therapies on both patient derived tumour- and healthy cells to better predict treatment effects and base the design of clinical trials on these findings[183].

Conclusions

Despite overwhelming preclinical evidence, solid clinical proof for surgery stimulated tumour growth in patients is still lacking. The advent of novel methodologies, such as improved imaging and more extensive use of patient derived material in combination with the use of human tumour derived organoid culture systems, can provide a platform necessary to elucidate which of the observed preclinical phenomena bears clinical relevance. Such knowledge should form the basis for developing adjuvant strategies that limit recurrence following surgical interventions.

Funding

This study was supported by the Dutch Cancer Society (grant numbers UU2010-4608 to K.M.G. and UU2013-5865 to J.M.J.).

References

1. McDowel, E., *Three cases of extirpation of diseased ovaria*. Eclectic Repertory, and Analytical Review, Medical and Philosophical, 1817. **7**: p. 242-244.
2. Récamier, J.C.A., *Recherches sur le traitement du cancer* 1829. **8(2)**: p. 1-12.
3. Hunter, J., *The Surgical Works*. 1835.
4. R., V., *Über den Mastdarmkrebs und die Exstirpatio recti [On rectal cancer and the exstirpatio recti]*. Volkmanns Sammlung klinischer Vorträge III Serie, 1878. **131**: p. 1113–1128.
5. Lortat-Jacob, J.L. and H.G. Robert, [*Well defined technic for right hepatectomy*]. Presse Med, 1952. **60(26)**: p. 549-51.
6. Virchow, R., *Die Cellularpathologie in ihrer Begründung auf physiologische und pathologische Gewebelehre*. August Hirschwald, Berlin 1858.
7. Ashworth, T.R., *A case of cancer in which cells similar to those of the tumour were seen in the blood after dead*. Med J Aust 1869. **14**: p. 146-147
8. Paget, S., *The distribution of secondary growths in cancer of the breast*. Lancet, 1889: p. 571-573.
9. Robinson, D.H. and A.H. Toledo, *Historical development of modern anesthesia*. J Invest Surg, 2012. **25(3)**: p. 141-9.
10. Lister, J., *On the Antiseptic Principle in the Practice of Surgery*. Br Med J, 1867. **2(351)**: p. 246-8.
11. Fleming, A., W. Walters, and et al., *Penicillin in surgery*. Lancet, 1947. **2(6474)**: p. 479.
12. Giangrande, P.L., *The history of blood transfusion*. Br J Haematol, 2000. **110(4)**: p. 758-67.
13. Koopman, M. and C.J. Punt, *Chemotherapy, which drugs and when*. Eur J Cancer, 2009. **45 Suppl 1**: p. 50-6.
14. Clunet, J., *Recherches expérimentales sur les tumeurs malignes*. Steinhil, Paris, 1910.
15. Marie, P.C., J. , *Fréquences des métastases viscérales chez les souris cancéreuses après ablation chirurgicale de leur tumeur*. Bull Assoc Franc L'Étude Cancér, 1910. **3**: p. 19-23.
16. Tyzzer, E.E., *Factors in the Production and Growth of tumor Metastases*. J Med Res, 1913. **28(2)**: p. 309-332.1.
17. Jones, F.S. and P. Rous, *ON THE CAUSE OF THE LOCALIZATION OF SECONDARY TUMORS AT POINTS OF INJURY*. J Exp Med, 1914. **20(4)**: p. 404-12.
18. Murthy, S.M., et al., *The influence of surgical trauma on experimental metastasis*. Cancer, 1989. **64(10)**: p. 2035-44.
19. Knox, L.C., *THE RELATIONSHIP OF MASSAGE TO METASTASIS IN MALIGNANT TUMORS*. Ann Surg, 1922. **75(2)**: p. 129-42.
20. Talmadge, J.E. and I.J. Fidler, *AACR centennial series: the biology of cancer metastasis: historical perspective*. Cancer Res, 2010. **70(14)**: p. 5649-69.
21. Ruthenborg, R.J., et al., *Regulation of wound healing and fibrosis by hypoxia and hypoxia-inducible factor-1*. Mol Cells, 2014. **37(9)**: p. 637-43.
22. Wilson, W.R. and M.P. Hay, *Targeting hypoxia in cancer therapy*. Nat Rev Cancer, 2011. **11(6)**: p. 393-410.

23. Govaert, K.M., et al., *Hypoxia after liver surgery imposes an aggressive cancer stem cell phenotype on residual tumor cells.* Ann Surg, 2014. **259**(4): p. 750-9.
24. Nijkamp, M.W., et al., *Accelerated perinecrotic outgrowth of colorectal liver metastases following radiofrequency ablation is a hypoxia-driven phenomenon.* Ann Surg, 2009. **249**(5): p. 814-23.
25. van der Bilt, J.D., et al., *Perinecrotic hypoxia contributes to ischemia/reperfusion-accelerated outgrowth of colorectal micrometastases.* Am J Pathol, 2007. **170**(4): p. 1379-88.
26. Yun, Z. and Q. Lin, *Hypoxia and regulation of cancer cell stemness.* Adv Exp Med Biol, 2014. **772**: p. 41-53.
27. Hongo, K., et al., *Hypoxia enhances colon cancer migration and invasion through promotion of epithelial-mesenchymal transition.* J Surg Res, 2013. **182**(1): p. 75-84.
28. Bao, B., et al., *The biological kinship of hypoxia with CSC and EMT and their relationship with deregulated expression of miRNAs and tumor aggressiveness.* Biochim Biophys Acta, 2012. **1826**(2): p. 272-96.
29. O'Leary, D.P., et al., *Effects of surgery on the cancer stem cell niche.* Eur J Surg Oncol, 2016. **42**(3): p. 319-25.
30. Gajewski, T.F., H. Schreiber, and Y.X. Fu, *Innate and adaptive immune cells in the tumor microenvironment.* Nat Immunol, 2013. **14**(10): p. 1014-22.
31. Seth, R., et al., *Surgical stress promotes the development of cancer metastases by a coagulation-dependent mechanism involving natural killer cells in a murine model.* Ann Surg, 2013. **258**(1): p. 158-68.
32. Tai, L.H., et al., *Preventing postoperative metastatic disease by inhibiting surgery-induced dysfunction in natural killer cells.* Cancer Res, 2013. **73**(1): p. 97-107.
33. Ananth, A.A., et al., *Surgical Stress Abrogates Pre-Existing Protective T Cell Mediated Anti-Tumor Immunity Leading to Postoperative Cancer Recurrence.* PLoS One, 2016. **11**(5): p. e0155947.
34. den Brok, M.H., et al., *In situ tumor ablation creates an antigen source for the generation of antitumor immunity.* Cancer Res, 2004. **64**(11): p. 4024-9.
35. Isbert, C., et al., *Enhancement of the immune response to residual intrahepatic tumor tissue by laser-induced thermotherapy (LITT) compared to hepatic resection.* Lasers Surg Med, 2004. **35**(4): p. 284-92.
36. Gameiro, S.R., et al., *Combination therapy with local radiofrequency ablation and systemic vaccine enhances antitumor immunity and mediates local and distal tumor regression.* PLoS One, 2013. **8**(7): p. e70417.
37. Behm, B., et al., *Additive antitumour response to the rabbit VX2 hepatoma by combined radio frequency ablation and toll like receptor 9 stimulation.* Gut, 2016. **65**(1): p. 134-43.
38. O'Reilly, M.S., et al., *Angiostatin: a novel angiogenesis inhibitor that mediates the suppression of metastases by a Lewis lung carcinoma.* Cell, 1994. **79**(2): p. 315-28.
39. Holmgren, L., M.S. O'Reilly, and J. Folkman, *Dormancy of micrometastases: balanced proliferation and apoptosis in the presence of angiogenesis suppression.* Nat Med, 1995. **1**(2): p. 149-53.

40. Maniwa, Y., et al., *Vascular endothelial growth factor increased by pulmonary surgery accelerates the growth of micrometastases in metastatic lung cancer*. *Chest*, 1998. **114**(6): p. 1668-75.
41. Aguirre-Ghiso, J.A., *Models, mechanisms and clinical evidence for cancer dormancy*. *Nat Rev Cancer*, 2007. **7**(11): p. 834-46.
42. Naumov, G.N., J. Folkman, and O. Straume, *Tumor dormancy due to failure of angiogenesis: role of the microenvironment*. *Clin Exp Metastasis*, 2009. **26**(1): p. 51-60.
43. Naumov, G.N., et al., *A model of human tumor dormancy: an angiogenic switch from the nonangiogenic phenotype*. *J Natl Cancer Inst*, 2006. **98**(5): p. 316-25.
44. Dunn, G.P., C.M. Koebel, and R.D. Schreiber, *Interferons, immunity and cancer immunoediting*. *Nat Rev Immunol*, 2006. **6**(11): p. 836-48.
45. Fisher, B. and E.R. Fisher, *Experimental evidence in support of the dormant tumor cell*. *Science*, 1959. **130**(3380): p. 918-9.
46. Sugarbaker, E.V., A.S. Ketcham, and A.M. Cohen, *Studies of dormant tumor cells*. *Cancer*, 1971. **28**(3): p. 545-52.
47. Rupertus, K., et al., *Rapamycin inhibits hepatectomy-induced stimulation of metastatic tumor growth by reduction of angiogenesis, microvascular blood perfusion, and tumor cell proliferation*. *Ann Surg Oncol*, 2009. **16**(9): p. 2629-37.
48. Shi, J.H., et al., *Growth of hepatocellular carcinoma in the regenerating liver*. *Liver Transpl*, 2011. **17**(7): p. 866-74.
49. Picardo, A., et al., *Partial hepatectomy accelerates local tumor growth: potential roles of local cytokine activation*. *Surgery*, 1998. **124**(1): p. 57-64.
50. Bellam, N. and B. Pasche, *Tgf-beta signaling alterations and colon cancer*. *Cancer Treat Res*, 2010. **155**: p. 85-103.
51. Calon, A., et al., *Dependency of colorectal cancer on a TGF-beta-driven program in stromal cells for metastasis initiation*. *Cancer Cell*, 2012. **22**(5): p. 571-84.
52. Paschkis, K.E., et al., *Tumor growth in partially hepatectomized rats*. *Cancer Res*, 1955. **15**(9): p. 579-82.
53. Rashidi, B., et al., *Minimal liver resection strongly stimulates the growth of human colon cancer in the liver of nude mice*. *Clin Exp Metastasis*, 1999. **17**(6): p. 497-500.
54. Nikfarjam, M., V. Muralidharan, and C. Christophi, *Altered growth patterns of colorectal liver metastases after thermal ablation*. *Surgery*, 2006. **139**(1): p. 73-81.
55. Ohno, T., et al., *Microwave coagulation therapy accelerates growth of cancer in rat liver*. *J Hepatol*, 2002. **36**(6): p. 774-9.
56. Ku, Y., et al., *Stimulation of haematogenous liver metastases by ischaemia-reperfusion in rats*. *Eur J Surg*, 1999. **165**(8): p. 801-7.
57. van der Bilt, J.D., et al., *Ischemia/reperfusion accelerates the outgrowth of hepatic micrometastases in a highly standardized murine model*. *Hepatology*, 2005. **42**(1): p. 165-75.
58. Jaeck, D., et al., *A two-stage hepatectomy procedure combined with portal vein embolization to achieve curative resection for initially unresectable multiple and bilobar colorectal liver metastases*. *Ann Surg*, 2004. **240**(6): p. 1037-49; discussion 1049-51.

59. Hoekstra, L.T., et al., *Enhanced tumor growth after portal vein embolization in a rabbit tumor model*. J Surg Res, 2013. **180**(1): p. 89-96.
60. Xing, M., et al., *Locoregional therapies for metastatic colorectal carcinoma to the liver--an evidence-based review*. J Surg Oncol, 2014. **110**(2): p. 182-96.
61. Rhee, T.K., et al., *Effect of transcatheter arterial embolization on levels of hypoxia-inducible factor-1alpha in rabbit VX2 liver tumors*. J Vasc Interv Radiol, 2007. **18**(5): p. 639-45.
62. Virmani, S., et al., *Comparison of hypoxia-inducible factor-1alpha expression before and after transcatheter arterial embolization in rabbit VX2 liver tumors*. J Vasc Interv Radiol, 2008. **19**(10): p. 1483-9.
63. Guo, W.J., et al., *Transient increased expression of VEGF and MMP-1 in a rat liver tumor model after hepatic arterial occlusion*. Hepatogastroenterology, 2004. **51**(56): p. 381-6.
64. Wang, G.Z., et al., *Increased metastatic potential of residual carcinoma after transarterial embolization in rat with McA-RH7777 hepatoma*. Oncol Rep, 2014. **31**(1): p. 95-102.
65. Coffey, J.C., et al., *Excisional surgery for cancer cure: therapy at a cost*. Lancet Oncol, 2003. **4**(12): p. 760-8.
66. van der Bij, G.J., et al., *The perioperative period is an underutilized window of therapeutic opportunity in patients with colorectal cancer*. Ann Surg, 2009. **249**(5): p. 727-34.
67. Demicheli, R., et al., *The effects of surgery on tumor growth: a century of investigations*. Ann Oncol, 2008. **19**(11): p. 1821-8.
68. Manfredi, S., et al., *Incidence and patterns of recurrence after resection for cure of colonic cancer in a well defined population*. Br J Surg, 2006. **93**(9): p. 1115-22.
69. Tilly, C., et al., *R1 rectal resection: look up and don't look down*. Ann Surg, 2014. **260**(5): p. 794-9; discussion 799-800.
70. Kobayashi, H., et al., *Characteristics of recurrence after curative resection for T1 colorectal cancer: Japanese multicenter study*. J Gastroenterol, 2011. **46**(2): p. 203-11.
71. M, A., et al., *The Cause and Prevention of Anastomotic Recurrence following Colectomy: An Immunohistochemical Approach for Detecting Transforming Colonocytes*. J Cancer, 2014. **5**(9): p. 784-9.
72. Mirnezami, A., et al., *Increased local recurrence and reduced survival from colorectal cancer following anastomotic leak: systematic review and meta-analysis*. Ann Surg, 2011. **253**(5): p. 890-9.
73. Lacy, A.M., et al., *Laparoscopy-assisted colectomy versus open colectomy for treatment of non-metastatic colon cancer: a randomised trial*. Lancet, 2002. **359**(9325): p. 2224-9.
74. Evrard, S., S. Mathoulin-Pelissier, and A. Kramar, *Open versus laparoscopy-assisted colectomy*. Lancet, 2003. **361**(9351): p. 73; author reply 75-6.
75. Ceulemans, R., et al., *Open versus laparoscopy assisted colectomy*. Lancet, 2003. **361**(9351): p. 73-4; author reply 75-6.
76. Lehnert, T., et al., *Open versus laparoscopy assisted colectomy*. Lancet, 2003. **361**(9351): p. 74; author reply 75-6.
77. Fiddian-Green, R.G., *Open versus laparoscopy assisted colectomy*. Lancet, 2003. **361**(9351): p. 74; author reply 75-6.
78. Bonjer, H.J., et al., *A randomized trial of laparoscopic versus open surgery for rectal cancer*. N Engl J Med, 2015. **372**(14): p. 1324-32.

79. Nelson, H., et al., *A comparison of laparoscopically assisted and open colectomy for colon cancer*. N Engl J Med, 2004. **350**(20): p. 2050-9.
80. Lacy, A.M., et al., *The long-term results of a randomized clinical trial of laparoscopy-assisted versus open surgery for colon cancer*. Ann Surg, 2008. **248**(1): p. 1-7.
81. Foss, O.P., et al., *Invasion of tumor cells into the bloodstream caused by palpation or biopsy of the tumor*. Surgery, 1966. **59**(5): p. 691-5.
82. Yamaguchi, K., et al., *Significant detection of circulating cancer cells in the blood by reverse transcriptase-polymerase chain reaction during colorectal cancer resection*. Ann Surg, 2000. **232**(1): p. 58-65.
83. Papavasiliou, P., et al., *Circulating tumor cells in patients undergoing surgery for hepatic metastases from colorectal cancer*. Proc (Bayl Univ Med Cent), 2010. **23**(1): p. 11-4.
84. Lindemann, F., et al., *Prognostic significance of micrometastatic tumour cells in bone marrow of colorectal cancer patients*. Lancet, 1992. **340**(8821): p. 685-9.
85. Schott, A., et al., *Isolated tumor cells are frequently detectable in the peritoneal cavity of gastric and colorectal cancer patients and serve as a new prognostic marker*. Ann Surg, 1998. **227**(3): p. 372-9.
86. Groot Koerkamp, B., et al., *Circulating tumor cells and prognosis of patients with resectable colorectal liver metastases or widespread metastatic colorectal cancer: a meta-analysis*. Ann Surg Oncol, 2013. **20**(7): p. 2156-65.
87. Rahbari, N.N., et al., *Meta-analysis shows that detection of circulating tumor cells indicates poor prognosis in patients with colorectal cancer*. Gastroenterology, 2010. **138**(5): p. 1714-26.
88. Iinuma, H., et al., *Clinical significance of circulating tumor cells, including cancer stem-like cells, in peripheral blood for recurrence and prognosis in patients with Dukes' stage B and C colorectal cancer*. J Clin Oncol, 2011. **29**(12): p. 1547-55.
89. Chang, J. and J. Erler, *Hypoxia-mediated metastasis*. Adv Exp Med Biol, 2014. **772**: p. 55-81.
90. Qing, G. and M.C. Simon, *Hypoxia inducible factor-2alpha: a critical mediator of aggressive tumor phenotypes*. Curr Opin Genet Dev, 2009. **19**(1): p. 60-6.
91. Semenza, G.L., *Defining the role of hypoxia-inducible factor 1 in cancer biology and therapeutics*. Oncogene, 2010. **29**(5): p. 625-34.
92. Shimomura, M., et al., *Overexpression of hypoxia inducible factor-1 alpha is an independent risk factor for recurrence after curative resection of colorectal liver metastases*. Ann Surg Oncol, 2013. **20 Suppl 3**: p. S527-36.
93. Warfel, N.A. and W.S. El-Deiry, *HIF-1 signaling in drug resistance to chemotherapy*. Curr Med Chem, 2014. **21**(26): p. 3021-8.
94. Sint Nicolaas, J., et al., *Risk of colorectal carcinoma in post-liver transplant patients: a systematic review and meta-analysis*. Am J Transplant, 2010. **10**(4): p. 868-76.
95. Sato, T., et al., *Objective criteria for the grading of venous invasion in colorectal cancer*. Am J Surg Pathol, 2010. **34**(4): p. 454-62.
96. Watanabe, T., et al., *Japanese Society for Cancer of the Colon and Rectum (JSCCR) guidelines 2010 for the treatment of colorectal cancer*. Int J Clin Oncol, 2012. **17**(1): p. 1-29.

97. Kazama, S., et al., *Six cases of primary colorectal cancer after living-donor liver transplantation: a single-institution experience in Japan.* Jpn J Clin Oncol, 2012. **42**(7): p. 586-90.
98. Espi, A., et al., *Relationship of curative surgery on natural killer cell activity in colorectal cancer.* Dis Colon Rectum, 1996. **39**(4): p. 429-34.
99. Tartter, P.I., et al., *The prognostic significance of natural killer cytotoxicity in patients with colorectal cancer.* Arch Surg, 1987. **122**(11): p. 1264-8.
100. Galon, J., et al., *Type, density, and location of immune cells within human colorectal tumors predict clinical outcome.* Science, 2006. **313**(5795): p. 1960-4.
101. Pages, F., et al., *Effector memory T cells, early metastasis, and survival in colorectal cancer.* N Engl J Med, 2005. **353**(25): p. 2654-66.
102. Maker, A.V., et al., *Genetic evidence that intratumoral T-cell proliferation and activation are associated with recurrence and survival in patients with resected colorectal liver metastases.* Cancer Immunol Res, 2015. **3**(4): p. 380-8.
103. Pugh, S.A., et al., *T cells but not NK cells are associated with a favourable outcome for resected colorectal liver metastases.* BMC Cancer, 2014. **14**: p. 180.
104. Wichmann, M.W., et al., *Fast-track rehabilitation in elective colorectal surgery patients: a prospective clinical and immunological single-centre study.* ANZ J Surg, 2007. **77**(7): p. 502-7.
105. Leaver, H.A., et al., *Lymphocyte responses following open and minimally invasive thoracic surgery.* Eur J Clin Invest, 2000. **30**(3): p. 230-8.
106. Griffith, J.P., et al., *Influence of laparoscopic and conventional cholecystectomy upon cell-mediated immunity.* Br J Surg, 1995. **82**(5): p. 677-80.
107. Belizon, A., et al., *Major abdominal surgery increases plasma levels of vascular endothelial growth factor: open more so than minimally invasive methods.* Ann Surg, 2006. **244**(5): p. 792-8.
108. Peeters, C.F., et al., *Metastatic dormancy imposed by the primary tumor: does it exist in humans?* Ann Surg Oncol, 2008. **15**(11): p. 3308-15.
109. Hurwitz, H., et al., *Bevacizumab plus irinotecan, fluorouracil, and leucovorin for metastatic colorectal cancer.* N Engl J Med, 2004. **350**(23): p. 2335-42.
110. Kabbinavar, F.F., et al., *Combined analysis of efficacy: the addition of bevacizumab to fluorouracil/leucovorin improves survival for patients with metastatic colorectal cancer.* J Clin Oncol, 2005. **23**(16): p. 3706-12.
111. Saltz, L.B., et al., *Bevacizumab in combination with oxaliplatin-based chemotherapy as first-line therapy in metastatic colorectal cancer: a randomized phase III study.* J Clin Oncol, 2008. **26**(12): p. 2013-9.
112. Chiringhelli, F., et al., *Bevacizumab efficacy in metastatic colorectal cancer is dependent on primary tumor resection.* Ann Surg Oncol, 2014. **21**(5): p. 1632-40.
113. Price, T.J., et al., *Current opinion on optimal treatment for colorectal cancer.* Expert Rev Anticancer Ther, 2013. **13**(5): p. 597-611.

114. Snoeren, N., et al., *A randomized two arm phase III study in patients post radical resection of liver metastases of colorectal cancer to investigate bevacizumab in combination with capecitabine plus oxaliplatin (CAPOX) vs CAPOX alone as adjuvant treatment.* BMC Cancer, 2010. **10**: p. 545.
115. Meng, S., et al., *Circulating tumor cells in patients with breast cancer dormancy.* Clin Cancer Res, 2004. **10**(24): p. 8152-62.
116. Nielsen, M., et al., *Breast cancer and atypia among young and middle-aged women: a study of 110 medicolegal autopsies.* Br J Cancer, 1987. **56**(6): p. 814-9.
117. Harach, H.R., K.O. Franssila, and V.M. Wasenius, *Occult papillary carcinoma of the thyroid. A "normal" finding in Finland. A systematic autopsy study.* Cancer, 1985. **56**(3): p. 531-8.
118. Sanchez-Chapado, M., et al., *Prevalence of prostate cancer and prostatic intraepithelial neoplasia in Caucasian Mediterranean males: an autopsy study.* Prostate, 2003. **54**(3): p. 238-47.
119. Sasturkar, S.V., et al., *Serial changes of cytokines and growth factors in peripheral circulation after right lobe donor hepatectomy.* Liver Transpl, 2016. **22**(3): p. 344-51.
120. Osada, S., et al., *Effect of hepatocyte growth factor on progression of liver metastasis in colorectal cancer.* Hepatogastroenterology, 2010. **57**(97): p. 76-80.
121. Tsushima, H., et al., *Circulating transforming growth factor beta 1 as a predictor of liver metastasis after resection in colorectal cancer.* Clin Cancer Res, 2001. **7**(5): p. 1258-62.
122. Christophi, C., N. Harun, and T. Fifis, *Liver regeneration and tumor stimulation--a review of cytokine and angiogenic factors.* J Gastrointest Surg, 2008. **12**(5): p. 966-80.
123. Narita, M., et al., *Two-stage hepatectomy for multiple bilobar colorectal liver metastases.* Br J Surg, 2011. **98**(10): p. 1463-75.
124. Wicherts, D.A., et al., *Long-term results of two-stage hepatectomy for irresectable colorectal cancer liver metastases.* Ann Surg, 2008. **248**(6): p. 994-1005.
125. Tanaka, K., et al., *Two-stage hepatectomy with effective perioperative chemotherapy does not induce tumor growth or growth factor expression in liver metastases from colorectal cancer.* Surgery, 2013. **153**(2): p. 179-88.
126. Mentha, G., et al., *'Liver first' approach in the treatment of colorectal cancer with synchronous liver metastases.* Dig Surg, 2008. **25**(6): p. 430-5.
127. Verhoef, C., et al., *The "liver-first approach" for patients with locally advanced rectal cancer and synchronous liver metastases.* Dis Colon Rectum, 2009. **52**(1): p. 23-30.
128. O'Neill, B.D., et al., *Non-operative treatment after neoadjuvant chemoradiotherapy for rectal cancer.* Lancet Oncol, 2007. **8**(7): p. 625-33.
129. Lykoudis, P.M., et al., *Systematic review of surgical management of synchronous colorectal liver metastases.* Br J Surg, 2014. **101**(6): p. 605-12.
130. Wong, S.L., et al., *American Society of Clinical Oncology 2009 clinical evidence review on radiofrequency ablation of hepatic metastases from colorectal cancer.* J Clin Oncol, 2010. **28**(3): p. 493-508.
131. Mulier, S., et al., *Local recurrence after hepatic radiofrequency coagulation: multivariate meta-analysis and review of contributing factors.* Ann Surg, 2005. **242**(2): p. 158-71.

132. Imamura, Y., et al., [*Two cases of hepatocellular carcinoma showing rapid progression after radio-frequency ablation therapy*]. *Nihon Shokakibyō Gakkai Zasshi*, 2002. **99**(1): p. 40-4.
133. Portolani, N., et al., *Aggressive recurrence after radiofrequency ablation of liver neoplasms*. *Hepatology*, 2003. **50**(54): p. 2179-84.
134. Seki, T., et al., *Rapid progression of hepatocellular carcinoma after transcatheter arterial chemoembolization and percutaneous radiofrequency ablation in the primary tumour region*. *Eur J Gastroenterol Hepatol*, 2001. **13**(3): p. 291-4.
135. Pringle, J.H., V. *Notes on the Arrest of Hepatic Hemorrhage Due to Trauma*. *Ann Surg*, 1908. **48**(4): p. 541-9.
136. van Duijnhoven, F.H., et al., *Factors influencing the local failure rate of radiofrequency ablation of colorectal liver metastases*. *Ann Surg Oncol*, 2006. **13**(5): p. 651-8.
137. Nijkamp, M.W., et al., *Prolonged portal triad clamping during liver surgery for colorectal liver metastases is associated with decreased time to hepatic tumour recurrence*. *Eur J Surg Oncol*, 2010. **36**(2): p. 182-8.
138. Giuliani, F., et al., *Does hepatic pedicle clamping affect disease-free survival following liver resection for colorectal metastases?* *Ann Surg*, 2010. **252**(6): p. 1020-6.
139. Matsuda, A., et al., *Hepatic pedicle clamping does not worsen survival after hepatic resection for colorectal liver metastasis: results from a systematic review and meta-analysis*. *Ann Surg Oncol*, 2013. **20**(12): p. 3771-8.
140. Weiss, M.J., et al., *Hepatic pedicle clamping during hepatic resection for colorectal liver metastases: no impact on survival or hepatic recurrence*. *Ann Surg Oncol*, 2013. **20**(1): p. 285-94.
141. Torzilli, G., et al., *Safety of intermittent Pringle maneuver cumulative time exceeding 120 minutes in liver resection: a further step in favor of the "radical but conservative" policy*. *Ann Surg*, 2012. **255**(2): p. 270-80.
142. Barbaro, B., et al., *Preoperative right portal vein embolization in patients with metastatic liver disease. Metastatic liver volumes after RPVE*. *Acta Radiol*, 2003. **44**(1): p. 98-102.
143. Kokudo, N., et al., *Proliferative activity of intrahepatic colorectal metastases after preoperative hemihepatic portal vein embolization*. *Hepatology*, 2001. **34**(2): p. 267-72.
144. Pamecha, V., et al., *Effect of portal vein embolisation on the growth rate of colorectal liver metastases*. *Br J Cancer*, 2009. **100**(4): p. 617-22.
145. Simoneau, E., et al., *Portal vein embolization stimulates tumour growth in patients with colorectal cancer liver metastases*. *HPB (Oxford)*, 2012. **14**(7): p. 461-8.
146. Hoekstra, L.T., et al., *Tumor progression after preoperative portal vein embolization*. *Ann Surg*, 2012. **256**(5): p. 812-7; discussion 817-8.
147. de Graaf, W., et al., *Induction of tumor growth after preoperative portal vein embolization: is it a real problem?* *Ann Surg Oncol*, 2009. **16**(2): p. 423-30.
148. Ardito, F., et al., *Right and extended-right hepatectomies for unilobar colorectal metastases: impact of portal vein embolization on long-term outcome and liver recurrence*. *Surgery*, 2013. **153**(6): p. 801-10.

149. Kubota, K., et al., *Growth rate of primary single hepatocellular carcinoma: determining optimal screening interval with contrast enhanced computed tomography*. Dig Dis Sci, 2003. **48**(3): p. 581-6.
150. Tezuka, M., et al., *Growth rate of locally recurrent hepatocellular carcinoma after transcatheter arterial chemoembolization: comparing the growth rate of locally recurrent tumor with that of primary hepatocellular carcinoma*. Dig Dis Sci, 2007. **52**(3): p. 783-8.
151. Fischer, C., et al., *Chemotherapy after portal vein embolization to protect against tumor growth during liver hypertrophy before hepatectomy*. JAMA Surg, 2013. **148**(12): p. 1103-8.
152. Ranieri, G., et al., *Vascular endothelial growth factor and tryptase changes after chemoembolization in hepatocarcinoma patients*. World J Gastroenterol, 2015. **21**(19): p. 6018-25.
153. Sergio, A., et al., *Transcatheter arterial chemoembolization (TACE) in hepatocellular carcinoma (HCC): the role of angiogenesis and invasiveness*. Am J Gastroenterol, 2008. **103**(4): p. 914-21.
154. Xu, W., et al., *Influence of preoperative transcatheter arterial chemoembolization on gene expression in the HIF-1alpha pathway in patients with hepatocellular carcinoma*. J Cancer Res Clin Oncol, 2014. **140**(9): p. 1507-15.
155. Zhou, W.P., et al., *A prospective, randomized, controlled trial of preoperative transarterial chemoembolization for resectable large hepatocellular carcinoma*. Ann Surg, 2009. **249**(2): p. 195-202.
156. Francia, G. and R.S. Kerbel, *Raising the bar for cancer therapy models*. Nat Biotechnol, 2010. **28**(6): p. 561-2.
157. Begley, C.G. and L.M. Ellis, *Drug development: Raise standards for preclinical cancer research*. Nature, 2012. **483**(7391): p. 531-3.
158. Prinz, F., T. Schlange, and K. Asadullah, *Believe it or not: how much can we rely on published data on potential drug targets?* Nat Rev Drug Discov, 2011. **10**(9): p. 712.
159. Arrowsmith, J., *Trial watch: Phase II failures: 2008-2010*. Nat Rev Drug Discov, 2011. **10**(5): p. 328-9.
160. Tuveson, D. and D. Hanahan, *Translational medicine: Cancer lessons from mice to humans*. Nature, 2011. **471**(7338): p. 316-7.
161. Fleming, I.N., et al., *Imaging tumour hypoxia with positron emission tomography*. Br J Cancer, 2015. **112**(2): p. 238-50.
162. Walsh, J.C., et al., *The clinical importance of assessing tumor hypoxia: relationship of tumor hypoxia to prognosis and therapeutic opportunities*. Antioxid Redox Signal, 2014. **21**(10): p. 1516-54.
163. Horsman, M.R., et al., *Imaging hypoxia to improve radiotherapy outcome*. Nat Rev Clin Oncol, 2012. **9**(12): p. 674-87.
164. Garcia-Figueiras, R., et al., *Imaging of Tumor Angiogenesis for Radiologists--Part 1: Biological and Technical Basis*. Curr Probl Diagn Radiol, 2015. **44**(5): p. 407-24.
165. Kienast, Y., et al., *Real-time imaging reveals the single steps of brain metastasis formation*. Nat Med, 2010. **16**(1): p. 116-22.
166. Rashidian, M., et al., *Noninvasive imaging of immune responses*. Proc Natl Acad Sci U S A, 2015. **112**(19): p. 6146-51.

167. van der Vorst, J.R., et al., *Near-infrared fluorescence-guided resection of colorectal liver metastases*. *Cancer*, 2013. **119**(18): p. 3411-8.
168. Oliveira, S., et al., *Rapid visualization of human tumor xenografts through optical imaging with a near-infrared fluorescent anti-epidermal growth factor receptor nanobody*. *Mol Imaging*, 2012. **11**(1): p. 33-46.
169. Lewandowski, R.J., et al., (90) *Y radiation lobectomy: Outcomes following surgical resection in patients with hepatic tumors and small future liver remnant volumes*. *J Surg Oncol*, 2016. **114**(1): p. 99-105.
170. Goldberg, S.N., et al., *Treatment of intrahepatic malignancy with radiofrequency ablation: radiologic-pathologic correlation*. *Cancer*, 2000. **88**(11): p. 2452-63.
171. Scudamore, C.H., et al., *Radiofrequency ablation followed by resection of malignant liver tumors*. *Am J Surg*, 1999. **177**(5): p. 411-7.
172. Hoogstraat, M., et al., *Detailed imaging and genetic analysis reveal a secondary BRAF(L505H) resistance mutation and extensive intrapatient heterogeneity in metastatic BRAF mutant melanoma patients treated with vemurafenib*. *Pigment Cell Melanoma Res*, 2015. **28**(3): p. 318-23.
173. Dillner, J. and K. Andersson, *Biobanks collected for routine healthcare purposes: build-up and use for epidemiologic research*. *Methods Mol Biol*, 2011. **675**: p. 113-25.
174. Kawamata, H., et al., *Discrepancies between the K-ras mutational status of primary colorectal cancers and corresponding liver metastases are found in codon 13*. *Genomics*, 2015. **106**(2): p. 71-5.
175. Sato, T., et al., *Single Lgr5 stem cells build crypt-villus structures in vitro without a mesenchymal niche*. *Nature*, 2009. **459**(7244): p. 262-5.
176. Boj, S.F., et al., *Organoid models of human and mouse ductal pancreatic cancer*. *Cell*, 2015. **160**(1-2): p. 324-38.
177. Emmink, B.L., et al., *Differentiated human colorectal cancer cells protect tumor-initiating cells from irinotecan*. *Gastroenterology*, 2011. **141**(1): p. 269-78.
178. Sato, T., et al., *Long-term expansion of epithelial organoids from human colon, adenoma, adenocarcinoma, and Barrett's epithelium*. *Gastroenterology*, 2011. **141**(5): p. 1762-72.
179. Sato, T. and H. Clevers, *SnapShot: Growing Organoids from Stem Cells*. *Cell*, 2015. **161**(7): p. 1700-1700.e1.
180. Huh, D., G.A. Hamilton, and D.E. Ingber, *From 3D cell culture to organs-on-chips*. *Trends Cell Biol*, 2011. **21**(12): p. 745-54.
181. Skardal, A., et al., *A reductionist metastasis-on-a-chip platform for in vitro tumor progression modeling and drug screening*. *Biotechnol Bioeng*, 2016. **113**(9): p. 2020-32.
182. Bhatia, S.N. and D.E. Ingber, *Microfluidic organs-on-chips*. *Nat Biotechnol*, 2014. **32**(8): p. 760-72.
183. Esch, E.W., A. Bahinski, and D. Huh, *Organs-on-chips at the frontiers of drug discovery*. *Nat Rev Drug Discov*, 2015. **14**(4): p. 248-60.



CHAPTER 3

Downregulation of DNA repair proteins and increased DNA damage in hypoxic Aldefluor^{bright} colon cancer cells is a therapeutically exploitable vulnerability

J.M.J. Jongen
L.M. van der Waals
K. Trumpi
J. Laoukili
N.A. Peters
S.J. Schenningen-van Schelven
K.M. Govaert
I.H.M. Borel Rinkes
O. Kranenburg

Abstract

Surgical removal of colorectal liver metastases generates areas of tissue hypoxia, which imposes a stem-like (Aldefluor^{bright}) phenotype on residual tumor cells and promotes tumor recurrence. Gene expression signatures reflecting both a stem-like phenotype and hypoxia as distinguishing features of the most aggressive primary colon cancer subtype (Consensus Molecular Subtype 4, CMS4). We hypothesize that surgery-induced hypoxic Aldefluor^{bright} cells are sensitive to hypoxia-targeted treatment and thereby limit recurrence following resection of primary tumors or metastases.

We demonstrated strongly suppressed DNA-repair mechanisms in CMS4 in addition to being inversely correlated with hypoxia. We next showed increased DNA damage and downregulation of key DNA-repair proteins RAD51, KU70 and RIF1 in human hypoxic primary colon tumors and metastases, with surgery treated livers of tumor-bearing mice as well as in *in vitro* hypoxia exposure of patient derived colonospheres. Hypoxia-induced DNA damage could be prevented by upregulating the ROS-neutralizing enzyme glutathione peroxidase 2 (GPx2), indicating that ROS is essential for hypoxia-induced DNA damage. Strikingly, the hypoxia-activated prodrug Tirapazamine reduced the Aldefluor^{bright} fraction, which was accompanied by downregulation of DNA repair protein expression.

We conclude that Aldefluor^{bright}-enriched hypoxic colon cancer tissue possesses decreased expression of DNA repair proteins and increased DNA damage and may be therapeutically exploited with hypoxia-activated prodrugs.

Keywords

DNA repair, Colon cancer, DNA damage, Tirapazamine, Cancer stem cells

Introduction

Colorectal cancer (CRC) is the third most common cancer worldwide and a major cause of cancer-related mortality [1]. The prognosis of patients with CRC is mostly determined by the presence of distant metastases. After distant spread – predominantly to the liver – 5-year survival drops to ~20% and the only curative treatment option is radical resection of the primary tumor and metastases. However, recurrence after liver surgery is seen in more than half of the patients [2].

Currently, treatment strategies that can limit disease recurrence following primary tumor resection or partial liver resection are not effective enough. The development of such strategies should be based on an understanding of the pathways that drive metastasis and recurrence. Gene-based tumor classification has recently identified 4 distinct molecular subtypes, reflecting differences in the activity of signaling pathways, tumor behavior and clinical outcome. Where Consensus Molecular Subtype 1 (CMS1) is known as the microsatellite instability immune related CRC type, CMS2 the canonical and epithelial subtype with marked WNT and MYC signaling activation and CMS3 as the metabolic and epithelial subtype with evident metabolic dysregulation, CMS4 is identified with highest propensity to form metastases. CMS4 is characterized by atypical expression of gene signatures reflecting a mesenchymal and a stem cell-like phenotype [3]. In addition, we have recently shown that mesenchymal-type primary colon tumors express high levels of hypoxia-related genes [4]. This is in line with the observation that CMS4 is characterized by expression of angiogenesis-stimulating genes [3]. Hypoxia is also a driving force behind tumor recurrence following liver surgery: hypoxic tissue areas in the remnant liver form a niche for stem-like tumor cells that can subsequently drive recurrence [5, 6]. In general, hypoxia is associated with more aggressive tumor phenotypes across different types of cancer (clear cell renal carcinoma, non-small cell lung carcinoma, neuroblastoma) [7].

We hypothesized that hypoxia-targeting strategies may have value in limiting disease recurrence. Insight into the mechanisms that underlie hypoxia-stimulated tumor growth and/or the identification of vulnerabilities in hypoxic cancer cells is key to the development of such strategies. One of the consequences of hypoxia in multiple cancer types, including colon cancer, is an increased proportion of cancer stem cells (CSCs). These CSCs have a high regenerative and tumorigenic potential and are generally resistant to standard chemotherapy [8-13], amongst others due to drug efflux pumps expressed on the surrounding differentiated tumor cells [14]. Since there is a lack of consensus on the topic how to identify CSCs, we decided upon referring to the cell population with clonogenic and tumorigenic potential as the Aldefluor^{bright} population. We, and others, have previously shown that the cell population high in aldehyde dehydrogenase 1 (ALDH1) activity display in vitro features of CSCs including clonogenic and tumorigenic potential [14-16]. Interestingly, hypoxia suppresses DNA repair pathways [17-21] which contributes to genomic instability [18, 21, 22]. However, impaired DNA repair capacity



could also lead to an increased vulnerability to DNA-damaging agents. One way to target hypoxic tumor tissue, enriched in Aldefluor^{bright} cells, is through the use of hypoxia-activated prodrugs (HAPs) such as the topoisomerase-II inhibitor Tirapazamine (TPZ) [23].

Here, we have assessed the effect of hypoxia on DNA damage and DNA repair pathways in human colon cancer cells by using three-dimensional patient-derived cell cultures. We show that increased DNA damage in hypoxia is dependent on high ROS levels. Hypoxia reduces expression of various DNA repair proteins, which precedes tumor cell apoptosis. Targeting hypoxic cancer cells with TPZ further reduced DNA repair protein expression in Aldefluor^{bright} cells, and reduced Aldefluor^{bright} content. We conclude that reduced repair capacity in a subset of human colorectal cancers and in post-treatment tumor tissue provides a clear opportunity for therapeutic intervention with the hypoxia-activated topoisomerase inhibitor TPZ.

Results

Hypoxia and DNA repair in CMS4 colorectal tumors

We have previously shown that expression of a gene signature comprising the genes most significantly co-expressed with hypoxia-inducible factor 2 (HIF2 α) was strongly enriched in aggressive mesenchymal-type tumors [4], now commonly referred to as CMS4. In addition, tumor hypoxia has previously been related to reduced DNA repair activity [17-19, 22]. Therefore, we studied expression of gene sets involved in specific DNA repair pathways (KEGG pathways; www.genome.jp/kegg/) and the HIF2 α signature in relation to the CMSs. The studied genes are based on magnitude of correlation (Supplementary Table 1), use in literature and commercially available antibodies for further analyses. Strikingly, all DNA repair pathways were down-regulated in CMS4 tumors (Figure 1a) and were negatively correlated with the HIF2 α signature (Figure 1b). Many chemotherapeutic drugs cause double strand breaks, which are repaired through homologous recombination (HR) and/or non-homologous end-joining (NHEJ). We found that colon tumors with high expression of the HIF2 α signature, generally had low expression of HR pathway genes (RAD51, BRCA1), and NHEJ pathway genes (RIF1, KU70) (Figure 1c and d). Moreover, tumor classification based on the median expression of any of these DNA repair genes and the HIF2 α signature revealed that the HIF2 α -high/DNA-repair-low tumors were strongly enriched in CMS4 (Figure 1c and d, Supplementary Figure 1, and Supplementary Table 2). Taken together, these data show that tumors with a high expression of a HIF2 α signature are mostly CMS4 tumors and characterized by low expression of DNA repair genes.

Tumors with a high hypoxia signature and low expression of DNA repair genes have a poor prognosis.

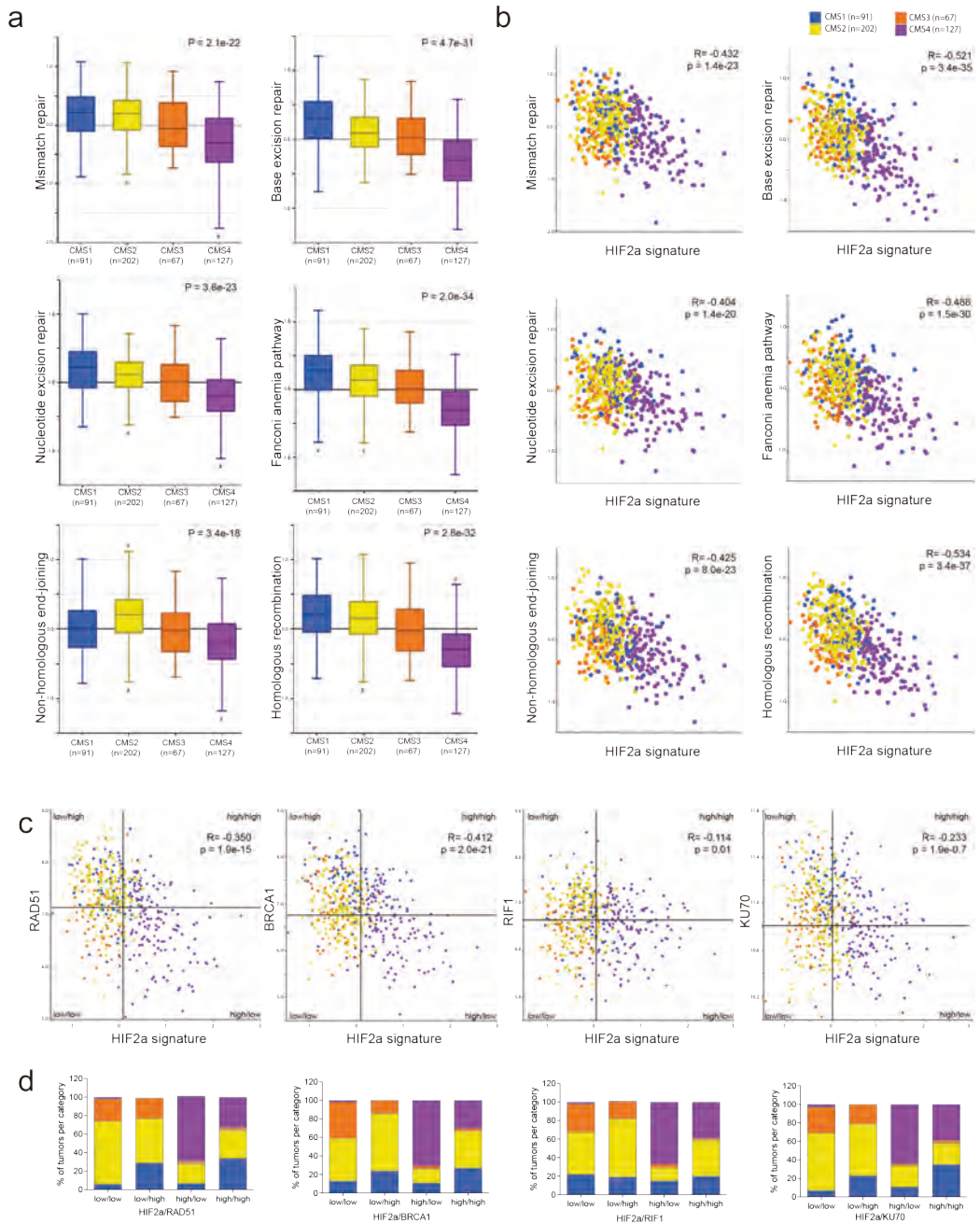
Next, we wanted to show the clinical relevance of focusing on this selected group of tumors with a high expression of HIF2 α and a low expression of DNA repair genes. Therefore, survival was compared between the different populations. Although survival in the HIF2 α -high/repair-high tumors are, in all 4 cases, better than in the HIF2 α -high/repair-low subgroups, the population 'HIF2 α high/ DNA repair proteins low' appeared to have worst survival (Figure 2a-d). In case all 4 repair proteins were low in expression level, prognosis was very poor compared to the group with high expression of all 4 repair proteins (Figure 2e). Interestingly, 2-year DFS for 'HIF2 α low / DNA repair protein high' is 94%, while the population 'HIF2 α high / DNA repair protein low' has 50% DFS at 2-years after diagnosis (Figure 2e). In conclusion, tumors with a high hypoxia signature and low DNA repair protein expression have worst prognosis.

Hypoxic tumor tissue is characterized by DNA damage and low expression of the DNA repair proteins RAD51 and RIF1.

The data so far show an inverse correlation between HIF2 α and DNA repair gene expression. This indicates that hypoxic tumor areas may have low repair capacity and therefore are prone to DNA damage. To study this further, we stained tissue sections of human colon tumors for the hypoxia markers CAIX and HIF1 α and for the DNA damage marker phosphorylated histone γ H2AX. Peri-necrotic areas in human primary colorectal tumors and liver metastases showed strong HIF1 α and CAIX staining, reflecting the hypoxic nature of this tissue. γ H2AX was also highly expressed in peri-necrotic tissue, indicating increased DNA damage in these areas (Figure 3a-e). To assess a potential causal relationship between surgery-induced hypoxia and DNA damage, we experimentally induced hypoxia in mice with pre-established liver metastases through vascular clamping as described previously [24]. Clamping caused an increase of necrotic tumor tissue, as we have shown before [5, 25, 26]. As expected, the peri-necrotic areas were characterized by strong CAIX staining. Again, γ H2AX staining was also high in peri-necrotic hypoxic tumor tissue (Figure 3f). Within the clamped liver, we saw that peri-necrotic (hypoxic) areas were accompanied by a clear downregulation of the DNA repair proteins RAD51 and RIF1, while expression of KU70 was similar in hypoxic and normoxic areas (Figure 3g). These results show that both spontaneous and surgery-induced intra-tumor hypoxia suppresses expression of DNA repair proteins, which may contribute to increased DNA damage.

Hypoxia induces DNA damage and suppresses expression of DNA repair proteins in patient-derived colonospheres

The correlation between hypoxia and DNA damage observed in human cancer and *in vivo* experiments could be due to a direct effect of hypoxia on the tumor cells. To test this, we exposed 2 independent patient-derived colonospheres to hypoxia for 24 hours and analyzed γ H2AX staining by immunofluorescence (Figure 4a and b), Comet assay (Figure 4c and d) and FACS analysis (Figure 4e).



Expression values of all genes comprising specific DNA repair pathways (www.KEGG.jp) were condensed into a single 'meta-gene' expression value by using the R2 platform (<http://r2.amc.nl>). (a) The box-and-whisker plots show the meta-gene expression values of 6 DNA repair pathways in relation to the 4 CMS groups (CMS1-4)[3] in the CIT dataset with CMS annotation (n=487; GSE39582). (b) The scatterplots show the association between the expression values of the 6 DNA repair pathway meta-genes and the expression of the HIF2 α signature [4] in relation to the CMS. Blue: CMS1; Yellow: CMS2; Orange: CMS3; Purple: CMS4. (c) Median expression values of 4 DNA repair genes and the HIF2 α signature were used to generate quadrants (tumor subgroups). In all cases the HIF2 α -high/DNA repair gene-low quadrants turn out to be mostly CMS4. (d) Bar graphs showing the tumor subtype distribution per quadrant.

All analyses showed that hypoxia causes a marked increase in γ H2AX in both colonosphere cultures. Apoptotic cells can acquire a strong secondary γ H2AX signal resulting from the activation of caspase-activated DNase (CAD) and the resulting DNA cleavage. To test whether hypoxia-induced DNA damage in human colonospheres was secondary to caspase activation we analyzed HIF stabilization, γ H2AX accumulation, DNA repair protein expression, autophagy and caspase cleavage over time. We show that co-expression signatures with HIF1 α and HIF2 α have a very strong and highly significant correlation and that both are stabilized in hypoxic conditions (Supplementary Figure 2 and 3). Hypoxia induced a rapid and strong induction of HIF1 α which was accompanied by an equally rapid accumulation of γ H2AX (Figure 3f). The induction of DNA damage was accompanied by simultaneous suppression of the DNA repair proteins RAD51, RIF1 and 53BP1 and, to a lesser extent, KU70. Importantly, during the time frame of the experiment hypoxia did increase autophagy but did not affect caspase cleavage. The latter result shows that hypoxia-induced suppression of DNA repair proteins and increased DNA damage are not secondary to caspase activation and apoptosis.

Overexpression of glutathione peroxidase-2 inhibits hypoxia-induced DNA damage and apoptosis
Hypoxia leads to the generation of reactive oxygen species (ROS), which could contribute to DNA damage [27, 28]. To study the contribution of ROS generation to hypoxia-induced DNA damage we used colonospheres overexpressing glutathione peroxidase 2 (GPx2) [29]. GPx2 uses glutathione to neutralize peroxides and is one of the most powerful intracellular anti-oxidant enzymes. Overexpression of GPx2 reduces cellular H₂O₂ levels and protects cells against oxidative stress induced by chemotherapy, single cell making, or exogenous H₂O₂ [30]. We found that prolonged exposure to hypoxia (72 hours) reduced proliferation and increased caspase cleavage and cell death, presumably resulting from chronic DNA damage (Figure 5a). Hypoxia-induced effects on proliferation, caspase processing and cell death hardly occur in a cell line overexpressing GPx2. This indicates that the hypoxia mediated changes are at least in part due to generation of ROS (Figure 5b-d). To further study hypoxia-induced oxidative damage we analyzed incorporation of the oxidized nucleotide 8-oxo-dG into DNA and accumulation of the oxidized lipid 4-hydroxy-nonenal (4-HNE). I

Immunohistochemistry analysis of 4-HNE on paraffin-embedded colonospheres showed an increased level of lipid peroxidation in colonospheres that had been exposed to hypoxia (Figure 5e). Likewise, immunofluorescence analysis of live FACS-sorted cells showed an accumulation of 8-oxo-dG in hypoxia-exposed colonospheres (Figure 5f). Accumulation is seen in both the nucleotide precursor pool and to a smaller extent in the nucleus [31]. Together the data show that prolonged hypoxia results in reduced proliferation and increased cell death which is accompanied by oxidative DNA and lipid damage.

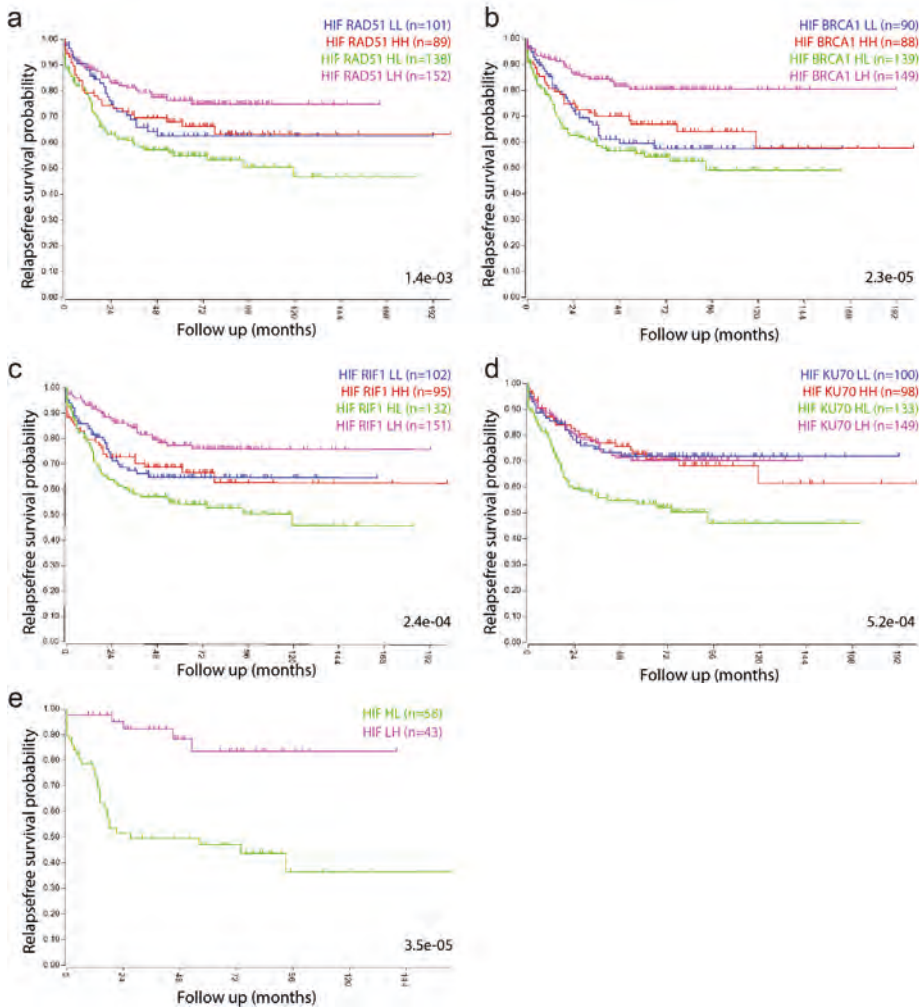


Figure 2. Tumors with a high hypoxia signature and low expression of DNA repair genes have a poor prognosis.

Kaplan Meier curves show the survival differences between the subgroups identified in Figure 1c, based on median expression values. (a) HIF2-BRCA1. (b) HIF2-RAD51. (c) HIF2-RIF1. (d) HIF2-Ku70. (e) Tumors belonging to each high-high, low-low, high-low and low-high quadrants in all four analyses (a-d) were identified by GeneVenn (www.genevenn.sourceforge.net) and analyzed separately. Tumors with high expression of the HIF2 signature and low levels of all 4 repair proteins had a very poor prognosis (green), when compared to tumors with low expression of the HIF2 signature and high expression of all 4 repair proteins (magenta).

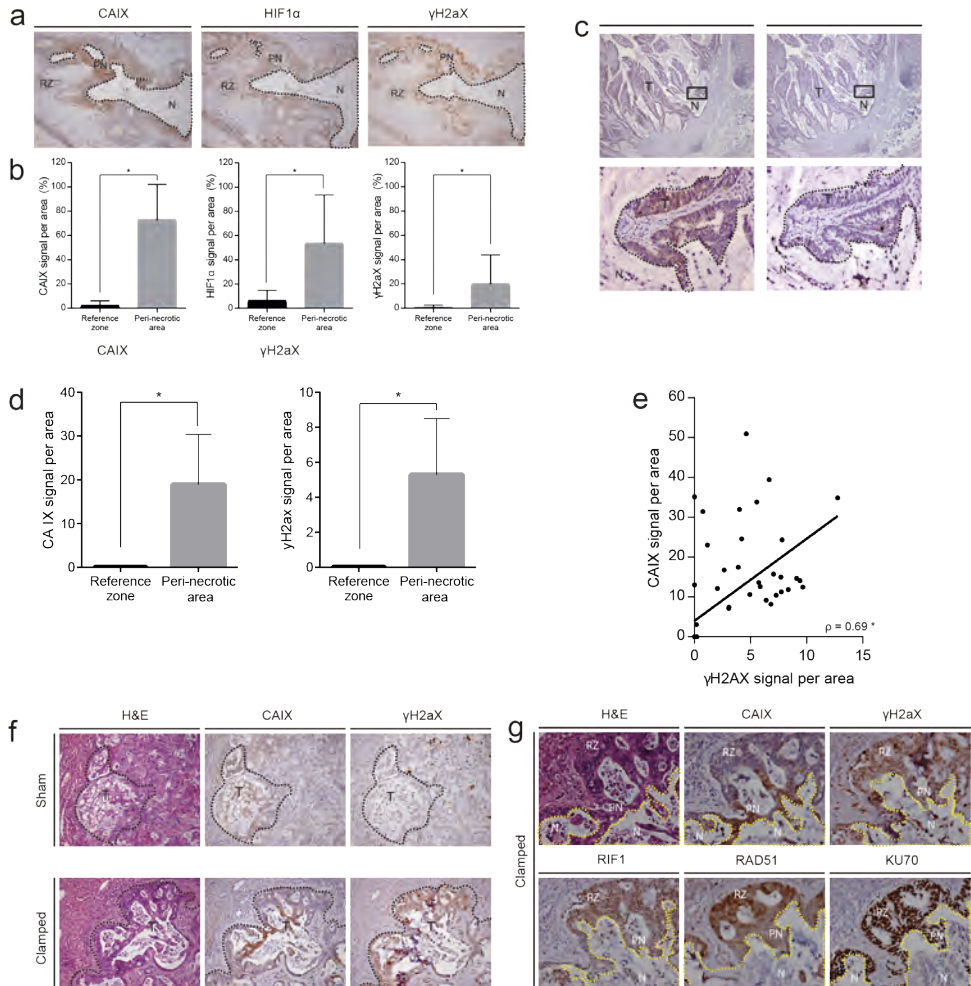


Figure 3. Hypoxic areas in primary tumors and liver metastases are characterized by DNA damage and low expression of the DNA repair proteins RAD51 and RIF1. (a) Immunohistochemistry (IHC) for CAIX, HIF1 α and γ H2ax in human primary colorectal tumours. Robust expression of all three markers was observed surrounding necrotic lesions. (b) Quantification of CAIX, HIF1 α

and γ H2AX expression in peri-necrotic areas and reference zones in primary human colon tumors by IHC (n=20). (c) Analysis of CAIX and γ H2AX expression in human liver metastases by IHC. A 20x magnification of the area depicted in the square in lower panel. (d) Quantification of CAIX and γ H2AX staining (IHC) in peri-necrotic and reference tissue in liver metastases (n=30). (e) Scatterplot showing the correlation between the expression of (randomly chosen microscopic field areas of) CAIX and γ H2AX, assessed with the Spearman test (ρ) (n=60). (f) Patient-derived colonospheres were injected into the liver parenchyma of immune-deficient mice. Following tumor initiation, the tumor-bearing liver lobes were subjected to a vascular clamping or sham protocol [24] to induce hypoxia. After 24 hours, the livers were excised and expression of CAIX and γ H2AX was examined by IHC. (g) IHC on peri-necrotic areas of clamped livers (experiment as in (f)) for CAIX, γ H2AX, RIF1, RAD51, and KU70. * $p < 0.001$, N=necrosis, T=tumor, PN=peri-necrotic, RZ=Reference Zone.

The hypoxia-activated pro-drug Tirapazamine (TPZ) reduces the stem-like Aldefluor^{bright} population in vitro and in liver metastases.

So far, the data indicate that DNA repair is reduced in hypoxic conditions, which may create a therapeutically exploitable vulnerability. Tirapazamine (TPZ) is a hypoxia-activated prodrug which causes primarily DNA double-strand breaks by inhibiting topoisomerase II [23]. To analyze DNA damage in TPZ-treated cells, we cultured human colonospheres in normoxia and hypoxia in the absence or presence of TPZ. Immunofluorescence (Figure 6a and b), comet assay (Figure 6c and d) and western blotting (Figure 6e) showed that TPZ strongly enhanced DNA double strand break formation (γ H2AX) and apoptosis (as evidenced by caspase-3 cleavage) in hypoxic colonospheres. We also analyzed DNA repair protein expression in TPZ-treated cells. TPZ treatment in hypoxia caused strong suppression of RIF1, RAD51, 53BP1 and KU70 expression (Figure 6e). We previously showed that a subpopulation of cancer stem cells (CSCs) reside in hypoxic tumor niches [4, 6] from where they may drive tumor recurrence. As described in the introduction, colon CSCs can be identified by high aldehyde dehydrogenase (ALDH) activity, which is measured with the Aldefluor assay [32-34].

Therefore, we tested whether TPZ would differently affect the induction of DNA damage and suppression of repair proteins in hypoxic CSCs and non-CSCs (operationally defined as Aldefluor^{bright} and Aldefluor^{dim}). Intact colonospheres were cultured in hypoxia and were treated with TPZ. After treatment, cells were FACS-sorted into Aldefluor^{bright} and Aldefluor^{dim} populations, and DNA damage and repair was analyzed in these populations by western blotting. DNA double strand break formation (γ H2AX) was similar in Aldefluor^{bright} and Aldefluor^{dim} cells (Figure 6f). RAD51, and to a lesser extent KU70, were downregulated under hypoxia and expression of both repair proteins was further reduced by TPZ treatment. We found that TPZ reduced the Aldefluor^{bright} fraction in hypoxic colonospheres (Figure 6g and Supplementary Figure 4). The same results were found *in vivo*; clamped liver lobes of mice treated with TPZ showed reduced levels of ALDH1 expression (Figure 6h and i). Therefore, hypoxia-induced suppression of DNA

repair proteins may enhance general sensitivity to TPZ and may explain the abolished upregulation of the Aldefluor^{bright} population in the cells treated with TPZ in hypoxia.

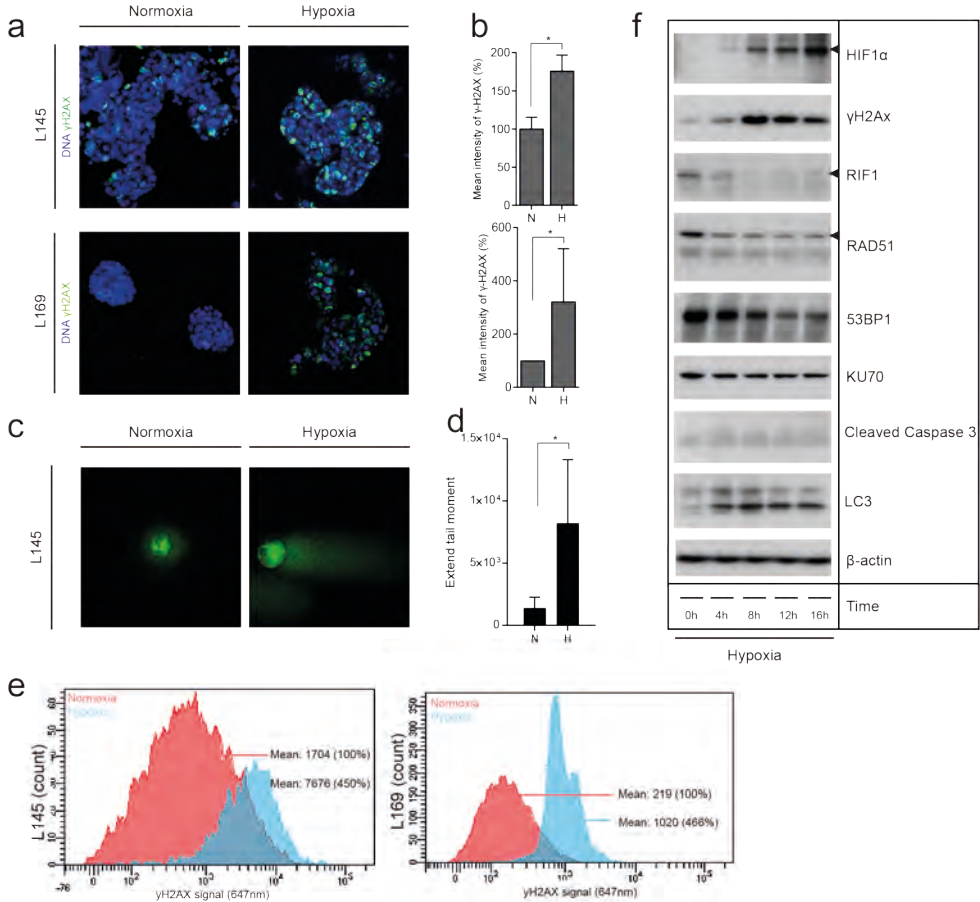


Figure 4. *In vitro* exposure of patient-derived colonosphere cultures to hypoxia. (a) Two independent patient-derived colonospheres were cultured in normoxia (21%) or hypoxia (0.1%) for 24 hours. Immunofluorescence was then used to assess γ H2AX (green) in the nuclei DAPI (blue). (b) Bar graphs showing the quantification of γ H2AX observed in (a) ($n=3$), shown as percentage of the mean γ H2AX intensity at normoxia. (c) Representative confocal pictures of the comet assay of colonospheres cultured as in (a). (d) Bar graphs showing the quantification of DNA damage observed with the comet assay (Extend tail moment) ($n=73$). (e) Colonospheres were cultured as in (a) and γ H2AX was assessed by FACS. The plots show normoxic γ H2AX levels in red and hypoxic γ H2AX levels in blue in two independent cell lines. (f) Human colonospheres were exposed to hypoxia for the indicated periods of time. Cell lysates were then analyzed by Western blotting for the indicated markers (cropped).

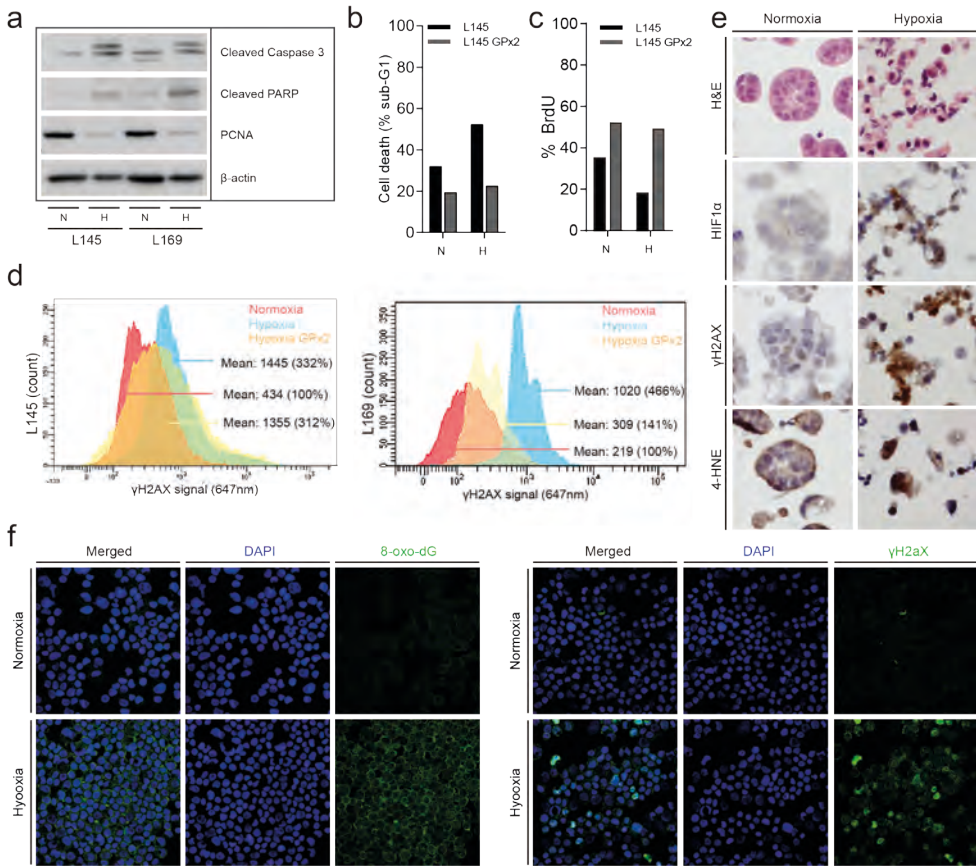


Figure 5. Chronic hypoxia induces oxidative damage and promotes tumor cell death. (a) Human colonospheres were cultured in hypoxia (0.1%) and normoxia (21%) for 72 hours. Cells were lysed and analyzed by Western blotting for PCNA (proliferation) and cleaved caspase-3 (apoptosis) (cropped gels). (b) Experiment performed as in (a) but human colonospheres overexpressing GPx2 were included. FACS analysis of PI-stained cells was then used to assess cell death. The bar graph shows the percentage of cells with sub-G1 DNA content. (c) The culture conditions were similar to a and b. Cells were pulse labeled with BrdU just prior to FACS analysis to assess the percentage of proliferating cells. (d) FACS analysis of γ H2AX levels in control and GPx2-overexpressing colonospheres. Cells were exposed to hypoxia for 24 hours. (e) Colonospheres were cultured in normoxia or hypoxia for 24 hours and were subsequently embedded in agar and fixed in formalin for IHC analysis of HIF1 α , γ H2AX and 4-HNE levels. (f) Colonospheres were cultured in normoxia or hypoxia for 24 hours. After single cell making living cells were FACS sorted and processed for immunofluorescence analysis of 8-oxo-dG (left panel) and γ H2AX (right panel). DAPI was used to visualize cell nuclei.

Discussion

In the present study, we show that increased DNA damage, possibly caused by reduced repair protein expression, is a therapeutically exploitable feature of aggressive colon tumors. Besides, an increase in DNA damage can also be caused by hypoxia-induced increase of reactive oxygen species (ROS) levels, and ROS-induced damage to the nucleotide pool. The link between hypoxia and DNA damage was found in primary tumors, in resected liver metastases, and in residual tumor tissue following liver surgery. The latter finding is important as it suggests a potential avenue for the development of adjuvant therapy, which is currently lacking. Since current adjuvant treatment regimens with standard chemotherapy have minimal effects on the survival of this patient population [35], HAPs may be employed to prevent outgrowth of residual tumor cells following an intentionally curative partial liver resection. We showed that hypoxia reduces DNA damage repair capacity by suppressing repair protein expression. In itself this can lead to accumulation of damage and tumor cell death without the addition of drugs. However, a double strand break-generating drug like TPZ greatly augments this process and can be used to exploit the lower repair capacity that is intrinsic to the hypoxic state.

RNA analysis of the primary tumors showed a general inverse association between hypoxia and repair protein expression, regardless of the specific repair pathway. Although this may be partially explained by a general lower proliferation rate of hypoxic tumors [36], our data also shows that hypoxia has a rapid down-regulatory effect on the expression of some of the repair proteins, even preceding HIF stabilization and DNA damage induction. This is in line with previous studies [18, 20, 21] and demonstrates a direct link between hypoxia, reduced DNA repair, and the accumulation of DNA damage. Future work should reveal how hypoxia leads to decreased repair protein expression and to what extent this contributes to DNA damage accumulation, since this could eventually lead to an even more target-based approach. Regardless of the underlying mechanism, there was a striking enrichment of aggressive mesenchymal-type CMS4 tumors in the [HIF2 α ^{high}/Repair-Protein^{low}] quadrants, showing also decreased DFS in all cases examined. A potential explanation for the observed connection between low repair a decreased survival probability could be that lower repair capacity leads to an increased mutation rate and an increased chance of the generation of metastasis-competent (and/or therapy resistant) sub-clones. This suggests that hypoxia targeting, for instance with TPZ or related hypoxia-activated topoisomerase inhibitors like AQ4N [37] and Q6 [38], should be explored as a therapeutic strategy in selected patients with CMS4-type tumors [39, 40]. In this respect, it is interesting to note that CSCs are intrinsically sensitive to the topoisomerase-I inhibitor irinotecan, but that CSCs – in the context of tumor tissue or colonosphere structure – are protected from the drug by efflux pumps expressed on the surrounding differentiated tumor cells [14]. By an increase in the Aldefluor^{bright} population, hypoxia could indirectly interfere with this drug resistance mechanism, yielding the hypoxic tumor tissue sensitive to topoisomerase inhibitors, such as TPZ.

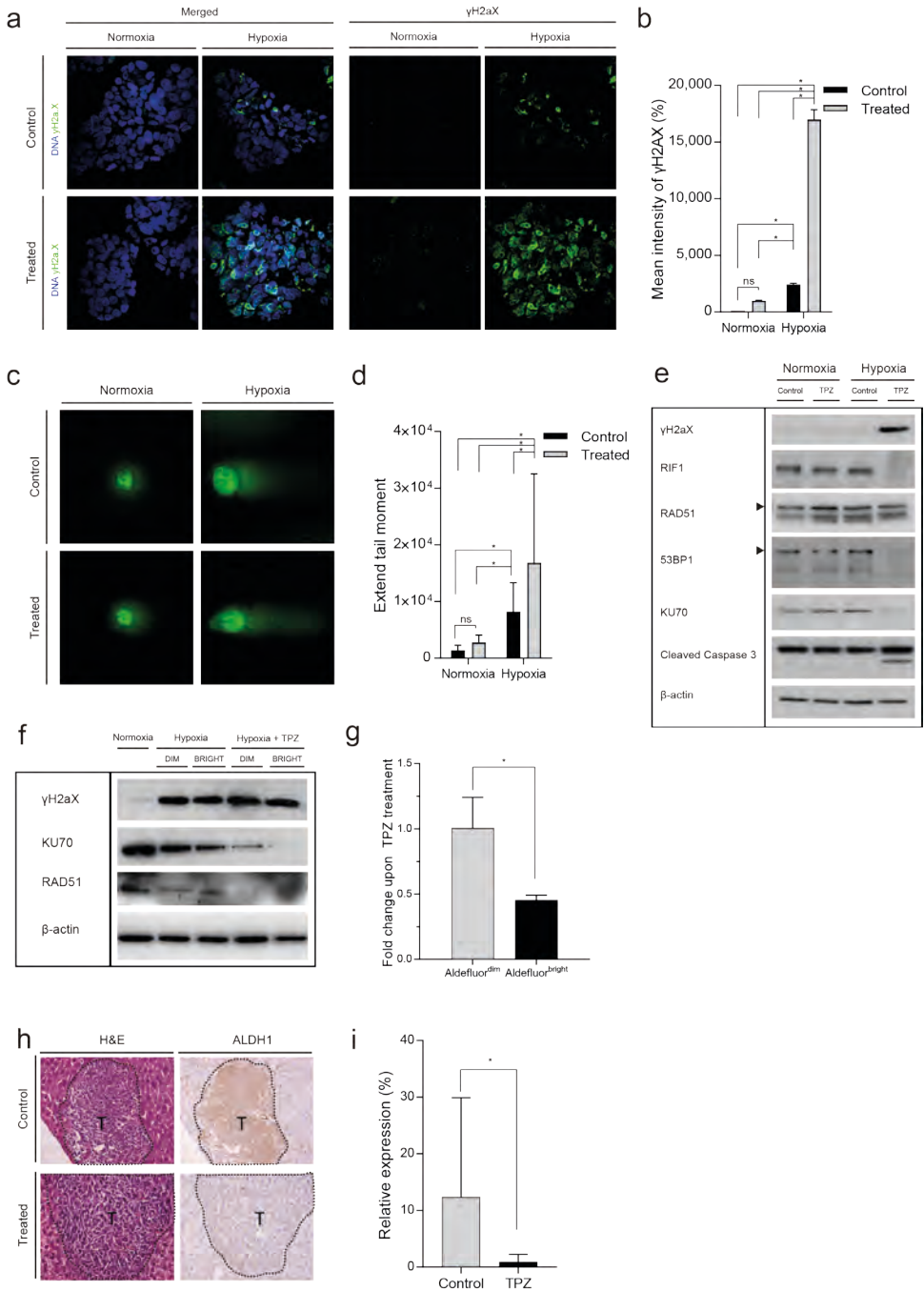


Figure 6. (left) **The hypoxia-activated pro-drug Tirapazamine (TPZ) reduces the stem-like Aldefluor^{bright} population in vitro and in liver metastases.** (a) Human colonospheres were cultured in hypoxia (0.1%) and normoxia (21%) for 24 hours in the absence or presence of TPZ for 4 hours. Cells were processed for immunofluorescence analysis of γ H2AX (green). DAPI (blue) was used to visualize cell nuclei. (b) Bar graphs showing the quantification of γ H2AX foci observed in (a), shown as percentage of the mean γ H2AX intensity at normoxia (n=3). (c) Representative confocal pictures of the comet assay of colonospheres cultured as in (a). (d) Bar graphs showing the quantification of DNA damage observed with the comet assay (Extend tail moment) (n=77). (e) The experiment was performed as in (a), but cells were either treated or untreated for 16 hours. Cells were lysed and analyzed by Western blotting for the indicated markers (cropped). (f) Colonospheres were cultured in hypoxia and treated with TPZ for 16 hours. The cells were FACS sorted into Aldefluor^{bright} and Aldefluor^{dim} populations and analyzed by western blotting for the indicated markers. (g) Human colonospheres were cultured in hypoxia (0.1%) for 24 hours in the absence or presence of TPZ for 4 hours and FACS sorted into Aldefluor^{bright} and Aldefluor^{dim} populations. The bar graph shows the fold change Aldefluor^{dim} and Aldefluor^{bright} cells upon TPZ treatment (n=3). (h) C26 tumor cells were injected into the liver parenchyma of immune-deficient mice. Following tumor initiation, the tumor-bearing liver lobes were subjected to a vascular clamping protocol [24] to induce hypoxia and treated with saline (control) or TPZ (treatment) for 10 days. At endpoint, the livers were excised and expression of ALDH1 was examined by IHC. Magnification 20x, T=tumor. (i) Bar graphs showing the quantification of ALDH1 (n=28) observed in (h) (n=14). * = significant (p>0.05). ns = not significant.

Interestingly, studies on DNA repair-deficient cancer syndromes like Lynch syndrome for CRC and BRCA-associated ovarian and breast cancer have led to the concept of synthetic lethality: the genetic deficiency of one repair pathway (e.g. mismatch repair) leads to a hypersensitivity to drugs targeting additional repair pathways (e.g. through PARP inhibition) [41, 42]. It will therefore be interesting to assess whether hypoxia - by suppressing the activity of one or more repair pathways - causes hypersensitivity to inhibitors of other repair pathways. Some studies indeed show that hypoxia sensitizes tumor tissue to PARP inhibitors in combination with radiation, supporting this treatment concept [19, 22, 43-46]. Although we have not found synergistic responses of hypoxic colon cancer cells and tumors to a combination of TPZ and the PARP inhibitor Olaparib (J), unpublished observations), this is an area that deserves further investigation. Novel platforms in translational oncology, including organoid culturing technology [47-49] and PDX-models [50] are now widely used to develop personalized cancer treatment. Interestingly, a subset of human colon tumors can only be established as organoids at low oxygen tension [49]. This hypoxia-addicted subgroup of colon cancer organoids can now be used in drug screens and transplantation models to identify treatment combinations with hypoxia-activated prodrugs and/or DNA repair inhibitors that effectively eradicate hypoxic tumor tissue.

Hypoxia within tumors is, by definition, heterogeneous. However, features of hypoxia are clearly overrepresented in the CMS4 subtype, providing a potential diagnostic strategy to select patients for hypoxia/repair-targeting therapy. Multiple robust diagnostic tools for selecting patients with CMS4 tumors have recently been developed and are now available [39, 40]. As an alternative to CMS4 tests, patients may also be selected by immunohistochemistry for hypoxia-, DNA damage-, and/or DNA DSB repair markers. In addition, hypoxia-generating procedures such as liver surgery or (radio-) embolization, may be followed by such therapy regardless of tumor subtype, aiming to kill hypoxic tumor residue and prevent recurrence. In such cases, hypoxia is externally generated rather than a consequence of tumor genetics. Another factor potentially influencing response to hypoxia/repair-targeting therapy is variation in DNA repair capacity between individuals and tumors. For instance, polymorphisms in miRNA binding sites in genes encoding DNA DSB repair genes can be used to study differences in DNA repair capacity in CRC patients [51]. Eventually, the analysis of such genetic variations may also have predictive value and could help select patients for hypoxia/repair targeting therapy. Whatever the selection strategies will be, we propose that reduced repair capacity in a subset of human colorectal cancers and in post-treatment tumor tissue provides a clear opportunity for therapeutic intervention. DNA repair defects and sensitivity to hypoxia-activated topoisomerase inhibitors are the basis for further developing combination therapies aimed at eradicating hypoxic tumor tissue.

Materials and Methods

Bioinformatics analyses

All bioinformatics analyses were performed by using the R2 Genomics analysis and visualization platform (<http://r2.amc.nl>). To visualize expression of particular gene sets in distinct tumor subgroups the option 'relate two tracks' was used. Condensation of gene set expression into single values per tumor was performed with the 'View Gene Set' option and storing the obtained values as a track for subsequent analysis. The HIF2 α signature was previously published [4].

All dot plots visualizing the comparative expression of gene sets were created using the 'relate two tracks option'. Pearson correlation (r) values and accompanying p -values were obtained by selecting the xy plot option.

Immunohistochemistry

Both human and mice tumors were immediately after respectively resection and necropsy fixed in 4-10% neutral-buffered formalin and embedded in paraffin. Spheroid pellets were fixed in 4% phosphate-buffered formalin, first embedded in a 2.5% agar droplet and subsequently embedded in paraffin. Serial sections (4 μ m) were used for immunohistochemical analyses and stained with CAIX (1:1000 ab15086, abcam), Hif1 α (1:50, 610959, BD Transduction Laboratories), γ H2AX (Ser139) (1:50, sc-2557, Cell

signaling, Littleton, MA), RIF1 (1:16000, A300-569A, Bethyl), KU70 (A-9) (1:6000, sc-5309, Santa Cruz), RAD51 (1:100, HPA039310, Sigma Atlas), Anti-4 OH nonenal (1:100, ab46545, abcam), ALDH1 (1:500, 611195, BD Transduction Laboratories). Briefly, tissue sections were deparaffinized with xylene and rehydrated through a series ethanol concentrations. Antigen retrieval was achieved by cooking for 20 minutes with citrate or EDTA, followed by blocking of the endogenous peroxidase activity for 1 hour at room temperature with 0.3% H₂O₂. Primary antibody was either applied for 1 hour at room temperature (CAIX, RAD51, KU70) or overnight at 4 degrees of Celcius (γ H2AX, HIF1 α , 4-OH-HNE, RIF1). HRP-labelled secondary antibody (Powerservision Immunologic, Immunovision Technologies, Brisbane, CA) was applied after washing and tissue sections were stained with DAB reagent (Dako). Nuclei were counterstained with Hematoxylin (Mayer). Tissue architecture and identification of necrotic areas was achieved by Hematoxylin and Eosin staining. Areas are subdivided into areas of necrosis (N), tumour (T), peri-necrotic (PN) and Reference Zone (RZ). The Novolink Polymer Detection System (Leica Biosystems Inc, Buffalo Grove, IL) was used according to the manufacture's protocol for some stainings (HIF1 α , γ H2AX, 4HNE). Staining was analyzed by ImageJ after subtracting background staining. Areas were defined as microscopic fields (20x).

Patient-derived colonosphere culture

Human colonosphere cell lines (L145 and L169) were derived from patients harboring colorectal liver metastases and cultured in stem cell medium as described previously [14]. Generation of colonospheres stably expressing GPx2-expression constructs was established as described before [29]. All cell culture was carried out at 37°C in a 5% CO₂-humidified incubator under normoxic (21% O₂) or hypoxic (0.1% O₂) conditions, the latter using an Invivo2 Hypoxia Workstation (Biotrace International, Spennymoor, UK). Tumor tissue was obtained in accordance with the local medical ethical committee on human experimentation (protocol #09-145). Informed consent was obtained from all patients. Colonospheres were cultured with or without Tirapazamine (TPZ) (20 μ M; kindly provided by Dr Minchinton, BC Cancer Agency, Vancouver, Canada) for the indicated time.

Immunofluorescence

Colonospheres were harvested and fixed for 20 minutes in PBS containing 4% of formaldehyde and permeabilized with 1% Triton X-100 at room temperature for 10 minutes and overnight in ice-cold (-20°C) methanol or PBS. Cells were blocked in PBS containing 0.1% Tween and 5% BSA and incubated overnight at 4°C with primary antibodies in PBS containing 0.1% Tween and 2% BSA; p- γ H2AX (Ser139) (1:100, 05-636, Millipore), Anti-8 OH guanosine (1:200 ab48508, abcam). Colonospheres were subsequently washed and incubated for 1 hour at room temperature with secondary antibody (goat anti-mouse Alexa Fluor568; Invitrogen) in PBS containing 0.1% Tween and 2% BSA. DAPI (0.5 μ g/mL) was used to stain the nuclei. Images (Z-stacks) were acquired using a Zeiss LSM510 Meta Confocal microscope. All images were acquired

with identical illumination settings and analyzed in 3D with Imaris version 8.2 Software (Bitplane AG, Zurich, Switzerland).

Comet Assay

The OxiSelect Comet Assay was used to analyze cellular DNA damage using single cell electrophoresis (Cell Biolabs, San Diego, CA, USA) according manufacturer instructions. In short, cells were trypsinized, washed and diluted to 10^5 /ml in PBS. Cells were then added to low-melting temperature agarose (10^4 /ml final) and immediately plated (75 μ l) on comet assay glass slides (Cell Biolabs) coated with normal-melting temperature agarose. After lysis, slides were placed in a horizontal gel electrophoresis chamber and covered with an alkaline buffer (5 mM NaOH and 200 mM Na₂ EDTA; pH >13). Following a 30 minute DNA “unwinding” period, electrophoresis was performed under standard conditions (21 V, 300 mA; distance between electrodes = 20 cm) for 30 minutes. Following neutralization to pH 7.5 using Trizma base (Sigma-Aldrich, St Louis, MO, USA), gels were stained with Vista Green DNA dye and stored at 4°C until analysis. Images were acquired with a Zeiss LSM 510 confocal microscope and LSM 710 version 3.2SP2 software. DNA damage was quantified per the manufacturer's instructions by calculating the extent tail moment: Extent Tail Moment = Tail DNA% \times Length of Tail; where Tail DNA% = $100 \times$ Tail DNA Intensity/Cell DNA intensity. For each time point, means \pm standard error of the mean were calculated. Statistical analysis was performed using an unpaired Student's t-test.

Western blot analysis

Lysates of colonospheres were prepared using laemmli buffer. Equal amounts of protein were loaded and run out on sodium dodecyl sulphate-containing gels and blotted onto nitro-cellulose membranes. Western blotting was performed using standard protocols. The following antibodies were used: Hif1 α (1:500, 610959, BD Transduction Laboratories), Hif2 α (1:500, ab8365, Abcam, Cambridge, MA), Cleaved Caspase 3 (Asp175) (1:1000, 9661, Cell Signaling, Littleton, MA), anti-PCNA (1:1000, SC-56 Santa Cruz), 53BP1 (1:1000, nb100-304 Novus Biologicals, Littleton, CO), p- γ H2AX (Ser139) (1:1000, 05-636, Millipore), RIF1 (1:2000, A300-569A, Bethyl.), KU70 (A-9) (1:200, sc-5309, Santa Cruz.), RAD51 (1:2500, ABE257, Millipore), cleaved PARP (1:1000, 9541, Cell Singalling, Littleton, MA), LC3 (5F10)(1:1000, 0231-100, Nanotools antibodies, Teningen, Germany) β -Actin AC15 (1:20000, NB600-501, Novus Biologicals, Littleton, CO).

Proliferation assay

A DNA synthesis-based cell proliferation assay using 10 mM 5-Bromo-2'-Deoxyuridine (BrdU) (BD Biosciences, Franklin Lakes, NJ, USA) was performed according manufacturer instructions.

Flow cytometry

L145 and L169 (with or without GPx2 construct) colonosphere cell lines were cultured under normoxia or hypoxia for the indicated time points. FACS analyses for γ H2AX is

performed according to the previous published protocol [52] in combination with 7-AAD for cell viability. We used γ H2A.X (Ser139) (1:200, sc-2557, Cell signaling, Littleton, MA), via-probe cell viability solution (7-AAD) (10 μ l/1 \times 10⁶ cells, 555816, BD Transduction Laboratories), RNase 10mg/ml 1:400. Aldefluor activity and γ H2AX were analyzed by fluorescence-activated cell sorting (FACS) using DIVA software (BD Biosciences). For the Aldefluor experiments, colonosphere line L145 was either first treated or first sorted. If first treated, cells were cultured for the indicated time under normoxic or hypoxic conditions with or without TPZ (20 μ M). The concentration of TPZ (20 μ M) was based on previous work in our lab[6]. Next, cells were trypsinized to obtain single-cell suspensions. Cell doublets and clumps were excluded by prior filtration with a 40 μ M filter and by using doublet discrimination gating during FACS analysis. Nonviable cells were excluded based on 7-AAD expression. Aldefluor positive cells were analyzed according to the manufacturer's protocol by using the ALDH (aldehyde dehydrogenase isoform 1) substrate BAAA (1 μ mol/L per 1 \times 10⁶ cells; StemCell Technologies, Vancouver, Canada). Negative control samples were co-incubated with diethylaminobenzaldehyde (50 mM, StemCell Technologies). When indicated, cells were first sorted based on Aldefluor positivity and afterwards cultured for the indicated time under normoxic or hypoxic conditions with or without TPZ (20 μ M). Afterwards, percentage of γ H2AX expression in L145 cells was determined by immunofluorescence or Western blot as described. The cell sorting experiments were conducted with a 6-color FACS Aria III Cell Sorter (Becton Dickinson Biosciences, Mountain View, CA).

Animals

All experiments were performed in accordance with the guidelines of the Animal Welfare Committee of the University Medical Center Utrecht, The Netherlands. Male Balb/C mice (10-12 weeks) were purchased from Charles River (Sulzfeld, Germany) and were housed under standard laboratory conditions.

Murine Model of Hepatic Hypoxia

A mouse model for hepatic hypoxia was used as described previously [24], in which hypoxia was induced through vascular clamping of the left liver lobe for 45 minutes. TPZ was then administered one day after clamping for a period of 10 days. The livers were excised, formalin fixed and paraffin embedded and expression of ALDH1 was examined by IHC.

Statistical analyses

Box and Whisker plots are shown to display the variation of CMS in the DNA repair patterns. Scatter plots are used for regression analysis and shown by (R). Data is presented as mean \pm SD. The Student t test (unpaired, two-tailed) was performed to analyze if differences between the groups are statistically significant, using SPSS version 23 (IBM SPSS Statistics, Armond, NY) and GraphPad Prism version 5.0 (Graphpad Software, La Jolla, CA). Differences with a P value of less than 0.05 were considered statistically significant. Box and whisker plots showed non-normal distribution of the

used parameters (data not shown), therefore correlation is analyzed by Spearman's rank correlation coefficient correlation.

Abbreviations

4-HNE	4-hydroxy-nonenal
ALDH	aldehyde dehydrogenase
CAD	caspase-activated DNase
CMS4	consensus molecular subtype 4
CSC	cancer stem cell
FACS	fluorescence-activated cell sorting
GPx2	glutathione peroxidase 2
HAPs	hypoxia-activated prodrugs
HIF1 α	hypoxia-inducible factor 1 alpha
HIF2 α	hypoxia-inducible factor 2 alpha
HR	homologous recombination
NHEJ	non-homologous end-joining
ROS	reactive oxygen species
TPZ	Tirapazamine
γ H2ax	phosphorylated histone 2AX

Author contributions

All the experiments in this paper were conceived and designed by JJ, IBR and OK. JJ, LvdW, KT, JL, NP and SvS conducted the experiments. JJ analyzed the data, made the figures and wrote the manuscript. OK, IBR and LvdW contributed to the writing and the editing of the manuscript. All authors read and approved the final manuscript.

Acknowledgements

We thank Jeroen van Velzen and Pien van der Burgh from the flow cytometry facility at the University Medical Center Utrecht for their excellent technical assistance. This study was supported by the Dutch Cancer Society (grant no. UU2013–5865 to J.M.J.), UU2010-4608 to K.M.G., and UU-2015-8088 to JL), Gieskes-Strijbis fund (LvdW), PON foundation and 'Vrienden van het UMCU' (KT).

Funding

This study was supported by the Dutch Cancer Society (grant no. UU2013–5865 to J.M.J.), UU2010-4608 to K.M.G., and UU-2015-8088 to JL), Gieskes-Strijbis Fund (LvdW), PON foundation and 'Vrienden van het UMCU' (KT).

References

1. Siegel R, Naishadham D, Jemal A. Cancer statistics, 2012. *CA Cancer J Clin.* 2012; 62: 10-29. doi: 10.3322/caac.20138.
2. Abdalla EK, Vauthey JN, Ellis LM, Ellis V, Pollock R, Broglio KR, Hess K, Curley SA. Recurrence and outcomes following hepatic resection, radiofrequency ablation, and combined resection/ablation for colorectal liver metastases. *Ann Surg.* 2004; 239: 818-25; discussion 25-7. doi:
3. Guinney J, Dienstmann R, Wang X, de Reynies A, Schlicker A, Sonesson C, Marisa L, Roepman P, Nyamundanda G, Angelino P, Bot BM, Morris JS, Simon IM, et al. The consensus molecular subtypes of colorectal cancer. *Nat Med.* 2015; 21: 1350-6. doi: 10.1038/nm.3967.
4. Fatrai S, van Schelven SJ, Ubink I, Govaert KM, Raats D, Koster J, Verheem A, Borel Rinkes IH, Kranenburg O. Maintenance of Clonogenic KIT(+) Human Colon Tumor Cells Requires Secretion of Stem Cell Factor by Differentiated Tumor Cells. *Gastroenterology.* 2015; 149: 692-704. doi: 10.1053/j.gastro.2015.05.003.
5. Nijkamp MW, van der Bilt JD, de Bruijn MT, Molenaar IQ, Voest EE, van Diest PJ, Kranenburg O, Borel Rinkes IH. Accelerated perinecrotic outgrowth of colorectal liver metastases following radiofrequency ablation is a hypoxia-driven phenomenon. *Ann Surg.* 2009; 249: 814-23. doi: 10.1097/SLA.0b013e3181a38ef5.
6. Govaert KM, Emmink BL, Nijkamp MW, Cheung ZJ, Steller EJ, Fatrai S, de Bruijn MT, Kranenburg O, Borel Rinkes IH. Hypoxia after liver surgery imposes an aggressive cancer stem cell phenotype on residual tumor cells. *Ann Surg.* 2014; 259: 750-9. doi: 10.1097/SLA.0b013e318295c160.
7. Qing G, Simon MC. Hypoxia inducible factor-2alpha: a critical mediator of aggressive tumor phenotypes. *Curr Opin Genet Dev.* 2009; 19: 60-6. doi: 10.1016/j.gde.2008.12.001.
8. O'Brien CA, Pollett A, Gallinger S, Dick JE. A human colon cancer cell capable of initiating tumour growth in immunodeficient mice. *Nature.* 2007; 445: 106-10. doi: 10.1038/nature05372.
9. Ricci-Vitiani L, Lombardi DG, Pilozzi E, Biffoni M, Todaro M, Peschle C, De Maria R. Identification and expansion of human colon-cancer-initiating cells. *Nature.* 2007; 445: 111-5. doi: 10.1038/nature05384.
10. Ma S, Lee TK, Zheng BJ, Chan KW, Guan XY. CD133+ HCC cancer stem cells confer chemoresistance by preferential expression of the Akt/PKB survival pathway. *Oncogene.* 2008; 27: 1749-58. doi: 10.1038/sj.onc.1210811.
11. Pang R, Law WL, Chu AC, Poon JT, Lam CS, Chow AK, Ng L, Cheung LW, Lan XR, Lan HY, Tan VP, Yau TC, Poon RT, et al. A subpopulation of CD26+ cancer stem cells with metastatic capacity in human colorectal cancer. *Cell Stem Cell.* 2010; 6: 603-15. doi: 10.1016/j.stem.2010.04.001.
12. Wang Z, Li Y, Ahmad A, Azmi AS, Kong D, Banerjee S, Sarkar FH. Targeting miRNAs involved in cancer stem cell and EMT regulation: An emerging concept in overcoming drug resistance. *Drug Resist Updat.* 2010; 13: 109-18. doi: 10.1016/j.drug.2010.07.001.

13. Chen K, Huang YH, Chen JL. Understanding and targeting cancer stem cells: therapeutic implications and challenges. *Acta Pharmacol Sin.* 2013; 34: 732-40. doi: 10.1038/aps.2013.27.
14. Emmink BL, Van Houdt WJ, Vries RG, Hoogwater FJ, Govaert KM, Verheem A, Nijkamp MW, Steller EJ, Jimenez CR, Clevers H, Borel Rinkes IH, Kranenburg O. Differentiated human colorectal cancer cells protect tumor-initiating cells from irinotecan. *Gastroenterology.* 2011; 141: 269-78. doi: 10.1053/j.gastro.2011.03.052.
15. Jiang F, Qiu Q, Khanna A, Todd NW, Deepak J, Xing L, Wang H, Liu Z, Su Y, Stass SA, Katz RL. Aldehyde dehydrogenase 1 is a tumor stem cell-associated marker in lung cancer. *Mol Cancer Res.* 2009; 7: 330-8. doi: 10.1158/1541-7786.mcr-08-0393.
16. Lohberger B, Rinner B, Stueendl N, Absenger M, Liegl-Atzwanger B, Walzer SM, Windhager R, Leithner A. Aldehyde dehydrogenase 1, a potential marker for cancer stem cells in human sarcoma. *PLoS One.* 2012; 7: e43664. doi: 10.1371/journal.pone.0043664.
17. Meng AX, Jalali F, Cuddihy A, Chan N, Bindra RS, Glazer PM, Bristow RG. Hypoxia down-regulates DNA double strand break repair gene expression in prostate cancer cells. *Radiother Oncol.* 2005; 76: 168-76. doi: 10.1016/j.radonc.2005.06.025.
18. Bristow RG, Hill RP. Hypoxia and metabolism. Hypoxia, DNA repair and genetic instability. *Nat Rev Cancer.* 2008; 8: 180-92. doi: 10.1038/nrc2344.
19. Chan N, Koritzinsky M, Zhao H, Bindra R, Glazer PM, Powell S, Belmaaza A, Wouters B, Bristow RG. Chronic hypoxia decreases synthesis of homologous recombination proteins to offset chemoresistance and radioresistance. *Cancer Res.* 2008; 68: 605-14. doi: 10.1158/0008-5472.can-07-5472.
20. Chan N, Bristow RG. "Contextual" synthetic lethality and/or loss of heterozygosity: tumor hypoxia and modification of DNA repair. *Clin Cancer Res.* 2010; 16: 4553-60. doi: 10.1158/1078-0432.ccr-10-0527.
21. Kumareswaran R, Ludkovski O, Meng A, Sykes J, Pintilie M, Bristow RG. Chronic hypoxia compromises repair of DNA double-strand breaks to drive genetic instability. *J Cell Sci.* 2012; 125: 189-99. doi: 10.1242/jcs.092262.
22. Luoto KR, Kumareswaran R, Bristow RG. Tumor hypoxia as a driving force in genetic instability. *Genome Integr.* 2013; 4: 5. doi: 10.1186/2041-9414-4-5.
23. Siim BG, Pruijn FB, Sturman JR, Hogg A, Hay MP, Brown JM, Wilson WR. Selective potentiation of the hypoxic cytotoxicity of tirapazamine by its 1-N-oxide metabolite SR 4317. *Cancer Res.* 2004; 64: 736-42. doi: 10.1158/0008-5472.can-03-3817.
24. van der Bilt JD, Kranenburg O, Nijkamp MW, Smakman N, Veenendaal LM, Te Velde EA, Voest EE, van Diest PJ, Borel Rinkes IH. Ischemia/reperfusion accelerates the outgrowth of hepatic micrometastases in a highly standardized murine model. *Hepatology.* 2005; 42: 165-75. doi: 10.1002/hep.20739.
25. van der Bilt JD, Kranenburg O, Verheem A, van Hillegersberg R, Borel Rinkes IH. Selective portal clamping to minimize hepatic ischaemia-reperfusion damage and avoid accelerated outgrowth of experimental colorectal liver metastases. *Br J Surg.* 2006; 93: 1015-22. doi: 10.1002/bjs.5382.

26. van der Bilt JD, Soeters ME, Duyverman AM, Nijkamp MW, Witteveen PO, van Diest PJ, Kranenburg O, Borel Rinkes IH. Perinecrotic hypoxia contributes to ischemia/reperfusion-accelerated outgrowth of colorectal micrometastases. *Am J Pathol.* 2007; 170: 1379-88. doi:10.2353/ajpath.2007.061028.
27. Wiseman H, Halliwell B. Damage to DNA by reactive oxygen and nitrogen species: role in inflammatory disease and progression to cancer. *Biochem J.* 1996; 313 (Pt 1): 17-29. doi:
28. Wang M, Kirk JS, Venkataraman S, Domann FE, Zhang HJ, Schafer FQ, Flanagan SW, Weydert CJ, Spitz DR, Buettner GR, Oberley LW. Manganese superoxide dismutase suppresses hypoxic induction of hypoxia-inducible factor-1 α and vascular endothelial growth factor. *Oncogene.* 2005; 24: 8154-66. doi:10.1038/sj.onc.1208986.
29. mmink BL, Laoukili J, Kipp AP, Koster J, Govaert KM, Fatrai S, Verheem A, Steller EJ, Brigelius-Flohe R, Jimenez CR, Borel Rinkes IH, Kranenburg O. GPx2 suppression of H₂O₂ stress links the formation of differentiated tumor mass to metastatic capacity in colorectal cancer. *Cancer Res.* 2014; 74: 6717-30. doi: 10.1158/0008-5472.can-14-1645.
30. Brigelius-Flohe R. Tissue-specific functions of individual glutathione peroxidases. *Free Radic Biol Med.* 1999; 27: 951-65. doi:
31. Nakabeppu Y. Cellular levels of 8-oxoguanine in either DNA or the nucleotide pool play pivotal roles in carcinogenesis and survival of cancer cells. *Int J Mol Sci.* 2014; 15: 12543-57. doi: 10.3390/ijms150712543.
32. Charafe-Jauffret E, Ginestier C, Iovino F, Tarpin C, Diebel M, Esterni B, Houvenaeghel G, Extra JM, Bertucci F, Jacquemier J, Xerri L, Dontu G, Stassi G, et al. Aldehyde dehydrogenase 1-positive cancer stem cells mediate metastasis and poor clinical outcome in inflammatory breast cancer. *Clin Cancer Res.* 2010; 16: 45-55. doi: 10.1158/1078-0432.ccr-09-1630.
33. Deng S, Yang X, Lassus H, Liang S, Kaur S, Ye Q, Li C, Wang LP, Roby KF, Orsulic S, Connolly DC, Zhang Y, Montone K, et al. Distinct expression levels and patterns of stem cell marker, aldehyde dehydrogenase isoform 1 (ALDH1), in human epithelial cancers. *PLoS One.* 2010; 5: e10277. doi: 10.1371/journal.pone.0010277.
34. Shenoy A, Butterworth E, Huang EH. ALDH as a marker for enriching tumorigenic human colonic stem cells. *Methods Mol Biol.* 2012; 916: 373-85. doi: 10.1007/978-1-61779-980-8_27.
35. Kornprat P, Jarnagin WR, Conen M, DeMatteo RP, Fong Y, Blumgart LH, D'Angelica M. Outcome after hepatectomy for multiple (four or more) colorectal metastases in the era of effective chemotherapy. *Ann Surg Oncol.* 2007; 14: 1151-60. doi: 10.1245/s10434-006-9068-y.
36. Tannock IF. The relation between cell proliferation and the vascular system in a transplanted mouse mammary tumour. *Br J Cancer.* 1968; 22: 258-73. doi:
37. Patterson LH, McKeown SR. AQ4N: a new approach to hypoxia-activated cancer chemotherapy. *Br J Cancer.* 2000; 83: 1589-93. doi: 10.1054/bjoc.2000.1564.



38. Chang L, Liu X, Wang D, Ma J, Zhou T, Chen Y, Sheng R, Hu Y, Du Y, He Q, Yang B, Zhu H. Hypoxia-Targeted Drug Q6 Induces G2-M Arrest and Apoptosis via Poisoning Topoisomerase II under Hypoxia. *PLoS One*. 2015; 10: e0144506. doi: 10.1371/journal.pone.0144506.
39. Trinh A, Trumpi K, De Sousa EMF, Wang X, de Jong JH, Fessler E, Kuppen PJ, Reimers MS, Swets M, Koopman M, Nagtegaal ID, Jansen M, Hooijer GK, et al. Practical and Robust Identification of Molecular Subtypes in Colorectal Cancer by Immunohistochemistry. *Clin Cancer Res*. 2016. doi: 10.1158/1078-0432.ccr-16-0680.
40. Ubink I, Elias SC, Moelans CB, Lacle MM, van Grevenstein WM, van Diest PJ, Borel Rinkes IH, Kranenburg O. A Novel Diagnostic Tool for Selecting Patients With Mesenchymal-Type Colon Cancer Reveals Intratumor Subtype Heterogeneity. *J Natl Cancer Inst*. 2017; 109. doi: 10.1093/jnci/djw303.
41. Bryant HE, Schultz N, Thomas HD, Parker KM, Flower D, Lopez E, Kyle S, Meuth M, Curtin NJ, Helleday T. Specific killing of BRCA2-deficient tumours with inhibitors of poly(ADP-ribose) polymerase. *Nature*. 2005; 434: 913-7. doi: 10.1038/nature03443.
42. Guillotin D, Martin SA. Exploiting DNA mismatch repair deficiency as a therapeutic strategy. *Exp Cell Res*. 2014; 329: 110-5. doi: 10.1016/j.yexcr.2014.07.004.
43. Chan N, Pires IM, Bencokova Z, Coackley C, Luoto KR, Bhogal N, Lakshman M, Gottipati P, Oliver FJ, Helleday T, Hammond EM, Bristow RG. Contextual synthetic lethality of cancer cell kill based on the tumor microenvironment. *Cancer Res*. 2010; 70: 8045-54. doi: 10.1158/0008-5472.can-10-2352.
44. Gani C, Coackley C, Kumareswaran R, Schutze C, Krause M, Zafarana G, Bristow RG. In vivo studies of the PARP inhibitor, AZD-2281, in combination with fractionated radiotherapy: An exploration of the therapeutic ratio. *Radiother Oncol*. 2015; 116: 486-94. doi: 10.1016/j.radonc.2015.08.003.
45. Ghiringhelli F, Richard C, Chevrier S, Vegran F, Boidot R. Efficiency of olaparib in colorectal cancer patients with an alteration of the homologous repair protein. *World J Gastroenterol*. 2016; 22: 10680-6. doi: 10.3748/wjg.v22.i48.10680.
46. Leichman L, Groshen S, O'Neil BH, Messersmith W, Berlin J, Chan E, Leichman CC, Cohen SJ, Cohen D, Lenz HJ, Gold P, Boman B, Fielding A, et al. Phase II Study of Olaparib (AZD-2281) After Standard Systemic Therapies for Disseminated Colorectal Cancer. *Oncologist*. 2016; 21: 172-7. doi: 10.1634/theoncologist.2015-0319.
47. Sato T, Stange DE, Ferrante M, Vries RG, Van Es JH, Van den Brink S, Van Houdt WJ, Pronk A, Van Gorp J, Siersema PD, Clevers H. Long-term expansion of epithelial organoids from human colon, adenoma, adenocarcinoma, and Barrett's epithelium. *Gastroenterology*. 2011; 141: 1762-72. doi: 10.1053/j.gastro.2011.07.050.
48. van de Wetering M, Francies HE, Francis JM, Bounova G, Iorio F, Pronk A, van Houdt W, van Gorp J, Taylor-Weiner A, Kester L, McLaren-Douglas A, Blokker J, Jaksani S, et al. Prospective derivation of a living organoid biobank of colorectal cancer patients. *Cell*. 2015; 161: 933-45. doi: 10.1016/j.cell.2015.03.053.

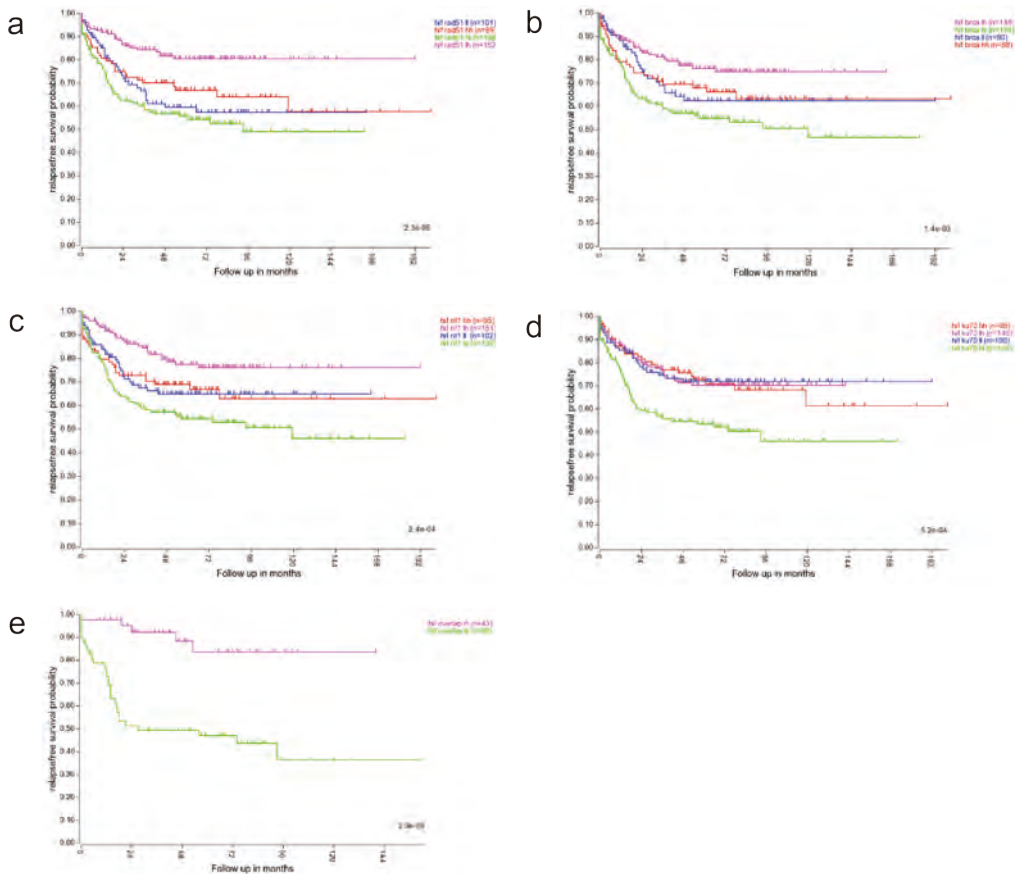
49. Fujii M, Shimokawa M, Date S, Takano A, Matano M, Nanki K, Ohta Y, Toshimitsu K, Nakazato Y, Kawasaki K, Uraoka T, Watanabe T, Kanai T, et al. A Colorectal Tumor Organoid Library Demonstrates Progressive Loss of Niche Factor Requirements during Tumorigenesis. *Cell Stem Cell*. 2016; 18: 827-38. doi: 10.1016/j.stem.2016.04.003.
50. Brown KM, Xue A, Mittal A, Samra JS, Smith R, Hugh TJ. Patient-derived xenograft models of colorectal cancer in pre-clinical research: a systematic review. *Oncotarget*. 2016; 7: 66212-25. doi: 10.18632/oncotarget.11184.
51. Naccarati A, Rosa F, Vymetalkova V, Barone E, Jiraskova K, Di Gaetano C, Novotny J, Levy M, Vodickova L, Gemignani F, Buchler T, Landi S, Vodicka P, et al. Double-strand break repair and colorectal cancer: gene variants within 3' UTRs and microRNAs binding as modulators of cancer risk and clinical outcome. *Oncotarget*. 2016; 7: 23156-69. doi: 10.18632/oncotarget.6804.
52. Huang X, Darzynkiewicz Z. Cytometric assessment of histone H2AX phosphorylation: a reporter of DNA damage. *Methods Mol Biol*. 2006; 314: 73-80. doi: 10.1385/1-59259-973-7:073.



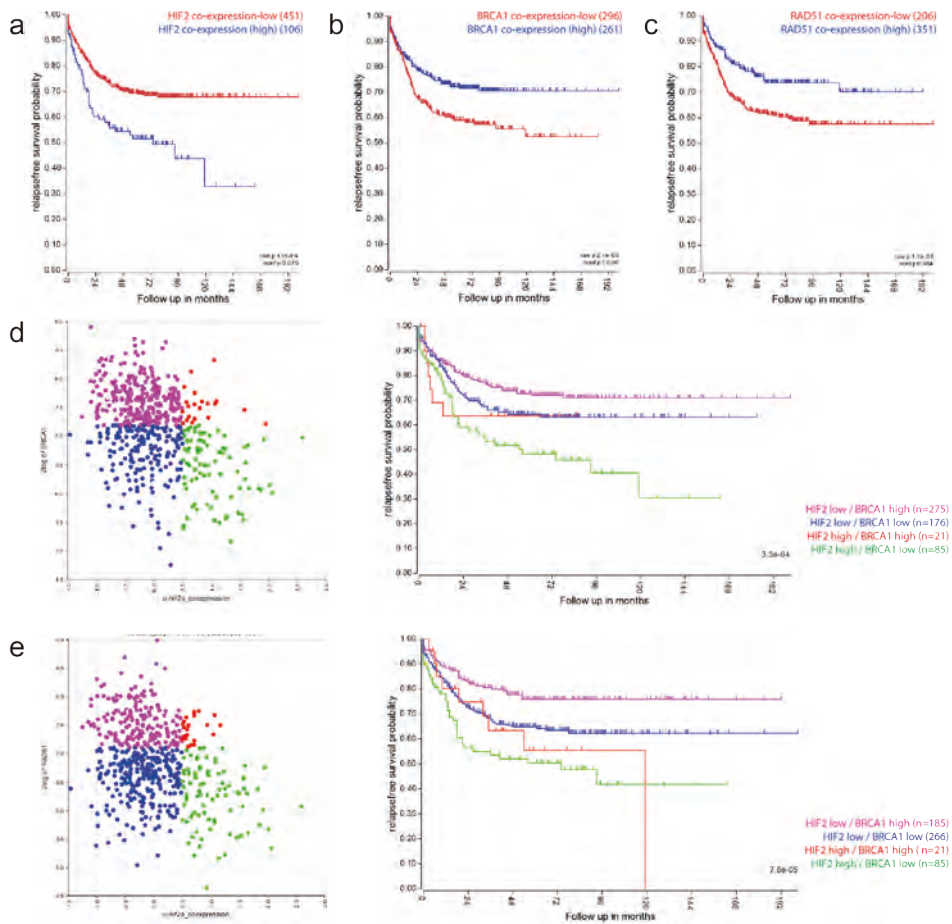
Supplementary information

HR		FA Pathway		MMR		NHEJ		NER	
POLD2	-0,436	UBE2T	-0,438	POLD2	-0,436	FEN1	-0,333	POLD2	-0,436
XRCC3	-0,392	BRCA1	-0,375	LIG1	-0,408	POLL	-0,257	LIG1	-0,408
RAD54L	-0,390	TELO2	-0,373	EXO1	-0,388	XRCC6	-0,222	POLE2	-0,377
RAD54B	-0,385	BRIP1	-0,369	RFC4	-0,349	PRKDC	-0,219	POLE	-0,364
BLM	-0,354	BLM	-0,354	POLD1	-0,345	MRE11A	-0,194	RFC4	-0,349
POLD1	-0,345	FANCA	-0,351	RFC3	-0,339	DNTT	-0,186	POLD1	-0,345
RPA3	-0,318	RMI2	-0,348	RPA3	-0,318	RAD50	-0,161	RFC3	-0,339
RAD51	-0,317	RMI1	-0,344	PCNA	-0,304	POLM	-0,137	RPA3	-0,318
BRCA2	-0,290	FANCC	-0,343	RFC2	-0,293	XRCC5	-0,118	PCNA	-0,304
RAD52	-0,268	FANCB	-0,339	SSBP1	-0,266	XRCC4	-0,117	RFC2	-0,293
SSBP1	-0,266	FANCD2	-0,339	MSH2	-0,264			CDK7	-0,264
SHFM1	-0,229	STRA13	-0,324	POLD3	-0,157			ERCC6	-0,241
TOP3A	-0,229	RPA3	-0,318	MSH3	-0,143			RAD23A	-0,226
TOP3B	-0,208	RAD51	-0,317	MSH6	-0,142			POLE3	-0,211
RAD51B	-0,197	PALB2	-0,313	RPA4	-0,140			POLD3	-0,157
MRE11A	-0,194	FANCG	-0,312					CUL4A	-0,156
SYCP3	-0,191	FAN1	-0,303					CCNH	-0,147
XRCC2	-0,179	FANCE	-0,294					ERCC2	-0,144
RAD50	-0,161	BRCA2	-0,290					RPA4	-0,140
POLD3	-0,157	FANCF	-0,269					GTF2H3	-0,132
EME1	-0,154	FANCI	-0,262					MNAT1	-0,128
RPA4	-0,140	FANCM	-0,239						
RAD51D	-0,114	TOP3A	-0,229						
		TOP3B	-0,208						
		USP1	-0,199						
		FANCL	-0,191						
		ATR	-0,168						
		EME2	-0,161						
		EME1	-0,154						
		RPA4	-0,140						
		POLH	-0,128						
		HES1	-0,126						
		POLI	0,181						
		REV3L	0,205						
		POLK	0,207						

Supplementary Figure 1. The correlation of the HIF2 α co-expression signature with DNA repair genes (a) R2 values of the correlation between HIF2 α and all separate gene sets involved in specific DNA repair pathways (KEGG pathways; www.genome.jp/kegg/).

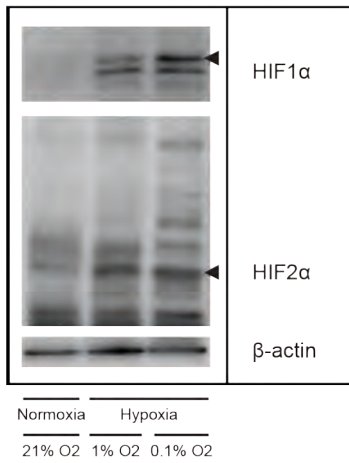


Supplementary Figure 2. Tumors with a high hypoxia signature and low expression of DNA repair genes have a poor prognosis. Kaplan Meier curves show the survival differences between the subgroups identified in Figure 1c, based on median expression values. (a) HIF2-BRCA1. (b) HIF2-RAD51. (c) HIF2-RIF1. (d) HIF2-Ku70. (e) Tumors belonging to each high-high, low-low, high-low and low-high quadrants in all four analyses (a-d) were identified by GeneVenn (www.genevenn.sourceforge.net) and analyzed separately. The Kaplan Meier graph shows the survival differences between the four HIF2-repair subgroups.

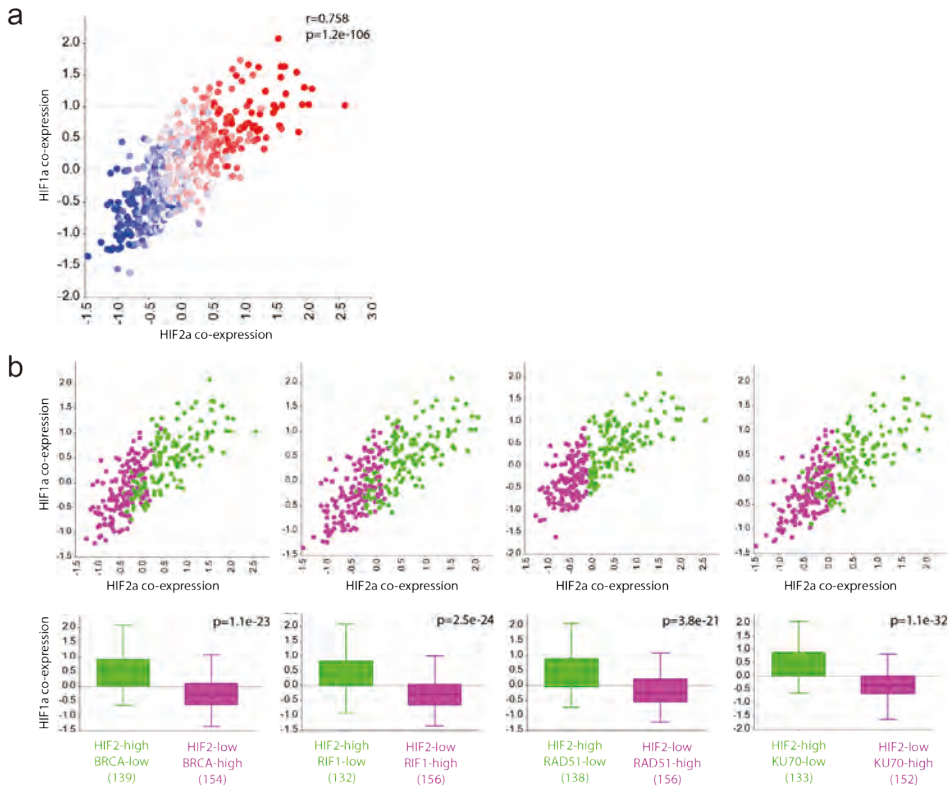


Supplementary Figure 3. HIF2-high/repair-low tumors have a poor prognosis. (a-c) Kaplan scan was performed in R2 (<http://r2.amc.nl>) to identify the optimal cutoff points for the HIF2 co-expression signature, BRCA1 and RAD51. The optimal cutoff points are indicated by the tumor numbers in each group. These cutoff points were then used to generate new quartiles, as in figure 1c. (d-e) Kaplan Meier curves showing the survival differences between the four HIF2-BRCA and HIF2-Rad51 subgroups, based on the Kaplan-scan generated cutoff points.

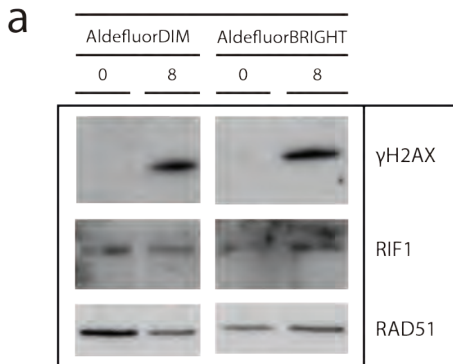
a



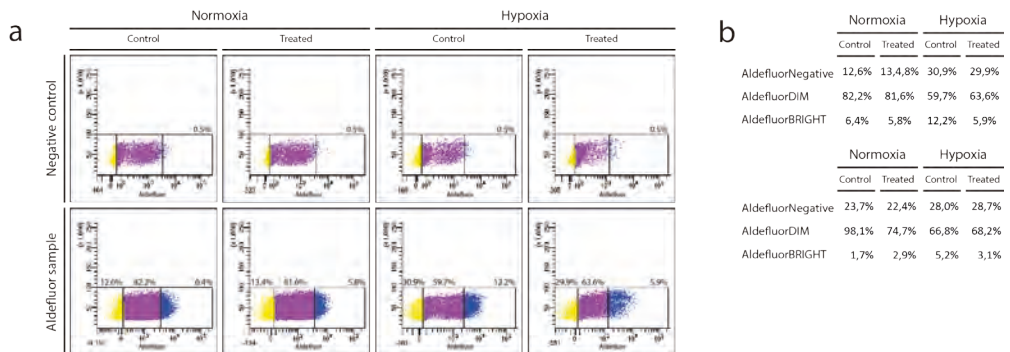
Supplementary Figure 4. In vitro exposure to hypoxia upregulates both HIF1 α and HIF2 α . (a) Human colonospheres were cultured in normoxia (21% O₂), hypoxia (1% O₂) or hypoxia (0.1% O₂) for 24 hours. Cells were lysed and analyzed by Western blotting for the hypoxia markers Hif1 α and Hif2 α (cropped gels).



Supplementary Figure 5. Co-expression of HIF1a and HIF2 a signatures shows an inverse correlation with repair gene expression. (a) Expression of HIF1alpha and HIF2alpha co-expression signatures was determined in 566 tumors of the CIT566 cohort. XY plot analysis shows highly significant co-expression of both signatures. Expression of the signature identifying mesenchymal-type tumors (CMS4) is color-coded from blue (low) to red (high). (b) Expression of the HIF1a signature is significantly higher in all HIF2a-HIGH/repair protein-LOW tumor subgroups.



Supplementary Figure 6. Aldefluor bright cells exposed to hypoxia show more DNA damage after TPZ treatment. (a) Human colonospheres were FACS sorted into Aldefluor^{dim} and Aldefluor^{bright} populations. The sorted cells were either immediately lysed or cultured in hypoxia (0.1% O₂) and treated with TPZ for 8 hours. Cells were lysed and analyzed by Western blotting for the indicated markers (cropped gels).



Supplementary Figure 7. Hypoxia induced increase of CSC is abolished by TPZ treatment. (a) Colonospheres cultured in normoxia or hypoxia, untreated or treated with TPZ and FACS-sorted based on Aldefluor activity. Yellow = Aldefluor^{Negative}, Purple = Aldefluor^{dim}, Blue = Aldefluor^{bright}. (b) Hypoxia- and TPZ-induced changes (in percentage) of Aldefluor activity in colonospheres.



CHAPTER 4

Increased levels of oxidative damage in liver metastases compared with corresponding primary colorectal tumors: association with molecular subtype and prior treatment

Lizet M van der Waals
Jennifer M J Jongen
Sjoerd G Elias
Kateryna Veremiyenko
Kari Trumpi
Anne Trinh
Jamila Laoukili
Inge Ubink
Susanne J van Schelven
Paul J van Diest
Inne HM Borel Rinkes
Onno Kranenburg

Abstract

High levels of oxidative stress in disseminated colorectal cancer (CRC) tumor cells may form a therapeutically exploitable vulnerability. However, it is unclear whether oxidative stress and damage persist in metastases. Therefore, we analyzed markers of oxidative damage in primary colorectal tumors and their corresponding liver metastases. Markers of generic and oxidative DNA damage (γ H2AX and 8-OHdG) were significantly higher in liver metastases compared to their corresponding primary tumors. Chemo- and/or radiotherapy prior to tumor resection was associated with increased persistent oxidative DNA damage and this effect was more pronounced in metastases. Immunohistochemistry-based molecular classification into epithelial-like and mesenchymal-like molecular subtypes, revealed that untreated mesenchymal-like tumors contained lower levels of oxidative DNA damage compared to epithelial-like tumors. Treated mesenchymal-like tumors, but not epithelial-like tumors, showed significantly higher levels of H2AX and 8-OHdG. Mesenchymal-like tumors expressed significantly lower levels of phospho-NRF2, a master regulator of the antioxidant response, and NRF2-controlled genes. Interestingly, a positive 8-OHdG status identified a subgroup of mesenchymal-like metastases with a poor overall survival. An increased capacity to tolerate therapy-induced oxidative damage in mesenchymal-like CRC may explain, at least in part, the poor responsiveness of these tumors to chemotherapy, which could contribute to the poor survival of this patient subgroup.

Introduction

Colorectal cancer (CRC) is a frequently lethal disease.^{1,2} Approximately 20% of patients with CRC present with metastases at diagnosis.² Despite multiple improvements in cancer care such as more effective systemic therapies and improved surgical techniques the median overall survival (OS) of metastatic CRC (mCRC) after chemotherapy combined with targeted agents is still poor, up to approximately 30 months.^{3,4} Clearly, more effective treatment approaches are needed. Characterization of the dependencies and vulnerabilities of metastasized tumor cells may help in designing such therapies.

Oxidative stress is characterized by an imbalance between the production of reactive oxygen species (ROS) and their neutralization by antioxidants. Oxidative stress is known to be a common characteristic of cancer cells that can be exploited therapeutically.⁵ Moderately increased levels of ROS stimulate tumorigenesis by acting as second messengers in tumor-promoting signaling pathways.⁷ Antioxidants are important for maintaining the redox balance in tumor cells, thereby preventing cell death and senescence.⁶ Interestingly, metastasizing tumor cells experience high levels of oxidative stress which is an important barrier to successful establishment of distant metastases.⁸⁻¹⁰ However, not much is known about oxidative stress in established metastases, which are the main targets of systemic therapy in mCRC. Chemotherapy regimens for mCRC are based on fluoropyrimidines (5-fluorouracil or capecitabine) in combination with oxaliplatin, and/or irinotecan.⁴ These chemotherapeutic drugs work, at least in part, by enhancing ROS levels and causing oxidative damage.^{11,12} Moreover, a signature reflecting increased oxidative signaling has been associated with the aggressive mesenchymal (MES) CRC subtype,⁹ now commonly referred to as consensus molecular subtype 4 (CMS4).¹³

Increased oxidative stress during metastatic outgrowth, following chemotherapy, or as a consequence of aggressive tumor biology, could create a therapeutically exploitable vulnerability.¹⁴ To gain insight into patient subgroup(s) that might benefit from such a therapeutic approach, we assessed the levels of oxidative damage and expression of an antioxidant transcription factor in a large series of primary CRC and corresponding colorectal liver metastases (CRLM) in relation to molecular subtypes. During data analysis, prior chemotherapy and/or radiotherapy and 'molecular subtype' were considered as potential factors influencing oxidative stress status.

Materials and Methods

Patients and tissues

The patient cohort was described before.¹⁵ CRC patients that underwent a resection for CRLM at the University Medical Center Utrecht between 2003 and 2014 were included in a prospective database. Their primary tumors were resected in the University Medical

Center Utrecht, Diaconessenhuis Utrecht, St. Antonius Hospital Nieuwegein or Rijnstate hospital at Arnhem. Patients with either synchronous or metachronous CRLM were included. Eventually, 158 mCRC patients were included. Clinicopathological data was available from 129 patients (86 males and 43 females). Median follow-up time was 76 months. Mean age was 62 years (range 37–83 years) at time of surgery for liver metastases. The use of anonymous or coded leftover material for scientific purposes is exempt from informed consent according to Dutch law. Standard treatment agreements include an opt-out for such use.^{16,17}

Tissue microarray construction

A 0.6 mm (triple-core) tissue microarray (TMA) of primary CRC tumors and corresponding CRLM was constructed,¹⁵ from which multiple 4 µm thick sections were cut for immunohistochemical staining.

Treatment status

Primary tumors were considered treated when neoadjuvant chemotherapy and/or radiotherapy was administered. Tissue from liver metastases was considered treated when patients received neoadjuvant chemotherapy for metachronous CRLM. Tissue from synchronous metastases was considered treated when neoadjuvant chemotherapy for primary tumors and/or liver metastases was administered. An overview of treatment status is given in Supplemental Table 1.

Mesenchymal versus epithelial subtypes

All tumors included within the TMA were previously classified as MES-like or epithelial (EPI)-like,¹⁵ using our validated immunohistochemistry (IHC) based classifier.¹⁸ In short, this assay identifies EPI- and MES-like CRC tumors using expression of homeobox protein CDX-2 (CDX2), FERM domain-containing protein 6 (FRMD6), 5-hydroxytryptamine receptor 2B (HTR2B), Zinc finger E-box-binding homeobox 1 (ZEB1), and pan-cytokeratin. High expression of the differentiation marker CDX2 and low immunohistochemical expression of the epithelial-mesenchymal marker ZEB1 identifies EPI-like cancers and increased levels of the vasoactive neurotransmitter HTR2B and goblet cell marker FRMD6 MES-like cancers. In addition, pan-cytokeratin was used to normalize the other markers for epithelial content. Based on the IHC-staining per marker a prediction probability for the MES-like subtype was calculated (MES-probability score). Each individual TMA core was classified as EPI- or MES-like using a MES-probability cut-off of 0.6 (EPI <0.6; MES ≥0.6) and subtype classification was obtained by majority consensus scoring. This individual per core MES-probability score was used to look for putative correlations between per core marker expression and the MES-probability scoring.

Immunohistochemistry

Three immunohistochemical stainings were performed on serial sections of the TMA: phospho-histone H2AX (γH2AX), 8-hydroxy-2'-deoxyguanosine (8-OHdG), and phospho-nuclear factor erythroid 2-related factor 2 (NRF2 also known as NFE2L2).

Supplemental Table 2 gives an overview of antibodies and dilutions, incubation conditions, and antigen-retrieval methods for each marker. For all stainings, sections were deparaffinized with xylene and rehydrated with serial dilutions of ethanol and water. Next, endogenous peroxidase activity was blocked with 1.5% hydrogen peroxide diluted in PBS for 30 minutes. Then, antigen retrieval was performed by boiling samples for 20 minutes in Citrate Buffer pH 6.0 for γ H2AX and 8-OHdG or EDTA buffer pH 9.0 for phospho-NRF2. Protein Block (Novolink Polymer detection Systems, Leica Biosystems, Newcastle Upon Tyne, UK) was applied according to the manufacturer's instructions to block non-specific binding of the anti-8-OHdG antibody. Primary antibody incubation was performed as follows: anti- γ H2AX (Ser139, rabbit, Cell Signaling, Danvers, MA, USA, 2577, 1:50, overnight 4°C), anti-8-OHdG ([N45.1], mouse monoclonal, Abcam, Cambridge, UK, ab48508, 1:500, 1 hour room temperature), anti-NRF2 (phospho S40, rabbit monoclonal, Abcam, ab76026, 1:500, 1 hour room temperature). Subsequently, the secondary antibodies BrightVision poly-HRP-conjugated anti-rabbit or anti-mouse IgG (ImmunoLogic, Duiven, The Netherlands, ready to use) were incubated for 30 minutes at room temperature. All sections were developed with diaminobenzidine for 10 minutes, followed by a hematoxylin counterstaining. Air-dried slides were mounted in a ClearVue Coverslipper (Thermo Fisher Scientific, Waltham, MA). To check for nonspecific binding of the secondary antibody slides were incubated without primary antibodies in the presence of the secondary antibody. Tissues previously validated in the literature as positive controls were used throughout.

Evaluation of staining

Scoring was performed by consensus of two investigators (L.M.W. and K.V.) blinded to clinicopathological data and EPI-versus MES-like subtype, after training by a pathologist (P.J.D.). Damaged and empty TMA cores and those not containing cancer cells were excluded. For 8-OHdG and phospho-NRF2 nuclear staining intensity was scored as 0 (negative), 1 (weak), 2 (moderate) or 3 (strong) (Supplemental Figure 1), ignoring cytoplasmic staining or staining within clearly necrotic regions. For 8-OHdG and phospho-NRF2 the percentage of positive nuclei was scored per intensity, calculating H-scores¹⁹ as follows $(1 \times (\% \text{ cells with intensity } 1) + 2 \times (\% \text{ cells with intensity } 2) + 3 \times (\% \text{ cells with intensity } 3))$. Due to highly heterogeneous intensity of the nuclear γ H2AX staining per cell, only the percentage of positive tumor cells was scored. The mean H-scores (8-OHdG and phospho-NRF2) or percentage positivity (γ H2AX) of 3 cores for each primary tumor specimen or metastatic specimen per patient were calculated. TMA raw data are provided in Supplemental Table 3.

Bioinformatic analyses

All bioinformatic analyses were performed using the R2 Genomics Analysis and Visualization Platform (<https://hgserver1.amc.nl/cgi-bin/r2/main.cgi> registration required). Expression data were obtained from a large composite primary CRC cohort dataset and a CRLM cohort dataset.^{13, 20}

Statistics

All analyses were carried out using IBM SPSS statistics version 23 (IBM corp., Armonk, NY) and Excel version 2013 (Microsoft Corp., Redmond, WA). GraphPad Prism version 7.0 for Windows (GraphPad Software, La Jolla, California, USA) was used for graphical presentation of the data. $p < 0.05$ (two-tailed) was considered statistically significant. All clinicopathological characteristics of the patients were assessed using a Chi-square Test and Independent-samples T-test for the continuous variable age. Correlations between expression of the different immunohistochemical markers within primary CRC tissue or CRLM tissue cores and MES-probability scoring were determined using the Kendall's Tau test. Hydrogen peroxide (H_2O_2) metagene expression within CRC molecular subtypes was compared using a one-way ANOVA. As the IHC expression data was right-skewed, we log-transformed the data before analyzing and comparing mean differences in expression. We report the results on the original scale by back transformation, yielding geometric means and corresponding 95% confidence intervals. To account for values of zero using this approach, we added 0.5 to all data-points before log-transformation, and subtracted this value again from the back transformed results. A paired T-test was applied to the log-transformed data to compare γ H2AX expression, 8-OHdG accumulation, and phospho-NRF2 expression in primary CRC samples and corresponding CRLM and an Independent-samples T-test to compare expression in treated and untreated tumor samples. All other outcomes were compared using a one-way ANOVA followed by a Fisher's LSD test to compare individual groups. For survival analysis, OS was measured from time of liver surgery until death or end of follow-up. Kaplan-Meier survival analyses were performed and survival curves were compared between the different groups by log-rank tests.

Results

Increased oxidative DNA damage in liver metastases compared to primary colorectal tumors

To study DNA damage accumulation in primary CRC tumors and corresponding liver metastases we analyzed phosphorylation of histone 2AX (γ H2AX) as a marker of the formation of DNA double strand breaks. γ H2AX initiates repair of double strand breaks and is a useful marker for their quantification.²¹ We found that γ H2AX levels were significantly increased ($p \leq 0.01$) in liver metastases compared to corresponding primary tumors (Figure 1A, B), indicating an increased load of DNA double strand breaks or repair in mCRC. ROS may cause oxidative damage to the nucleotide precursor pool, which – upon incorporation into DNA – can lead to DNA damage. DNA bases, predominantly guanine, are also susceptible to direct oxidation by ROS and the oxidized base 8-OHdG is therefore a frequently used marker of oxidative DNA damage.²² We observed a significantly increased accumulation of 8-OHdG ($p \leq 0.05$) in metastases compared to the primary tumors from which they were derived (Figure 1A, C).

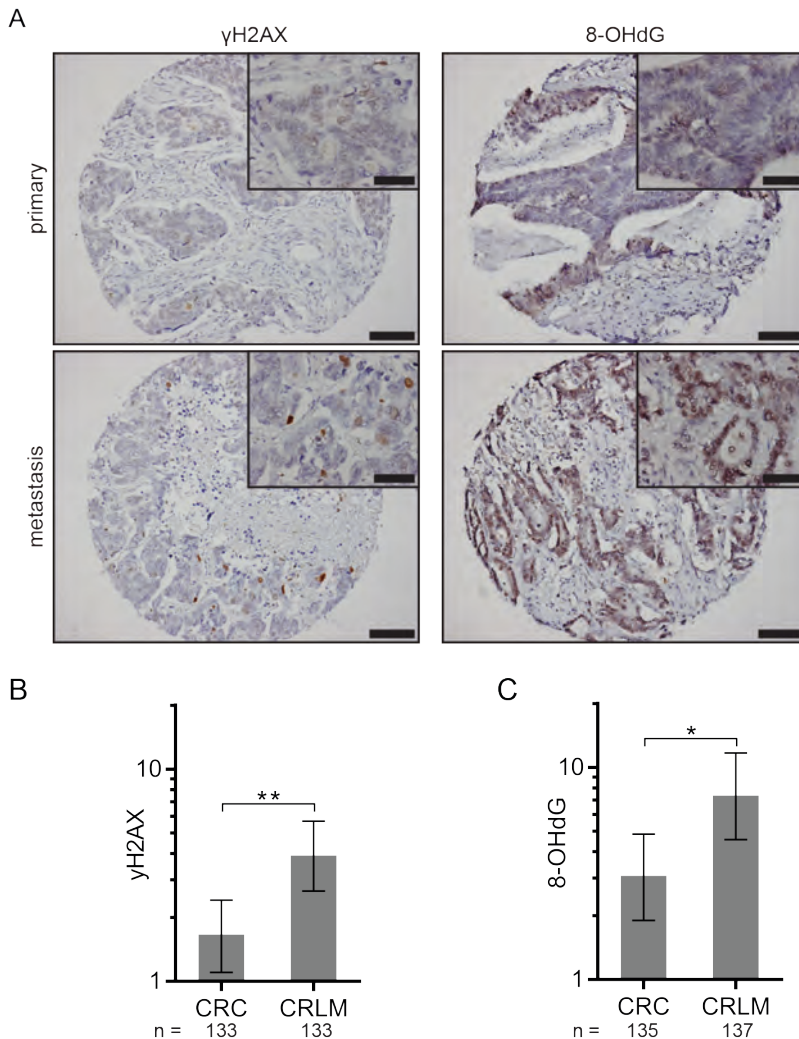


Figure 1. Increased oxidative DNA damage in colorectal liver metastases. (A) Representative images of immunohistochemical expression of γ H2AX and 8-OHdG in primary colorectal cancer (CRC) samples and corresponding colorectal liver metastases (CRLM). x10 microscope objective whole TMA tissue core and x40 microscope objective inset shown. Scale bars: 100 μ m; 50 μ m (inset). Bar graphs showing quantification of γ H2AX expression (B) and 8-OHdG accumulation (C) in CRC tumors versus CRLM. (B-C) A paired T-test was applied to the log-transformed data to compare γ H2AX expression and 8-OHdG accumulation as continuous variable in CRC versus CRLM. *, $p \leq 0.05$; **, $p \leq 0.01$. Error bars represent the geometric mean and corresponding 95% confidence intervals. CRC, colorectal cancer; CRLM, colorectal liver metastases

Accumulation of oxidative damage in therapy-exposed tumors

Chemo- and radiotherapy generate oxidative damage.^{11, 12, 23-25} Therefore, we speculated that the increased accumulation of oxidative DNA damage in CRC liver metastases could be a consequence of differences in treatment status between primary CRC tumors and their corresponding liver metastases. To test this, we stratified tissues according to their treatment status and re-analyzed expression of the different markers. This revealed that treatment prior to tumor resection was associated with a significant increase of γ H2AX levels, both in primary tumors and metastases (Figure 2A; $p \leq 0.05$). In addition, γ H2AX levels were higher in previously untreated metastases compared to untreated primary tumors (Figure 2A).

Levels of 8-OHdG were increased in therapy-exposed metastases (Figure 2B; $p \leq 0.01$) and a similar trend was observed in primary tumors (Figure 2B). Similar to γ H2AX, 8-OHdG levels were also increased in previously untreated liver metastases when compared to untreated primary tumors (Figure 2B).

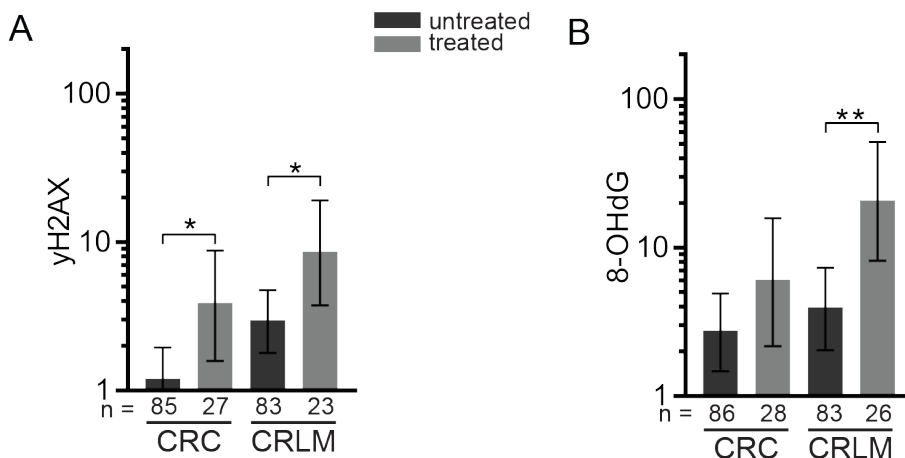


Figure 2. Prior treatment is associated with DNA damage and 8-OHdG accumulation. Bar graphs showing quantification of γ H2AX expression (A) or 8-OHdG accumulation (B) in primary colorectal cancer (CRC) and colorectal liver metastases (CRLM), treated versus untreated tumors. (A) Therapy-exposed CRC and CRLM express higher levels of the DNA damage marker γ H2AX. (B) Therapy-exposed CRC and CRLM accumulate 8-OHdG. (A-B) An unpaired T-test was applied to the log-transformed data to compare groups. *, $p \leq 0.05$; **, $p \leq 0.01$. Error bars represent the geometric mean and corresponding 95% confidence intervals. CRC, colorectal cancer; CRLM, colorectal liver metastases

Accumulation of oxidative damage in therapy-exposed mesenchymal-like tumors

The recent classification of colorectal tumors into molecular subtypes¹³ offers a new paradigm for developing subtype-targeted therapy. One of the subtypes, CMS4, is characterized by a mesenchymal gene expression profile and is associated with a poor prognosis¹³ and high expression of H₂O₂-regulated genes (Supplemental Figure 2 and 9). To assess whether high expression of H₂O₂-regulated genes in mesenchymal-like tumors is associated with increased oxidative damage, we used IHC-based molecular classification to discriminate between EPI-like and MES-like tumors.¹⁸ Previously untreated primary tumors and metastases of the MES-like subtype showed significantly less accumulation of γ H2AX and there was a trend towards less accumulation of 8-OHdG (Figure 3A, B: $p = 0.054$ 8-OHdG primary; $p = 0.057$ 8-OHdG metastasis). Interestingly, levels of γ H2AX and 8-OHdG lesions were significantly higher in MES-like tumors (primary and metastases) that received prior treatment, but not in EPI-like tumors (Figure 3A, B).

Low levels of phospho-NRF2 and its target genes in mesenchymal-like tumors

NRF2 is a transcription factor that induces expression of many antioxidant genes in normal and cancer cells and is considered to be (one of) the most important orchestrators of the cellular antioxidant response.¹⁴ Therefore, we tested whether the levels of active (phospho S40) NRF2 were different between primary tumors and metastases, and between MES- and EPI-like tumors. We found that primary tumors and liver metastases contained similar levels of phospho-NRF2 (Figure 4A). Furthermore, we found a highly significant negative correlation between phospho-NRF2 levels and a MES-like tumor phenotype (Figure 4B and Table 1). Analysis of NRF2 target genes (*i.e.* genes containing NRF2-binding sites, as demonstrated by chromatin immunoprecipitation (ChIP)-sequencing²⁶) in a large composite CRC cohort showed that MES-like tumors (CMS4) express NRF2 target genes – as a proxy for active NRF2 – at significantly lower levels than epithelial subtypes (CMS2, CMS3) (Figure 4C and Supplemental Figure 3). Additionally, low NRF2 mRNA levels in liver metastases were also associated with poor OS, and this effect was most prominent in MES-like tumors (Figure 4D).



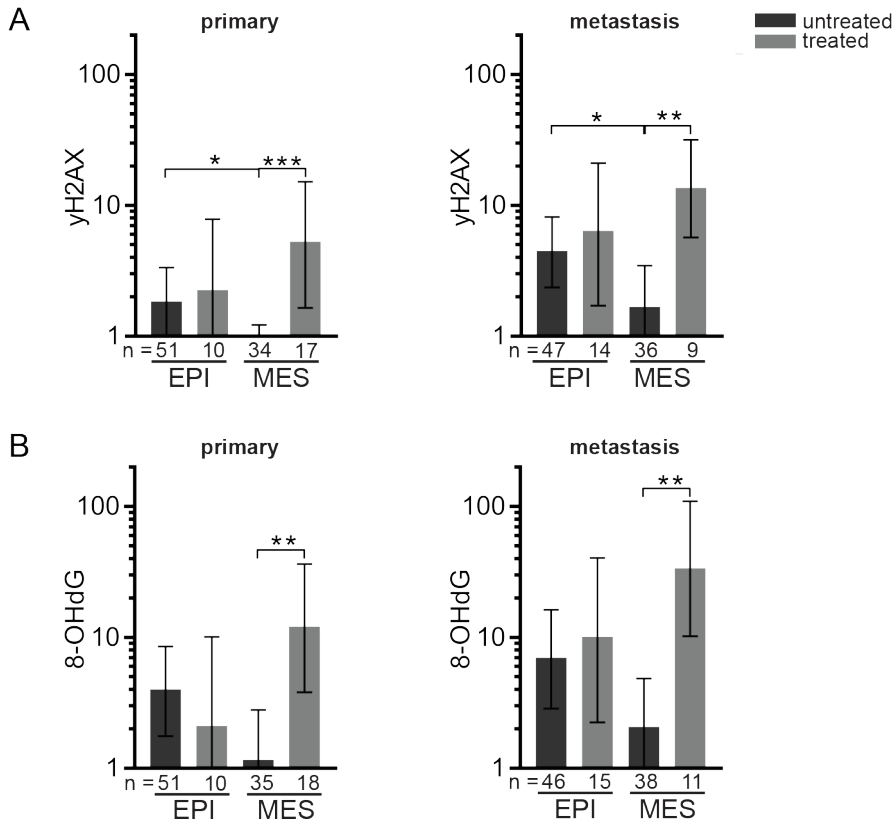


Figure 3. Oxidative DNA damage is increased in treatment-exposed MES-like tumors characterized by low basal levels of DNA damage. (A) Bar graphs showing expression of γ H2AX in primary colorectal cancer and colorectal liver metastases stratified according to treatment status and subtype. (B) Bar graphs showing levels of 8-OHdG in primary colorectal cancer and colorectal liver metastases stratified according to treatment status and subtype. (A-B) A one-way ANOVA and Fisher's LSD post hoc test was applied to the log-transformed data to compare groups. *, $p \leq 0.05$; **, $p \leq 0.01$; ***, $p \leq 0.001$. Error bars represent the geometric mean and corresponding 95% confidence intervals. CRC, colorectal cancer; CRLM, colorectal liver metastases; EPI, epithelial; MES, mesenchymal

Table 1. Correlations between expression of the different immunohistochemical markers within primary colorectal cancer tissue or liver metastatic tissue cores and mesenchymal probability scoring

	CRC			n§	CRLM			n§
	Kendall's τ^*	95% CI †	p-value‡		Kendall's τ^*	95% CI †	p-value‡	
γH2AX	-0.130	(-0.263-0.002)	0.0540	220	-0.057	(-0.190-0.075)	0.398	201
8-OHdG	-0.046	(-0.206-0.114)	0.573	233	-0.052	(-0.203-0.098)	0.496	215
phospho-NRF2	-0.206	(-0.312--0.099)	0.0002	220	-0.142	(-0.272--0.012)	0.0318	214

* Kendall's rank correlation coefficient (Kendall's τ); † 95% confidence interval; ‡ two-sided p-values are given; § n = number of XY pairs. CRC, colorectal cancer; CRLM, colorectal liver metastasis tumor cores.

8-OHdG staining in mesenchymal-like metastases is associated with poor survival

The abundance of oxidative damage in resected tumors may not only serve as an indicator of prior treatment but could also be related to pro-tumorigenic oxidative stress signaling. Therefore, we analyzed OS of patients with EPI- and MES-like metastases with positive (H-score >0) and negative 8-OHdG staining (H-score =0). A positive 8-OHdG status (n=23) in MES-like metastases showed a trend towards significance (p = 0.119) as marker for poor OS (Figure 5A). In contrast, a positive 8-OHdG status in EPI-like metastases was not associated with survival (Figure 5B). In addition, a positive treatment status was associated with a positive 8-OHdG status in MES-like metastases but not in EPI-like metastases (Table 2).

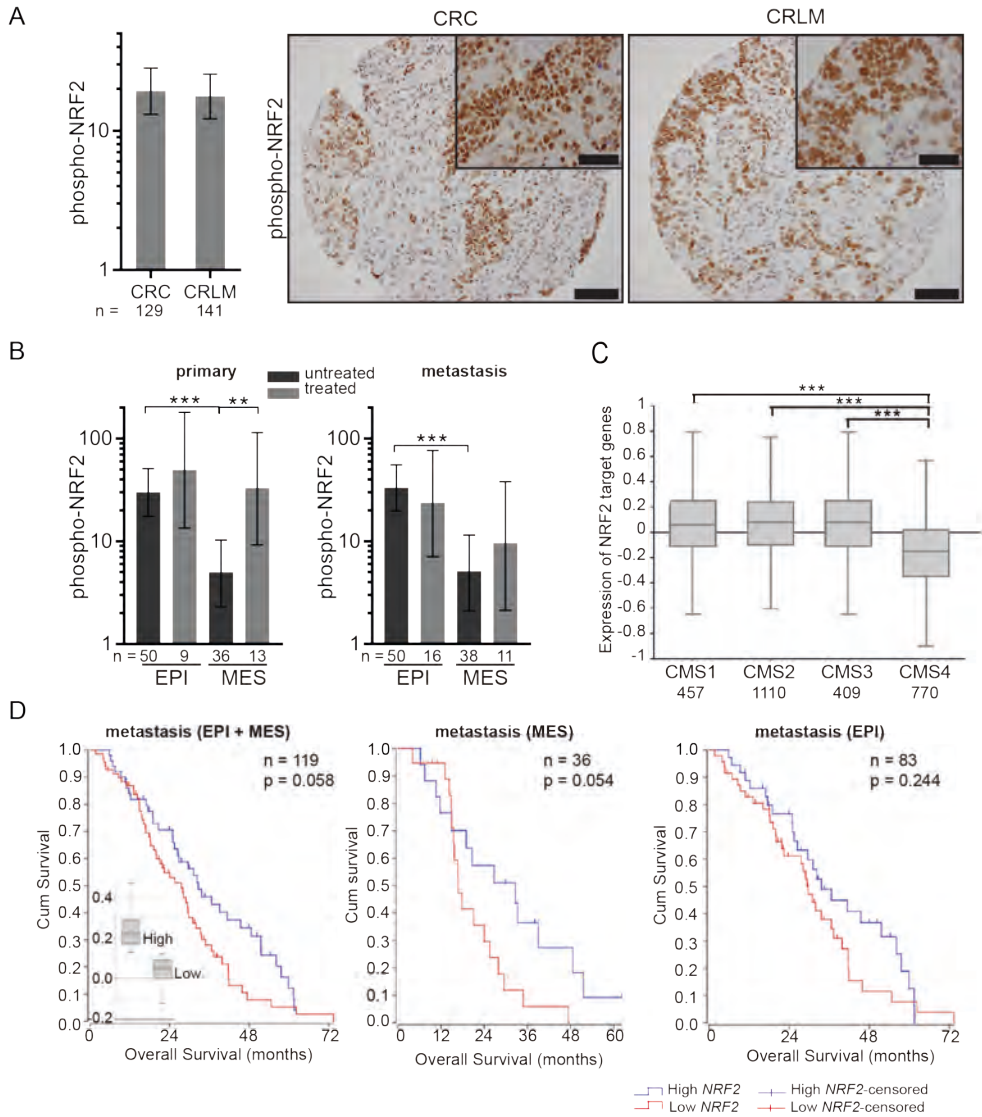


Figure 4. Low basal levels of phospho-NRF2 and its target genes in mesenchymal-like tumors.

(A) Bar graph showing quantification of phospho-NRF2 expression and representative images of immunohistochemical nuclear expression of phospho-NRF2 in primary colorectal cancer (CRC) and corresponding colorectal liver metastases (CRLM). $\times 10$ microscope objective whole TMA tissue core and $\times 40$ microscope objective inset shown. Scale bars: 100 μm ; 50 μm (inset). A paired T-test was applied to the log-transformed data to compare phospho-NRF2 expression as continuous variable in CRC versus CRLM. Error bars represent the geometric mean and corresponding 95%

confidence intervals. (B) Low basal levels of phospho-NRF2 in mesenchymal-like tumors. A one-way ANOVA and Fisher's LSD post hoc test was applied to the log-transformed data to compare groups. **, $p \leq 0.01$; ***, $p \leq 0.001$. Error bars represent the geometric mean and corresponding 95% confidence intervals. (C) Expression of NRF2 target genes within 3232 colorectal cancer tumors classified according to their molecular subtype¹³. The following NRF2 target genes were included in the analyses: *ABCC4*, *ALDH3A1*, *AOX1*, *CAT*, *CHAC1*, *ENTPD5*, *FAM3B*, *GCLC*, *GCLM*, *GSR*, *HMOX1*, *HTATIP2*, *IDH1*, *LRP8*, *MAGOHB*, *MGST1*, *MOCOS*, *NQO1*, *PRR13*, *RNF183*, *SLC19A2*, *SLC22A23*, *SLC7A11*, *TRIB3*, *VASN*, *ZFP36*. ANOVA p-values: ***, $p \leq 0.001$. The box represents the median and middle 50% of the scores. The upper and lower whiskers represent scores outside the middle 50%. (D) Kaplan-Meier curves showing the differences in overall survival between NRF2 'high' and 'low' subgroups in a cohort consisting of patients undergoing resection for their colorectal liver metastases²⁰. Levels of NRF2 mRNA in liver metastases was used to generate 'high' and 'low' subgroups, using the average as a cut-off point. NRF2 mRNA levels in both groups are shown in the inset. Significance was tested using the log-rank test. CRC, colorectal cancer; CRLM, colorectal liver metastases; EPI, epithelial; MES, mesenchymal.



Table 2. Patient and liver metastasis characteristics of the classified patients

	epithelial-like metastases (n=69)		mesenchymal-like metastases (n=60)		p-value*	
	8-OHdG UNK n=11 (%)	8-OHdG- 8OHdG+ n=27 (%)	8-OHdG UNK n=14 (%)	8-OHdG- 8OHdG+ n=24 (%)		
Mean age						
years, range	- -	63 (37-82)	- -	63 (46-83)	0.415 (42-77)	0.110 (43-78)
Sex						
Male	- -	20 74	- -	14 64	0.792	14 58
Female	- -	7 26	- -	8 36		10 42
Onset						
Synchronous	- -	14 52	- -	12 55	0.134	10 42
Metachronous	- -	13 48	- -	10 46		14 58
Treatment status						
Treated	- -	6 22	- -	0 0	0.555	9 38
Untreated	- -	21 78	- -	22 100		15 63

* All Chi-square Test (categorical data) except for the continuous variable age at surgery (Independent-samples T-test). UNK, unknown; -, negative; +, posi

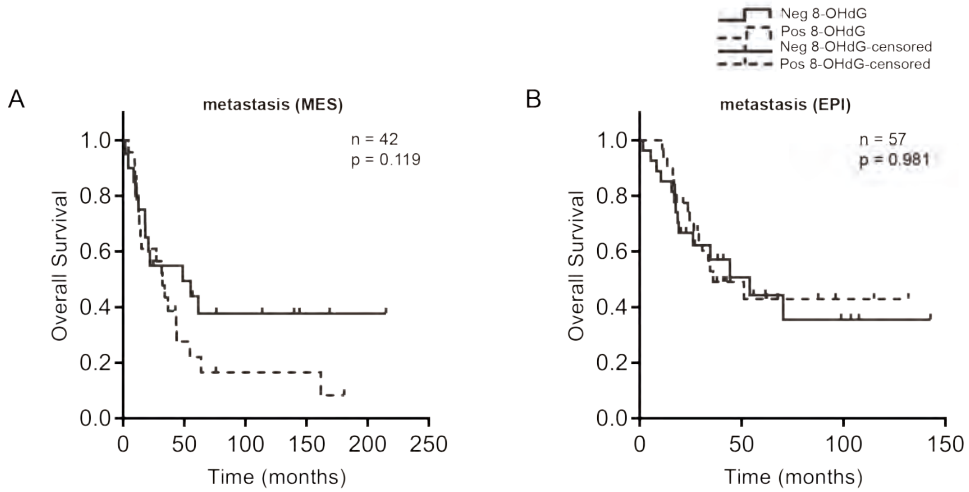


Figure 5. 8-OHdG positivity identifies a group of poor-prognostic mesenchymal-like metastases. (A) Kaplan-Meier curves showing the differences in overall survival between 8-OHdG positive and 8-OHdG negative MES-like metastases. Significance was tested using the log-rank test. (B) Kaplan-Meier curves showing the differences in overall survival between 8-OHdG positive and 8-OHdG negative EPI-like metastases. Significance was tested using the log-rank test. Neg, negative; Pos, positive

Discussion

CRC patients with metastatic disease have a poor prognosis^{3,4} and effective therapeutic approaches that have an impact on long-term survival are urgently needed. Targeting the increased redox status of tumor cells could be such an approach. Our data show that CRC liver metastases are characterized by high levels of oxidative DNA damage. This is in line with a recent report showing that metastatic melanoma nodules express significantly higher levels of ROS in a human melanoma xenograft model.¹⁰ Interestingly, our data points to higher oxidative stress levels in treatment-naïve CRC metastases compared to primary tumors. This indicates that factors distinct from treatment status, such as microenvironmental cues, and/or intrinsic differences between metastasis-competent and incompetent tumor cell clones could be responsible for the different levels of oxidative damage in primary tumors and metastases.

Expression of the DNA damage markers γ H2AX and 8-OHdG in CRC liver metastases was significantly higher in patients that had received treatment. This may be due to a sustained chemo- and radiotherapy-induced elevation of ROS^{12,23} and 8-OHdG lesions²⁴.

Additional experiments will be necessary to assess the causal relationship between treatment and redox status. Such studies will require the prospective collection of tumor biopsies before and after treatment.

Effective therapies for poor-prognosis MES-like CRC tumors^{13,15,18} are urgently needed. We observed that these tumors are characterized by low expression of γ H2AX, 8-OHdG and phospho-NRF2. Although phospho-NRF2 might not adequately reflect NRF2 activation status²⁷, MES-like tumors also expressed low levels of NRF2 target genes. Moreover, low mRNA levels of *NFE2L2* (the gene encoding NRF2) in primary tumors were associated with poor survival in the colorectal adenocarcinoma (COADREAD) cohort as shown by the Human Protein Atlas (<https://www.proteinatlas.org/ENSG00000116044-NFE2L2/pathology/tissue/colorectal+cancer+v18> Human Protein Atlas). Finally, low levels of *NRF2* mRNA in CRC metastases identified a subgroup of MES-like tumors with a poor OS.

The correlation of low phospho-NRF2 protein levels, low *NFE2L2* mRNA and low NRF2 target gene expression with an aggressive tumor phenotype is somewhat surprising, considering that sustained and constitutive activation of NRF2 is known to promote tumor growth²⁸ and chemotherapy-resistance²⁹. Possibly, mRNA or phospho-NRF2 levels may not adequately reflect total NRF2 activity. Alternatively, NRF2 regulation of cancer cell viability may be context-dependent. Finally, the levels of NRF2 expressed at the time of tumor resection may not reflect the ability of these tumors to mount a NRF2 response and increase their antioxidant capacity in response to ROS insults. Indeed, phospho-NRF2 protein levels were significantly higher in MES-like tumors that had been exposed to prior treatment. Although markers of oxidative damage were also higher in these tumors, they clearly survived treatment. This suggests that MES-like tumors may have a higher tolerance for therapy-induced oxidative damage than EPI-like tumors, which may (partly) explain their relative resistance to chemotherapy.³⁰ Importantly, a definitive assessment of the role of NRF2, its phosphorylation, and activation of its target genes in colorectal cancer progression requires further studies in model systems and human tissues. In particular, it will be interesting to investigate whether a higher tolerance for oxidative stress, possibly relying on NRF2 activity, contributes to the higher metastatic potential of aggressive MES-like tumors.

Given that moderately increased levels of oxidative stress may have tumor-promoting effects⁷ we explored whether a positive 8-OHdG status identifies aggressive CRC metastases. Interestingly, our data suggest that patients with 8-OHdG-positive MES-like metastases have a shorter OS, whereas 8-OHdG status did not seem to be associated with OS in patients with EPI-like tumors. Our results therefore suggest that a further sub-classification (on the basis of redox status) may improve the prognostic value of colon cancer subtyping, at least in the metastatic setting. Finally, this may help selecting patients for specific types of targeted therapies, particularly those targeting the redox status of tumor cells. The value of such an approach should now be evaluated in pre-clinical studies using models of MES-like and EPI-like CRC.

In conclusion, therapeutics that interfere with redox status might be particularly effective in targeting metastases, therapy-surviving tumor cells, and MES-like tumors and might be administered in combination with conventional oxidative stress-inducing radio- and chemotherapeutics. Further studies will be needed to clarify whether markers of redox status could have prognostic and/or predictive value.

List of abbreviations

CMS	– consensus molecular subtype
CRC	– colorectal cancer
CRLM	– colorectal liver metastases
EPI	– epithelial
H ₂ O ₂	– hydrogen peroxide
IHC	– immunohistochemistry
mCRC	– metastatic colorectal cancer
MES	– mesenchymal
NRF2	– nuclear factor erythroid 2-related factor 2
8-OHdG	– 8-hydroxy-2'-deoxyguanosine
OS	– overall survival
ROS	– reactive oxygen species
TMA	– tissue microarray
γH2AX	– phospho-histon



References

1. Ferlay J, Steliarova-Foucher E, Lortet-Tieulent J, Rosso S, Coebergh JW, Comber H, Forman D, Bray F: Cancer incidence and mortality patterns in Europe: estimates for 40 countries in 2012. *European journal of cancer (Oxford, England : 1990)* 2013, 49:1374-403
2. Siegel R, Desantis C, Jemal A: Colorectal cancer statistics, 2014. *CA: a cancer journal for clinicians* 2014, 64:104-17
3. Loupakis F, Cremolini C, Masi G, Lonardi S, Zagonel V, Salvatore L, Cortesi E, Tomasello G, Ronzoni M, Spadi R, Zaniboni A, Tonini G, Buonadonna A, Amoroso D, Chiara S, Carlomagno C, Boni C, Allegrini G, Boni L, Falcone A: Initial therapy with FOLFOXIRI and bevacizumab for metastatic colorectal cancer. *The New England journal of medicine* 2014, 371:1609-18
4. Cremolini C, Schirripa M, Antoniotti C, Moretto R, Salvatore L, Masi G, Falcone A, Loupakis F: First-line chemotherapy for mCRC—a review and evidence-based algorithm. *Nature reviews Clinical oncology* 2015, 12:607-19
5. Trachootham D, Zhou Y, Zhang H, Demizu Y, Chen Z, Pelicano H, Chiao PJ, Achanta G, Arlinghaus RB, Liu J, Huang P: Selective killing of oncogenically transformed cells through a ROS-mediated mechanism by beta-phenylethyl isothiocyanate. *Cancer cell* 2006, 10:241-52
6. Cairns RA, Harris IS, Mak TW: Regulation of cancer cell metabolism. *Nature reviews Cancer* 2011, 11:85-95
7. Wiseman H, Halliwell B: Damage to DNA by reactive oxygen and nitrogen species: role in inflammatory disease and progression to cancer. *The Biochemical journal* 1996, 313 (Pt 1):17-29
8. Schafer ZT, Grassian AR, Song L, Jiang Z, Gerhart-Hines Z, Irie HY, Gao S, Puigserver P, Brugge JS: Antioxidant and oncogene rescue of metabolic defects caused by loss of matrix attachment. *Nature* 2009, 461:109-13
9. Emmink BL, Laoukili J, Kipp AP, Koster J, Govaert KM, Fatrai S, Verheem A, Steller EJ, Brigelius-Flohe R, Jimenez CR, Borel Rinke IH, Kranenburg O: GPx2 suppression of H₂O₂ stress links the formation of differentiated tumor mass to metastatic capacity in colorectal cancer. *Cancer research* 2014, 74:6717-30
10. Piskounova E, Agathocleous M, Murphy MM, Hu Z, Huddlestun SE, Zhao Z, Leitch AM, Johnson TM, DeBerardinis RJ, Morrison SJ: Oxidative stress inhibits distant metastasis by human melanoma cells. *Nature* 2015, 527:186-91
11. Alexandre J, Nicco C, Chereau C, Laurent A, Weill B, Goldwasser F, Batteux F: Improvement of the therapeutic index of anticancer drugs by the superoxide dismutase mimic mangafodipir. *Journal of the National Cancer Institute* 2006, 98:236-44

12. Arifa RD, Madeira MF, de Paula TP, Lima RL, Tavares LD, Menezes-Garcia Z, Fagundes CT, Rachid MA, Ryffel B, Zamboni DS, Teixeira MM, Souza DG: Inflammasome activation is reactive oxygen species dependent and mediates irinotecan-induced mucositis through IL-1 β and IL-18 in mice. *The American journal of pathology* 2014, 184:2023-34
13. Guinney J, Dienstmann R, Wang X, de Reynies A, Schlicker A, Sonesson C, Marisa L, Roepman P, Nyamundanda G, Angelino P, Bot BM, Morris JS, Simon IM, Gerster S, Fessler E, De Sousa EMF, Missiaglia E, Ramay H, Barras D, Homicsko K, Maru D, Manyam GC, Broom B, Boige V, Perez-Villamil B, Laderas T, Salazar R, Gray JW, Hanahan D, Taberero J, Bernardis R, Friend SH, Laurent-Puig P, Medema JP, Sadanandam A, Wessels L, Delorenzi M, Kopetz S, Vermeulen L, Tejpar S: The consensus molecular subtypes of colorectal cancer. *Nature medicine* 2015, 21:1350-6
14. Gorrini C, Harris IS, Mak TW: Modulation of oxidative stress as an anticancer strategy. *Nature reviews Drug discovery* 2013, 12:931-47
15. Trumpi K, Ubink I, Trinh A, Djafarimedani M, Jongen JM, Govaert KM, Elias SG, van Hooff SR, Medema JP, Lacle MM, Vermeulen L, Borel Rinkes IHM, Kranenburg O: Neoadjuvant chemotherapy affects molecular classification of colorectal tumors. *Oncogenesis* 2017, 6:e357
16. van Diest PJ: No consent should be needed for using leftover body material for scientific purposes. *For. BMJ (Clinical research ed)* 2002, 325:648-51
17. Coebergh JWW on behalf of the FMWV Society: Federa: Human tissue and medical research: code of conduct for responsible use (2011). Rotterdam, the Netherlands: FMWV, 2011
18. Trinh A, Trumpi K, De Sousa EMF, Wang X, de Jong JH, Fessler E, Kuppen PJ, Reimers MS, Swets M, Koopman M, Nagtegaal ID, Jansen M, Hooijer GK, Offerhaus GJ, Kranenburg O, Punt CJ, Medema JP, Markowitz F, Vermeulen L: Practical and Robust Identification of Molecular Subtypes in Colorectal Cancer by Immunohistochemistry. *Clinical cancer research : an official journal of the American Association for Cancer Research* 2017, 23:387-98
19. van Diest PJ, van Dam P, Henzen-Logmans SC, Berns E, van der Burg ME, Green J, Vergote I: A scoring system for immunohistochemical staining: consensus report of the task force for basic research of the EORTC-GCCG. European Organization for Research and Treatment of Cancer-Gynaecological Cancer Cooperative Group. *Journal of clinical pathology* 1997, 50:801-4
20. Snoeren N, van Hooff SR, Adam R, van Hillegersberg R, Voest EE, Guettier C, van Diest PJ, Nijkamp MW, Brok MO, van Leenen D, Koerkamp MJ, Holstege FC, Rinkes IH: Exploring gene expression signatures for predicting disease free survival after resection of colorectal cancer liver metastases. *PLoS one* 2012, 7:e49442
21. Kuo LJ, Yang LX: Gamma-H2AX - a novel biomarker for DNA double-strand breaks. *In vivo (Athens, Greece)* 2008, 22:305-9
22. Klaunig JE, Kamendulis LM, Hocevar BA: Oxidative stress and oxidative damage in carcinogenesis. *Toxicologic pathology* 2010, 38:96-109

23. Tulard A, Hoffschir F, de Boisferon FH, Luccioni C, Bravard A: Persistent oxidative stress after ionizing radiation is involved in inherited radiosensitivity. *Free radical biology & medicine* 2003, 35:68-77
24. Siomek A, Tujakowski J, Gackowski D, Rozalski R, Foksinski M, Dziaman T, Roszkowski K, Olinski R: Severe oxidatively damaged DNA after cisplatin treatment of cancer patients. *International journal of cancer* 2006, 119:2228-30
25. Preston TJ, Henderson JT, McCallum GP, Wells PG: Base excision repair of reactive oxygen species-initiated 7,8-dihydro-8-oxo-2'-deoxyguanosine inhibits the cytotoxicity of platinum anticancer drugs. *Molecular cancer therapeutics* 2009, 8:2015-26
26. Hirotsu Y, Katsuoka F, Funayama R, Nagashima T, Nishida Y, Nakayama K, Engel JD, Yamamoto M: Nrf2-MafG heterodimers contribute globally to antioxidant and metabolic networks. *Nucleic acids research* 2012, 40:10228-39
27. Sun Z, Huang Z, Zhang DD: Phosphorylation of Nrf2 at multiple sites by MAP kinases has a limited contribution in modulating the Nrf2-dependent antioxidant response. *PLoS one* 2009, 4:e6588
28. Ma Q: Role of nrf2 in oxidative stress and toxicity. *Annual review of pharmacology and toxicology* 2013, 53:401-26
29. Wang XJ, Sun Z, Villeneuve NF, Zhang S, Zhao F, Li Y, Chen W, Yi X, Zheng W, Wondrak GT, Wong PK, Zhang DD: Nrf2 enhances resistance of cancer cells to chemotherapeutic drugs, the dark side of Nrf2. *Carcinogenesis* 2008, 29:1235-43
30. Song N, Pogue-Geile KL, Gavin PG, Yothers G, Kim SR, Johnson NL, Lipchik C, Allegra CJ, Petrelli NJ, O'Connell MJ, Wolmark N, Paik S: Clinical Outcome From Oxaliplatin Treatment in Stage II/III Colon Cancer According to Intrinsic Subtypes: Secondary Analysis of NSABP C-07/NRG Oncology Randomized Clinical Trial. *JAMA oncology* 2016, 2:1162-9

Supplementary information

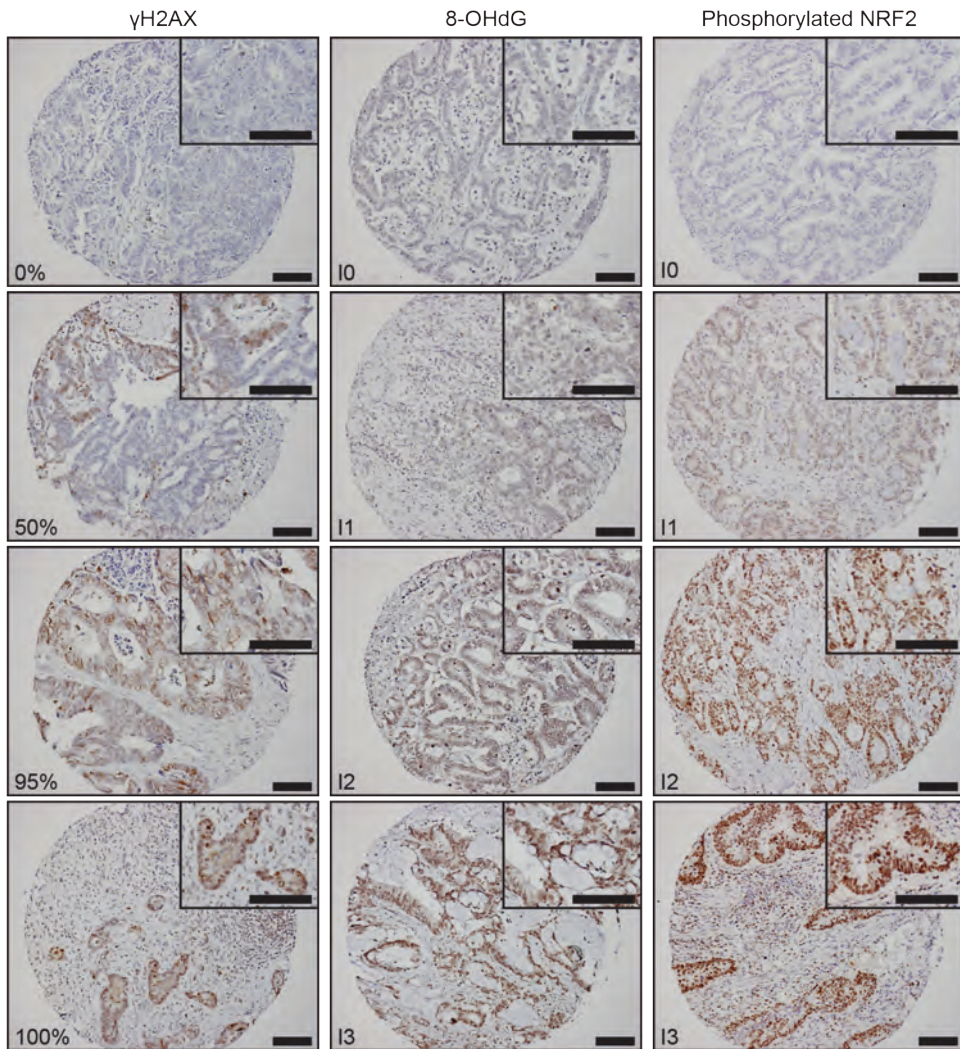
Supplemental Table 1. Treatment status of the tumor tissue included within the tissue microarray.

	All primary tumors		epithelial-like		mesenchymal-like		p-value*
	n=129	(%)	n=61	(%)	n=68	(%)	
Treatment status primary tumors							
Treated	34	26.4	10	16.4	24	35.3	0.015
Untreated	95	73.6	51	83.6	44	64.7	
	All metastases		epithelial-like		mesenchymal-like		p-value
	n=129	(%)	n=69	(%)	n=60	(%)	
Treatment status metastasis							
Treated	32	24.8	16	23.2	16	26.7	0.648
Untreated	97	75.2	53	76.8	44	73.3	

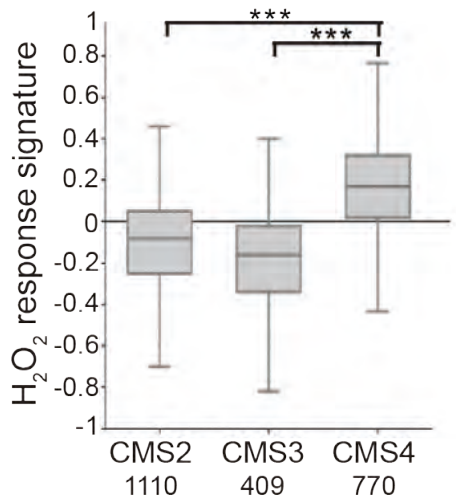
* All Chi-square Test (categorical data).

Supplemental Table 2. Overview of the immunohistochemical staining procedure per marker.

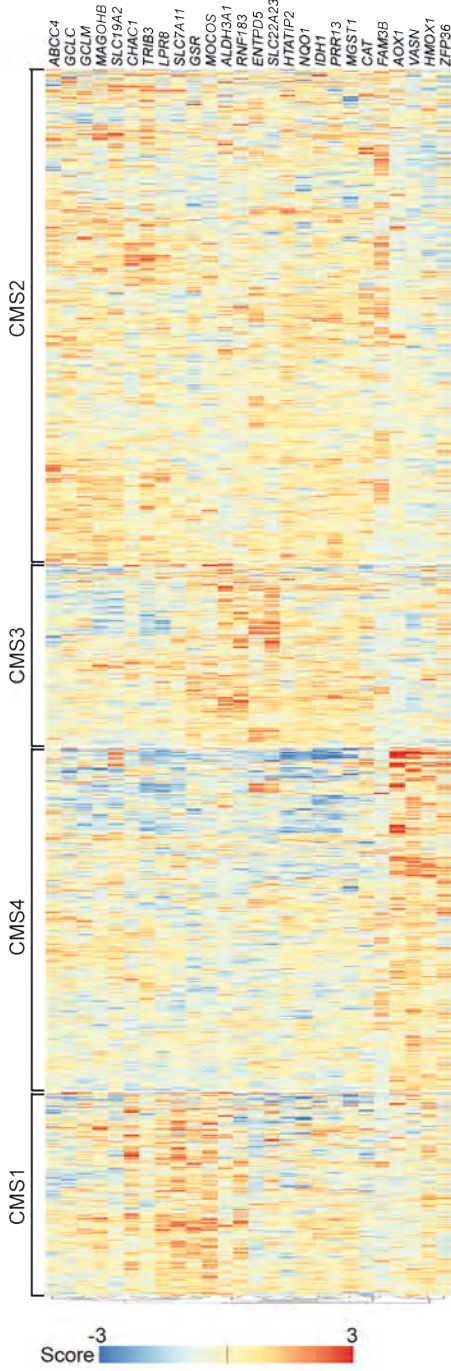
Marker	Primary Antibody	Dilution	Incubation time/ temp (primary antibody)	Antigen Retrieval	Re-marks	Positive control(s)
H2AX	anti-phospho-histone H2AX (Ser139) rabbit, Cell Signaling, 2577	1:50	overnight 4°C	Citrate		Seminoma
8-OHdG	anti-8-hydroxy-2'-deoxyguanosine mouse monoclonal [N45.1], Abcam, ab48508	1:500	1 hour room temperature	Citrate	Protein Block (No-volink)	Urinary bladder Fatty liver
phospho-NRF2	anti-NRF2 (phospho S40) rabbit monoclonal, Abcam, ab76026	1:500	1 hour room temperature	EDTA		Kidney Urinary bladder



Supplemental Figure 1. Representative pictures as example of immunohistochemical percentage (γ H2AX) and intensity (8-OHdG and phospho-NRF2) scoring of colorectal carcinoma TMA cores. Scale bar: 100 μ m (\times 10 microscope objective). For γ H2AX representative images of different percentages positivity are shown. For 8-OHdG and phospho-NRF2 representative images of the different staining intensities: 0 (negative), 1 (weak), 2 (moderate) or 3 (strong) are shown. I = intensity



Supplemental Figure 2. MES-like colon tumors express high levels of an H₂O₂-response signature. mRNA levels of genes upregulated by H₂O₂ within 3232 colorectal cancer tumors classified according to their molecular subtype.¹³ ANOVA p-values: ***, p ≤ 0.001. The box represents the median and middle 50% of the scores. The upper and lower whiskers represent scores outside the middle 50%. CMS, consensus molecular subtype.



Supplemental Figure 3. (left) Heatmap showing low expression of NRF2 target genes in CMS4 (MES-like) tumors. Expression of NRF2 target genes within 3232 colorectal cancer tumors clustered according to their molecular subtype¹³ and gene expression profile.

PART II

Radioembolization in metastatic Colorectal Cancer



CHAPTER 5

Progressive disease after treatment with radioembolization in patients with metastatic colorectal cancer is most often due to new lesions

Jennifer M.J. Jongen
Caren van Roekel
Maarten Smits
Sjoerd G. Elias
Miriam Koopman
Onno Kranenburg
Inne H.M. Borel Rinkes
Marnix G.E.H. Lam

Abstract

Background: Despite adequate tumor targeting, most metastatic colorectal cancer patients experience progressive disease early after radioembolization treatment. To investigate the need for a more restricted patient selection, the mode of progression was assessed.

Materials and Methods: Intra- and extrahepatic lesions from 90 eligible patients were evaluated according to RECIST 1.1 at baseline and 3 months after treatment. Correlations between baseline characteristics and mode of progression and survival, were evaluated.

Results: Progressive disease at three months (69 patients; 77%) was based on growth of existing intrahepatic lesions (n=20), new intrahepatic lesions (n=35), growth of existing extrahepatic lesions (n=37) and/or new extrahepatic lesions (n=57). Progression on multiple levels was seen in 46 patients. Seventy-three percent of the total cohort presented with extrahepatic lesions at 3-month follow-up. Progression was solely based on new extrahepatic lesions in 17 patients. Presence of extrahepatic lesions at baseline increased the chance of development of new extrahepatic lesions (OR 3.06 [1.28;7.72]) and new lesions in general (OR 2.86 [1.14;7.66]). Sixty percent of the patients without extrahepatic lesions at baseline were diagnosed with progressive disease at 3-month follow-up compared to 95% with extrahepatic lesions at baseline ($p < 0.0001$). Patients with extrahepatic disease at baseline compared to those without, had worse median OS: 6 versus 10 months ($p = 0.0005$) (HR=1.93, 95% CI [1.33;2.79]).

Conclusion: Progressive disease after radioembolization was most often based on the presence of new lesions at 3-month follow-up. Patients with extrahepatic disease at baseline had a significantly higher chance of progression compared to patients without extrahepatic disease at baseline.

Keywords

Metastatic Colorectal Cancer, Radioembolization, Progression, RECIST, Extrahepatic Lesions

Introduction

About 45% of the patients with colorectal cancer (CRC) develops metastases [1, 2]. This makes metastatic CRC (mCRC) one of the most lethal diseases worldwide [3, 4]. So far, surgery remains the only treatment with curative intent, either with or without (neo) adjuvant systemic therapy. However, in 80% of all patients with liver metastases, these are irresectable [5]. These patients are treated with doublet or triplet chemotherapy regimens with or without targeted agents, potentially followed by second or third line therapy, after which patients eventually will reach a refractory state.

Radioembolization (RE) is a potential locoregional treatment for refractory patients with liver-only or liver-dominant disease. Intra-arterial administration of radioactive microspheres is proven to be safe and effective [6]. Microspheres (± 30 μm) are loaded with the radioactive isotope yttrium-90 (^{90}Y) or holmium-166 (^{166}Ho) and injected via the hepatic artery [7]. The injected microspheres embolize the microvasculature surrounding the tumour and emit high-energy beta radiation. The remainder of the liver is largely spared since healthy liver tissue is mainly supplied by the portal vein [8-10].

Response of RE in mCRC patients is usually evaluated by the Response Evaluation Criteria in Solid Tumors (RECIST) [11-13]. When using these criteria, the results of most RE clinical studies in metastatic (liver) disease are modest [14-17]. This raises the question how to increase response rates, for instance by optimizing dosage and delivery [18] [19], but also with respect to patient selection and possible concomitant therapies. To study this, first an inventory of the mode of progression in mCRC patients after RE has to be made. Whether these patients show progression based on growth of intrahepatic lesions, growth of extrahepatic lesions, new lesions or a combination of those is currently underexplored. Hence, the aim of this study was to assess the mode of progression and explore its relation with baseline determinants in mCRC patients after RE.

Materials and Methods

Patient selection and study design

A total of 129 patients with irresectable, liver-dominant mCRC were treated with RE at our institution between August 2009 and January 2017, predominantly as part of the HEPAR-2 (Radioactive Holmium Microspheres for the Treatment of Unresectable Liver Metastases) [19], or RADAR trial (RADioembolization: Angiogenic factors and Response) [18]. These studies were all conducted in accordance with the Medical Ethical Committee of the University Medical Center Utrecht and informed consent was obtained from all patients before study inclusion. The need for informed consent for this additional retrospective analysis was waived. Patients were only included if CT and/or MRI scans were available at baseline and after 3-months follow-up. Patients were treated with either ^{166}Ho -microspheres or glass (TheraSphere[®], BTG) / resin (SIR-spheres[®], SIRTEX



medical) 90Y-microspheres. The electronic medical record was reviewed to obtain all patient characteristics. Several baseline characteristics were compared because they have proven to be independent prognostic factors in patients with mCRC [17, 20-27].

Radioembolization

The injected activity for the patients that were treated with glass 90Y-microspheres was calculated according to the so-called MIRD method, with a desired absorbed dose of 80-120 Gy [28-30]. For the patients that were treated with resin 90Y-microspheres, the body surface area (BSA) method was used. The injected activity for 166Ho-microspheres was calculated based on the MIRD method with an aimed whole-liver absorbed dose of 60 Gy (Supplementary table 1) [31].

Response assessments

Measurements for tumour diameter were performed on abdominal contrast enhanced CT or MRI by two independent blinded readers (JJ and CvR) at baseline and 3-months follow-up using RECIST 1.1 [13]. Both readers measured 2 self-chosen target lesions in the liver and identified and measured extrahepatic disease at both time points. In case an FDG-PET scan was available, it was used to identify extrahepatic metastases. For liver only response, percentage change was calculated based on the measurements of the 2 target lesions and the response category was defined according to RECIST 1.1. (complete response (CR) / partial response (PR) / stable disease (SD) / progressive disease (PD)). In case no consensus was reached, a third reader (ML) gave the final call. Finally, inter-observer variability between the two raters was assessed for the liver only RECIST categories.

Progression of disease at three months was subdivided in 4 categories: growth of intrahepatic lesions (GIHL), growth of extrahepatic lesions (GEHL), new intrahepatic lesions (NIHL), and new extrahepatic lesions (NEHL). All extrahepatic lesions were taken into account, regardless of their size. These scores were also compared between the two readers.

Statistical Analysis

Standard descriptive statistics were used to display patient demographics and summarize response measures. Cohen's kappa was used to determine agreement based on RECIST categories. Chi-Square was used to test for differences in whole body response classification. Firth's bias-reduced logistic regression was used to explore associations between baseline characteristics and mode of progression. This type of analysis was chosen to correct for small-sample bias. Univariable survival analysis by the Kaplan-Meier method was used to estimate median overall survival (OS). A Cox proportional hazards model was used to test for differences between median OS estimates across patients with and without extrahepatic disease at baseline. All analyses were performed using GraphPad Prism version 5.0 (Graphpad Software, La Jolla, CA) and R version 3.1.2.

Results

Patient demographics

Of the total cohort of 129 treated patients in our institution, 39 patients (30%) were lost to follow-up due to various reasons: 1 patients had excessive disease progression and could not undergo RE, the 3-month follow-up scan was not evaluable in 1 patient due to RFA artefacts, and there was no 3-months follow-up scan of 37 patients. Twenty-four of these patients died within 4 months after RE. Therefore, clinical deterioration due to disease progression may be a likely cause for the missing data. Baseline- and treatment characteristics for the remaining 90 patients are summarized in Table 1. FDG-PET imaging was available in 76% of the patients at baseline and 74% at 3-months follow-up.

Inter-observer variability

First, the percentage change in target lesion and extrahepatic lesion diameter between baseline and 3-months follow-up was calculated. The percentages of change were converted to RECIST categories and in 5 patients the third rater gave the final call. The level of agreement in RECIST categories was almost perfect with a Cohen's kappa of 0.895 ($p < 0.001$), 95% CI (0.805-0.985).

Mode of progression in patients with progressive disease

Of the 90 patients, according to RECIST 1.1 criteria, no patients showed CR, 5 (5.5%) patients were evaluated as PR, 16 (17.8%) as SD and 69 (76.7%) as PD. According to RECIST, progressive disease can be based on growth of intrahepatic lesions, growth of extrahepatic lesions or new lesions (either intra- or extrahepatic). Growth of intrahepatic lesions was observed in 20 patients, new intrahepatic lesions in 35 patients, growth of extrahepatic lesions in 37 patients, and 57 patients were diagnosed with new extrahepatic lesions. In total, 46 (67% of all progressive patients) patients had progression on multiple levels. Most, 63 of the progressive patients (91%), had new (intra- and/or extrahepatic) lesions.

At baseline, 43/90 (48%) patients had extrahepatic lesions, which increased to 66/90 (73%) patients at 3-months follow-up (Figure 1). Although many organs can be affected, the lymph nodes and lungs were most affected (Figure 2).

Correlations between baseline characteristics and mode of progression

The association between several baseline characteristics and the mode of progression was assessed (Table 2). For previous treatment with first-line chemotherapy versus second-line chemotherapy, a reduced risk was seen for all modes of progression, with the strongest association between this factor and NIHL (OR=0.37, 95% CI 0.14-0.91). Extrahepatic lesions at baseline increased the risk of progressive disease for all modes of progression. The relation was strongest for NEHL (OR=3.06, 95% CI 1.28-7.72). There was an increased risk for every mode of progression for patients with KRAS wild type, with the strongest association for NIHL (OR=4.78, 95% CI 1.52-16.5). There were no other



significant relations between baseline characteristics and mode of progression (Table 2). When looking at growth of lesions (intra- and/or extrahepatic) and development of new lesions (intra- and/or extrahepatic), penalized regression showed a significant association between extrahepatic lesions at baseline and development of new lesions (OR 2.86, 95% CI 1.14-7.66) (Table 2). The odds for new lesions is higher for patients with extrahepatic disease at baseline.

The difference in response evaluation was compared for patients with- or without extrahepatic lesions at baseline. Forty-eight percent of the patients presented with- and 52% without extrahepatic lesions. Of the group presenting with extrahepatic lesions at baseline, 95% was diagnosed with PD at 3m FU. Significantly less patients (60%) were diagnosed with PD in the group of patients presenting without extrahepatic lesions at baseline ($p < 0.0001$) (Table 3).

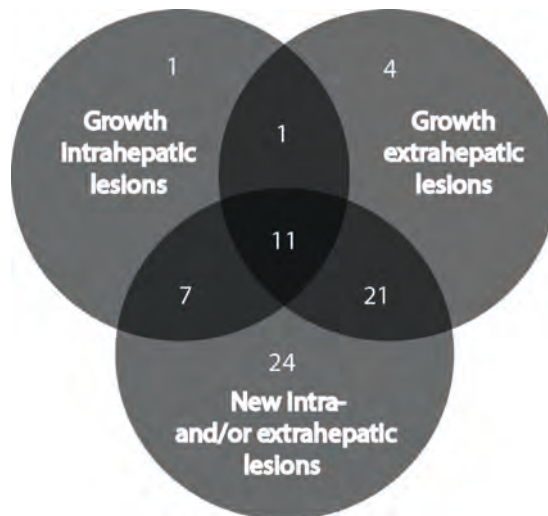


Figure 1. Types of progression. Lesions scored according to RECIST 1.1 criteria. Venn diagram for progressive patients at 3-month post treatment (n=69). Numbers indicate the number of patients in the indicated (overlapping) group. The vast majority of progressive patients (91%) had new lesions.

Table 1: Baseline Characteristics (90 patients)

Gender	
Female	25 (28%)
Male	65 (72%)
Age (years)	
Mean (range)	65 (35 - 84)
Performance status	
WHO = 0	54 (60%)
WHO = 1	25 (28%)
WHO = 2	2 (2%)
Unknown	9 (10%)
Previous chemotherapy lines ¹	
0	1 (1%)
1	36 (40%)
2 or more	51 (56%)
Unknown	2 (3%)
Previous bevacizumab ²	
Yes	54 (60%)
No	34 (38%)
Unknown	2 (2%)
Type of radioembolization	
Holmium-166	24 (27%)
Yttrium-90 (resin)	46 (51%)
Yttrium-90 (glass)	20 (22%)
KRAS status	
Wildtype	32 (36%)
Mutation	20 (22%)
Unknown	38 (42%)
Primary Tumor in Situ	
Yes	7 (8%)
No	83 (92%)
Extrahepatic disease (all lesions)	
None	47 (52%)
Lymph node	32
Lung	16
Abdominal wall	1
Spleen	1

This table shows the baseline characteristics for the 90 included patients. The numbers represent number of patients (% of total) or mean (range). No percentage of total is given for the extrahepatic disease site categories, since patients can have multiple sites of extrahepatic disease. ¹Chemotherapy used: capecitabine, oxaliplatin, 5-FU, Irinotecan, leucovorin, panitumumab/cetuximab, mitomycin (n=1), oxaliplatin (n=1). ²Mostly given in combination with Capecitabine and Oxaliplatin (CAPOX-B).

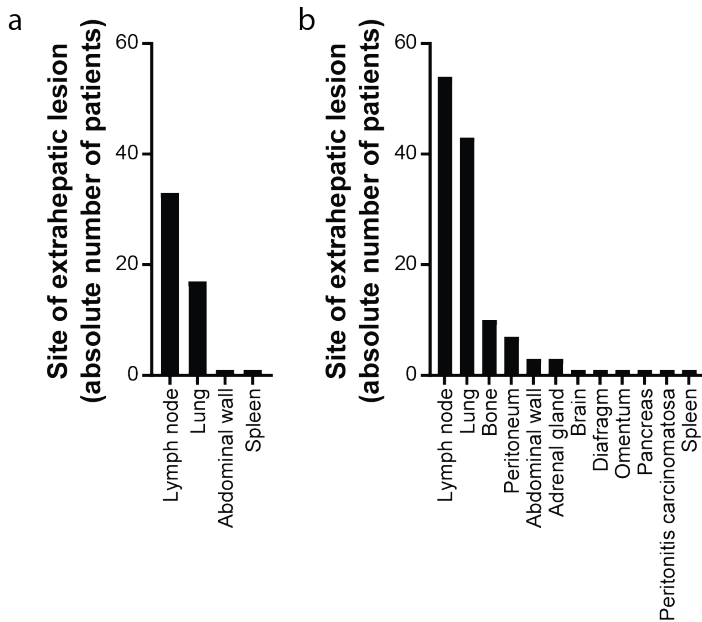


Figure 2. Site of extrahepatic lesions at baseline and 3-months follow-up. (a) Type and number of affected organs in patients with extrahepatic lesions at baseline. Bars depict absolute number of patients. In total 50 affected organs in 43 patients. (b) As in (a), for 3-months follow-up. In total 119 affected organs in 66 patients. Lymph nodes and lung are most affected at baseline and 3-months follow-up.

Prognostic value of extrahepatic disease at baseline based on overall survival (OS)

Finally, the prognostic value of extrahepatic disease at baseline was determined by comparing OS. Of the 129 patients, 6 were still alive and 123 had died at the time of analysis. Median OS for the entire cohort was 8 months (95% CI 7-10 months). Presence of extrahepatic lesions at baseline showed a difference in median OS estimates with 6 months (95% CI: 5-9) for patients with extrahepatic lesions at baseline and 10 months (95% CI: 8-14) for patients without extrahepatic lesions at baseline (Hazard ratio for survival with extrahepatic disease at baseline: 1.93, 95%CI (1.33-2.79), $p=0.0005$) (Figure 3).

Table 3: Whole body response classification at 3-months post treatment

No extrahepatic lesions at baseline	Complete response	47 (52%)
	Partial response	0 (0%)
	Stable disease	5 (10%)
	Progressive disease	14 (30%)
		28 (60%)
Extrahepatic lesions at baseline	Complete response	43 (48%)
	Partial response	0 (0%)
	Stable disease	0 (0%)
	Progressive disease	2 (5%)
		41 (95%)*

This table shows a comparison of the whole-body response classification at 3-months post treatment for patients with or without extrahepatic lesions at baseline. Numbers represent number of patients (% of total/subcategory). * $p < 0.0001$

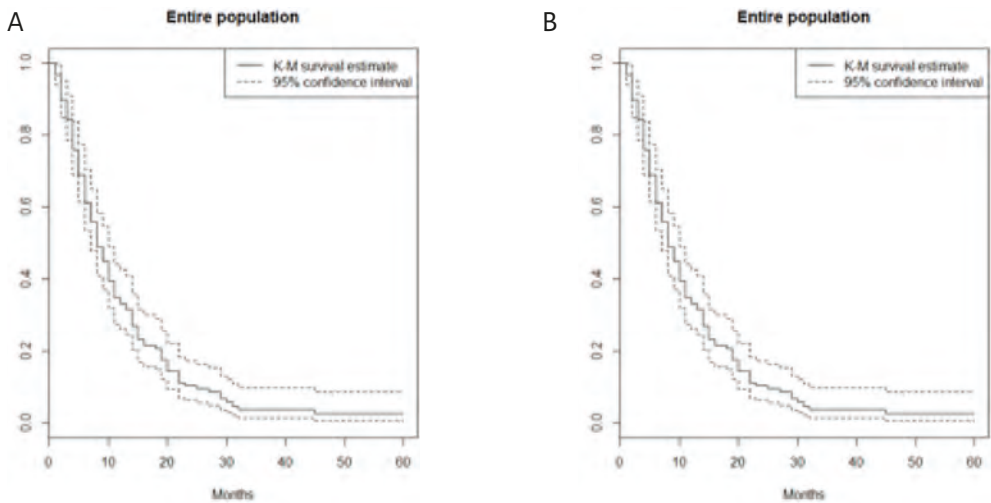


Figure 3. Kaplan-Meier survival curves, overall, and stratified for extrahepatic (EH) lesions at baseline (BL). (a) Kaplan-Meier Survival curve for the entire study population (n=129) (b) Kaplan-Meier Survival curve for patients with- or without EH lesions at BL.

Table 2: Univariable penalized logistic regression analysis for baseline characteristics and type of progression: OR (95%CI)

	GIHL (n=20)	GEHL (n=37)	NIHL (n=35)	NEHL (n=57)	GL (n=45)	NL (n=63)
Age in years	0.99 (0.02;9.75)	1.01 (0.97;1.06)	1.02 (0.98;1.06)	1.00 (0.96;1.05)	1.01 (0.97;1.06)	1.01 (0.97;1.05)
Chemotherapy*	0.74 (0.26;2.01)	0.87 (0.37;2.05)	0.37 [^] (0.14;0.91)	0.63 (0.26;1.51)	0.57 (0.24;1.33)	0.48 (0.19;1.19)
Type of RE**	1.09 (0.35;3.74)	0.40 (0.14;1.11)	0.58 (0.21;1.60)	0.76 (0.25;2.15)	0.45 (0.15;1.24)	0.66 (0.20;2.01)
Extrahepatic lesions at baseline	2.39 (0.89;6.84)	NA	1.83 (0.79;4.32)	3.06 [^] (1.28;7.72)	NA	2.86 [^] (1.14;7.66)
Primary tumor in situ	0.76 (0.08;3.96)	1.12 (0.24;4.88)	3.86 (0.87;22.5)	2.73 (0.54;27.1)	1.32 (0.30;6.21)	2.00 (0.39;19.9)
WHO status***	0.43 (0.10;1.43)	0.91 (0.35;2.33)	0.90 (0.33;2.33)	0.50 (0.19;1.31)	0.86 (0.34;2.19)	0.81 (0.30;2.27)
KRAS status§	1.88 (0.56;6.45)	2.75 (0.90;8.78)	4.78 [^] (1.52;16.5)	3.92 [^] (1.11;17.2)	2.85 (0.92;9.48)	2.67 (0.74;11.86)

This table shows the associations (odds ratio and 95%CI) between baseline characteristics and modes of progressions as described by RECIST at 3 months post-treatment.

* previous treatment with 1st versus 2nd line chemotherapy

** Yttrium-90 versus holmium-166

*** WHO performance status 0 versus 1,2

[^] significant

§ KRAS wild type versus KRAS mutation

Abbreviations: GIHL = growth of intrahepatic lesions. GEHL = growth of extrahepatic lesions. NIHL = new intrahepatic lesions. NEHL = new extrahepatic lesions. GL = growth of lesions (GEHL + GIHL). NL = new lesions (NEHL + NIHL). NA = not applicable. RE = radioembolization. OR = odds ratio. 95% CI = 95% confidence interval.

Discussion

The aim of this study was to assess the mode of early progression and identify possible correlations with baseline characteristics. Tumor targeting was adequate in the vast majority of the patients [18, 19]. Despite this, the results showed that the majority (77%) of patients was diagnosed with progressive disease at 3 months follow-up. This progression was mainly based on the development of new metastases, and to a lesser extent on the growth of existing lesions. The presence of extrahepatic disease at baseline significantly increases the chance of development of new lesions, in particular extrahepatic lesions. Moreover, patients with extrahepatic lesions at baseline had a worse overall survival. Taken together, this raises the question whether the risks of RE outweigh the advantages in patients with extrahepatic lesions at baseline.

In our institution, indications for RE include liver-dominant, irresectable, systemic therapy refractory disease. Patients with significant extrahepatic metastases are not considered eligible, but patients with stable, limited extrahepatic disease (defined as a maximum of 5 lung nodules <1 cm and lymph nodes <2 cm) are. Recently, several large phase III trials have been conducted in mCRC patients. Some of these used the same inclusion criteria with respect to extrahepatic disease [32]. First of all, the SIRFLOX, FOXFIRE and FOXFIRE-Global assessed the added value of RE to chemotherapy in first line mCRC patients. The EPOCH trial (clinicaltrials.gov identifier NCT01483027) studies the added value of RE plus chemotherapy in second line mCRC patients. However, the study by Hendlisz et al., which assessed the addition of RE to intravenous chemotherapy in mCRC patients, excluded patients with extrahepatic disease [33]. In the randomized controlled trial of Gray et al., patients with extrahepatic disease other than lymph nodes in the porta hepatis were also excluded [34].

The addition of systemic therapy to a local treatment of hepatic metastases seems logical, especially if we look at the results of our study, in which a significant number of patients developed new extrahepatic metastases. However, the possible role for systemic therapy in combination with RE in the salvage setting is currently debated. In the SIRFLOX, FOXFIRE and FOXFIRE-Global studies, no difference in OS or progression-free survival (PFS) was observed [35]. Progression-free survival confined to the liver was also not significantly better in patients in the combination group. Interestingly the cumulative incidence of first progression occurring outside the liver or death was higher in patients treated with RE; 33% (95% CI 29-37%) in the combination group, versus 19% in the chemotherapy alone group (95% CI 16-23%). This may be explained by a better intrahepatic tumor control for these patients. Furthermore, this may have been one of the reasons that no survival differences were found with regard to PFS and eventually OS [35].

The median overall survival in our total cohort was 8 months. The group of progressive patients (that underwent a follow-up scan) had an OS of 8.6 months, which is in line



with the previously described OS in end stage treatment for mCRC patients ranging from 7.1-8.8 months [17]. At baseline, 48% of our study population was diagnosed with extrahepatic lesions. This is also in line with other studies in which 35-77% of the included patients had extrahepatic lesions at baseline [14-16, 36-40]. We showed a difference in median OS with- and without the presence of EH lesions at BL, respectively 6 versus 10 months ($p=0.0005$). In a previous study of our group, worse survival of patients with extrahepatic disease was also shown [41]. In a retrospective analysis of patients with colorectal liver metastases treated with RE, Tohme et al. also found that extrahepatic disease was a predictor of worse overall survival [42]. The study of Soydal et al. confirms this finding [43]. Last, Paprottka et al. also found that extrahepatic disease was an independent predictor of survival after RE [44].

The current study has several limitations. First of all, the overall number of patients in our study is rather small. Secondly, the retrospective setting is prone to selection bias and the lack of 3-months follow-up scans is a drawback. Especially since this seems to be a poor prognosis group with 44% mortality after 3 months and 62% after 4 months. Also, it was a single institution study with a heterogeneous study population. Since RE was used in a salvage setting, outcome was likely muddled by the effect of other, previous therapies (Table 1; footnote 1). However, since patients were selected for RE based on their chemo-resistant tumours, the contribution of this variation in our patient population on the outcome of our study was considered minimal. Also, it is important to keep in mind that we did not compare patients with EH disease at baseline undergoing RE with a group of patients treated with best supportive care. Therefore, it is unclear whether RE worked insufficiently or not at all in the 20 patients that show growth of intrahepatic lesions: lesions might have grown even harder without RE. Furthermore, three types of microspheres were used in our dataset. The differences with regard to the embolic nature of the treatment, the specific activity of the microspheres, the administered activities, and the absorbed doses may have influenced the incidence of early progressive disease, and potentially also the type of progression. KRAS status was unknown in 42% of the patients, making the number of patients for the subgroup analyses for KRAS rather small.

Conclusion

In conclusion, patients with extrahepatic disease at baseline seem to have a higher chance on early progression after RE. Most of the patients with early progressive disease develop new lesions in- and outside the liver. This implies the need for a more restricted patient selection which excludes patients with extrahepatic disease.

References

1. Norstein, J. and W. Silen, *Natural history of liver metastases from colorectal carcinoma.* J Gastrointest Surg, 1997. **1**(5): p. 398-407.
2. Ruers, T. and R.P. Bleichrodt, *Treatment of liver metastases, an update on the possibilities and results.* Eur J Cancer, 2002. **38**(7): p. 1023-33.
3. Torre, L.A., et al., *Global cancer statistics, 2012.* CA Cancer J Clin, 2015. **65**(2): p. 87-108.
4. Siegel, R.L., K.D. Miller, and A. Jemal, *Cancer statistics, 2016.* CA Cancer J Clin, 2016. **66**(1): p. 7-30.
5. Sabanathan, D., G.D. Eslick, and J. Shannon, *Use of Neoadjuvant Chemotherapy Plus Molecular Targeted Therapy in Colorectal Liver Metastases: A Systematic Review and Meta-analysis.* Clin Colorectal Cancer, 2016.
6. Murthy, R., A. Habbu, and R. Salem, *Trans-arterial hepatic radioembolisation of yttrium-90 microspheres.* Biomed Imaging Interv J, 2006. **2**(3): p. e43.
7. Smits, M.L., et al., *Intra-arterial radioembolization of breast cancer liver metastases: a structured review.* Eur J Pharmacol, 2013. **709**(1-3): p. 37-42.
8. Bierman, H.R., et al., *Studies on the blood supply of tumors in man. III. Vascular patterns of the liver by hepatic arteriography in vivo.* J Natl Cancer Inst, 1951. **12**(1): p. 107-31.
9. Breedis, C. and G. Young, *The blood supply of neoplasms in the liver.* Am J Pathol, 1954. **30**(5): p. 969-77.
10. Lien, W.M. and N.B. Ackerman, *The blood supply of experimental liver metastases. II. A microcirculatory study of the normal and tumor vessels of the liver with the use of perfused silicone rubber.* Surgery, 1970. **68**(2): p. 334-40.
11. Buyse, M., et al., *Relation between tumour response to first-line chemotherapy and survival in advanced colorectal cancer: a meta-analysis.* Meta-Analysis Group in Cancer. Lancet, 2000. **356**(9227): p. 373-8.
12. Therasse, P., et al., *New Guidelines to Evaluate the Response to Treatment in Solid Tumors.* J Natl Cancer Inst, 2000. **92**(3): p. 205-216.
13. Eisenhauer, E.A., et al., *New response evaluation criteria in solid tumours: revised RECIST guideline (version 1.1).* Eur J Cancer, 2009. **45**(2): p. 228-47.
14. Martin, L.K., et al., *Yttrium-90 radioembolization as salvage therapy for colorectal cancer with liver metastases.* Clin Colorectal Cancer, 2012. **11**(3): p. 195-9.
15. Sofocleous, C.T., et al., *Radioembolization as a Salvage Therapy for Heavily Pretreated Patients With Colorectal Cancer Liver Metastases: Factors That Affect Outcomes.* Clin Colorectal Cancer, 2015. **14**(4): p. 296-305.
16. Bester, L., et al., *Radioembolization versus standard care of hepatic metastases: comparative retrospective cohort study of survival outcomes and adverse events in salvage patients.* J Vasc Interv Radiol, 2012. **23**(1): p. 96-105.
17. Kennedy, A., et al., *Updated survival outcomes and analysis of long-term survivors from the MORE study on safety and efficacy of radioembolization in patients with unresectable colorectal cancer liver metastases.* J Gastrointest Oncol, 2017. **8**(4): p. 614-624.



18. van den Hoven, A.F., et al., *Insights into the Dose-Response Relationship of Radioembolization with Resin 90Y-Microspheres: A Prospective Cohort Study in Patients with Colorectal Cancer Liver Metastases.* J Nucl Med, 2016. **57**(7): p. 1014-9.
19. Prince, J.F., et al., *Efficacy of radioembolization with holmium-166 microspheres in salvage patients with liver metastases: a phase 2 study.* J Nucl Med, 2017.
20. Kosmider, S., et al., *Radioembolization in combination with systemic chemotherapy as first-line therapy for liver metastases from colorectal cancer.* J Vasc Interv Radiol, 2011. **22**(6): p. 780-6.
21. Ahmadzadehfar, H., et al., *The Importance of Tc-MAA SPECT/CT for Therapy Planning of Radioembolization in a Patient Treated With Bevacizumab.* Clin Nucl Med, 2012. **37**: p. 1129-1130.
22. Lam, M.G., et al., *Root cause analysis of gastroduodenal ulceration after yttrium-90 radioembolization.* Cardiovasc Intervent Radiol, 2013. **36**(6): p. 1536-47.
23. Lahti, S.J., et al., *KRAS Status as an Independent Prognostic Factor for Survival after Yttrium-90 Radioembolization Therapy for Unresectable Colorectal Cancer Liver Metastases.* J Vasc Interv Radiol, 2015. **26**(8): p. 1102-11.
24. Bhooshan, N., et al., *Pretreatment tumor volume as a prognostic factor in metastatic colorectal cancer treated with selective internal radiation to the liver using yttrium-90 resin microspheres.* J Gastrointest Oncol, 2016. **7**(6): p. 931-937.
25. Jakobs, T.F., et al., *Robust evidence for long-term survival with (90)Y radioembolization in chemorefractory liver-predominant metastatic colorectal cancer.* Eur Radiol, 2017. **27**(1): p. 113-119.
26. Sato, K., et al., *Unresectable Chemorefractory Liver Metastases: Radioembolization with 90Y Microspheres—Safety, Efficacy, and Survival.* Radiology, 2008. **247**(2): p. 507-515.
27. Abbott, A.M., et al., *Outcomes of Therasphere Radioembolization for Colorectal Metastases.* Clin Colorectal Cancer, 2015. **14**(3): p. 146-53.
28. Salem, R. and K.G. Thurston, *Radioembolization with 90Yttrium microspheres: a state-of-the-art brachytherapy treatment for primary and secondary liver malignancies. Part 1: Technical and methodologic considerations.* J Vasc Interv Radiol, 2006. **17**(8): p. 1251-78.
29. Salem, R. and K.G. Thurston, *Radioembolization with 90yttrium microspheres: a state-of-the-art brachytherapy treatment for primary and secondary liver malignancies. Part 2: special topics.* J Vasc Interv Radiol, 2006. **17**(9): p. 1425-39.
30. Salem, R. and K.G. Thurston, *Radioembolization with yttrium-90 microspheres: a state-of-the-art brachytherapy treatment for primary and secondary liver malignancies: part 3: comprehensive literature review and future direction.* J Vasc Interv Radiol, 2006. **17**(10): p. 1571-93.
31. Smits, M.L.J., et al., *Holmium-166 radioembolisation in patients with unresectable, chemorefractory liver metastases (HEPAR trial): a phase 1, dose-escalation study.* The Lancet Oncology, 2012. **13**(10): p. 1025-1034.
32. Virdee, P.S., et al., *Protocol for Combined Analysis of FOXFIRE, SIRFLOX, and FOXFIRE-Global Randomized Phase III Trials of Chemotherapy +/- Selective Internal Radiation Therapy as First-Line Treatment for Patients With Metastatic Colorectal Cancer.* JMIR Res Protoc, 2017. **6**(3): p. e43.

33. Hendlisz, A., et al., *Phase III trial comparing protracted intravenous fluorouracil infusion alone or with yttrium-90 resin microspheres radioembolization for liver-limited metastatic colorectal cancer refractory to standard chemotherapy.* J Clin Oncol, 2010. **28**(23): p. 3687-94.
34. Gray, B., et al., *Randomised trial of SIR-Spheres plus chemotherapy vs. chemotherapy alone for treating patients with liver metastases from primary large bowel cancer.* Ann Oncol, 2001. **12**(12): p. 1711-20.
35. Wasan, H.S., et al., *First-line selective internal radiotherapy plus chemotherapy versus chemotherapy alone in patients with liver metastases from colorectal cancer (FOXFIRE, SIRFLOX, and FOXFIRE-Global): a combined analysis of three multicentre, randomised, phase 3 trials.* Lancet Oncol, 2017. **18**(9): p. 1159-1171.
36. Seidensticker, R., et al., *Matched-pair comparison of radioembolization plus best supportive care versus best supportive care alone for chemotherapy refractory liver-dominant colorectal metastases.* Cardiovasc Intervent Radiol, 2012. **35**(5): p. 1066-73.
37. Kennedy, A.S., et al., *Hepatic imaging response to radioembolization with yttrium-90-labeled resin microspheres for tumor progression during systemic chemotherapy in patients with colorectal liver metastases.* J Gastrointest Oncol, 2015. **6**(6): p. 594-604.
38. Lewandowski, R.J., et al., *Twelve-year experience of radioembolization for colorectal hepatic metastases in 214 patients: survival by era and chemotherapy.* Eur J Nucl Med Mol Imaging, 2014. **41**(10): p. 1861-9.
39. Shady, W., et al., *Percutaneous Radiofrequency Ablation of Colorectal Cancer Liver Metastases: Factors Affecting Outcomes--A 10-year Experience at a Single Center.* Radiology, 2016. **278**(2): p. 601-11.
40. Shady, W., et al., *Surrogate Imaging Biomarkers of Response of Colorectal Liver Metastases After Salvage Radioembolization Using 90Y-Loaded Resin Microspheres.* AJR Am J Roentgenol, 2016. **207**(3): p. 661-70.
41. Rosenbaum, C.E., et al., *Yttrium-90 radioembolization for colorectal cancer liver metastases: a prospective cohort study on circulating angiogenic factors and treatment response.* EJNMMI Res, 2016. **6**(1): p. 92.
42. Tohme, S., et al., *Survival and tolerability of liver radioembolization: a comparison of elderly and younger patients with metastatic colorectal cancer.* HPB (Oxford), 2014. **16**(12): p. 1110-6.
43. Soydal, C., et al., *Prognostic Importance of the Presence of Early Metabolic Response and Absence of Extrahepatic Metastasis After Selective Internal Radiation Therapy in Colorectal Cancer Liver Metastasis.* Cancer Biother Radiopharm, 2016. **31**(9): p. 342-346.
44. Paprottka, K.J., et al., *Pre-therapeutic factors for predicting survival after radioembolization: a single-center experience in 389 patients.* Eur J Nucl Med Mol Imaging, 2017. **44**(7): p. 1185-1193.



Supplementary information

Supplementary Table 1: Radioembolization Characteristics (90 patients)

Approach RE	
Whole liver	70 (78%)
Lobar	17 (19%)
Unknown	3 (3%)
Injected activity (MBq)	
Average (range) (n=89)	
Holmium (range) (n=24)	3235 (636-11627)
Yttrium (range) (n=65)	7034 (2213-11627)
Unknown (n=1)	1836 (636-6277)
Longshunt	
Percentage (range) (n=83)	
No longshunt (n=7)	5.56 (0.1 - 27)
Previous therapies ¹	
None	60 (67%)
RFA	12 (13%)
Segmentectomy	18 (20%)
Hemihepatectomy	8 (9%)
Chemo-embolization	5 (6%)

This table shows the RE characteristics for the 90 included patients. The numbers represent number of patients (% of total) or average (range). Percentage of total exceeds 100% for previous therapy, since patients can have multiple previous therapies. ¹Fourteen patients received >1 other type of therapy previously to RE; combinations were: RFA + segmentectomy (n=7), RFA + segmentectomy + chemoembolization (n=2), RFA + hemihepatectomy (n=2), segmentectomy + chemoembolization (n=1), segmentectomy and hemihepatectomy (n=2).



CHAPTER 6

Anatomic versus metabolic tumor response
assessment after radioembolization treatment

Jennifer M.J. Jongen
Charlotte E.N.M. Rosenbaum
Manon N.G.J.A. Braat
Maurice A.A.J. van den Bosch
Daniel Y. Sze
Onno Kranenburg
Inne H.M. Borel Rinkes
Marnix G.E.H. Lam
Andor F. van den Hoven

Abstract

Purpose: To assess the applicability of metabolic tumor response assessment on ^{18}F -FDG-PET/CT after radioembolization (RE) in patients with colorectal liver metastases (CRLM) by comparison with one-dimensional size-based response assessment on MRI.

Materials and Methods: A prospective cohort study was performed on 38 patients with CRLM undergoing RE. MRI and ^{18}F -FDG-PET/CT imaging were performed at baseline, 1- (n=38) and 3-month (n=21) follow-up. Longest tumor diameter (LTD) reduction on MRI at these time-points was compared to reduction in total lesion glycolysis (TLG) on ^{18}F -FDG-PET/CT. Hepatic response was compared between RECIST and total liver TLG and correlated with overall survival (OS).

Results: TLG and LTD response were positively correlated in 106 analyzed metastases (38 patients) at 1-month, and 58 metastases (22 patients) at 3-month follow-up. Agreement was poor, with LTD underestimating TLG response. A significant association with prolonged OS was found in total liver TLG at 1 month (HR 0.64, $p < 0.01$) and 3 months (HR 0.43, $p < 0.01$). For LTD, a significant association with OS was found at 3 months (HR 0.10, $p < 0.01$). Important differences in liver response classification were found, with total liver TLG identifying more patients and situations where there appeared to be treatment benefit compared to RECIST.

Conclusion: TLG response assessment on ^{18}F -FDG-PET/CT appears more sensitive and accurate, especially at early follow-up, than size-based response assessment on MRI in patients with CRLM treated by RE. Semi-automated liver response assessment with total liver TLG is objective, reproducible, rapid, and prognostic.

Keywords

Radioembolization; Colorectal liver metastases; PET; MRI; Tumor response assessment

Introduction

Adequate posttreatment tumor response assessment is essential to enable timely intervention in cancer patients who show progression of disease. The Response Evaluation Criteria in Solid Tumors (RECIST) system has been widely adopted, and currently serves as standard method. This method is based on changes in one-dimensional tumor diameter on cross-sectional imaging and patient prognosis, and used in cytotoxic drug studies (1–3). It is, however, questionable whether RECIST is applicable for other therapies, since treatment response may not primarily be characterized by tumor shrinkage.

Therefore, other response criteria systems have been developed, such as the European Association for the Study of the Liver (EASL) criteria and modified RECIST (mRECIST) for intra-arterial therapy in hepatocellular carcinoma (4, 5), the Choi criteria for the treatment of gastrointestinal stromal tumors (GIST) (6), and the immune-related Response Criteria (ir-RC) and irRECIST for immunotherapy (7, 8).

As radioembolization (RE) is now increasingly applied in unresectable chemorefractory, colorectal cancer liver metastases (CRLM), it is important to critically reflect on the applicability of the current used RECIST in this setting as well. Using RECIST might introduce subjectivity by selecting only two lesions, disregarding both size and consistency of lesions, and most important disregarding tumor cell activity (8, 9). Using alternative response criteria systems based on tumor vascularization is not a suitable due to the relatively hypovascular nature of CRLM.

Metabolic tumor response on ^{18}F -fluorodeoxyglucose positron emission tomography/computed tomography (^{18}F -FDG-PET/CT) might offer a solution. Previously, several SUV-based parameters derived from ^{18}F -FDG-PET have been validated for prediction of survival, but these do not take the lesion volume into account (10). Total lesion glycolysis (TLG) – the product of the mean standardized uptake value (SUV) and metabolic volume of a tumor – reflects the metabolic activity of a tumor and can be automated. This allows for an unbiased, fast and reproducible comparison between baseline and follow-up scans, while taking all lesions into account.

Hence, the purpose of this prospective study was to assess the applicability of metabolic tumor response assessment on ^{18}F -FDG-PET/CT after RE in patients with CRLM by comparison with one-dimensional size-based response assessment on MRI.

Material and Methods

For a detailed information of image acquisition and response assessments, we refer to the Supplementary Methods (available online).



Patient selection and study design

Between November 2011 and August 2014, 42 patients with CRLM underwent radioembolization with resin yttrium-90 (⁹⁰Y) microspheres in a prospective single-arm cohort study.

Patients with unresectable, chemorefractory, liver-dominant metastases had to meet eligibility criteria for RE. None of the patients received chemotherapy within 4 weeks before the baseline scan of the study. Chemorefractory is defined as irresponsibility or toxicity to oxaliplatin- and/or irinotecan based therapy with or without cetuximab/panitumumab (based on KRAS status). RE workup and treatment were performed in accordance with current standards of practice (11). All patients underwent a magnetic resonance imaging (MRI) scan of the liver and an ¹⁸F-FDG-PET/CT at baseline and during follow-up. Posttreatment imaging was acquired at 1-month follow-up and at 3 months (unless progressive disease (RECIST criteria) was noted at 1 month). Patients were allowed to participate in other clinical studies after 3-months follow-up. Only patients with an in-house liver MRI and ¹⁸F-FDG-PET/CT, obtained per protocol, at baseline and follow-up, were included since mean SUVs are not interchangeable.

The Medical Ethical committee approved this study, and informed consent was obtained from all patients before study-inclusion. All study procedures were performed in accordance with the Declaration of Helsinki.

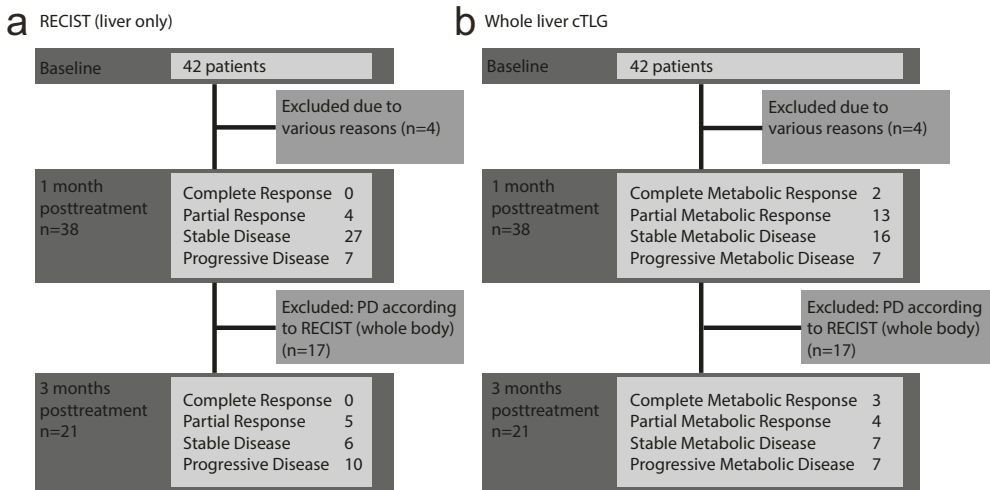


Figure 1. Patient outcome flow chart. Liver response classification at both 1- and 3 months posttreatment. (a) Flow chart of response classification based on Response Evaluation Criteria in Solid Tumors (RECIST). (b) Flow chart of response classification based on total liver Total Lesion Total Lesion Glycolysis (TLG).

Patient demographics

A total of 42 patients were treated with resin ⁹⁰Y-microspheres between November 2011 and August 2014. Four patients were excluded due to: inability to administer ¹⁸F-FDG (n=1), baseline ¹⁸F-FDG-PET/CT performed at a different center (n=1), and no MRI (n=1) or ¹⁸F-FDG-PET/CT (n=1) at 1-month follow-up. Complete baseline and treatment characteristics for the remaining 38 patients are summarized in Table 1 and 2 respectively and outcome flow chart in Figure 1a and b.

Table 1: Baseline Characteristics (38 patients)

Gender	
Female	11 (29%)
Male	27 (71%)
Age (years)	
Mean (range)	62 (34 - 83)
Liver metastases	
Synchronous	29 (76%)
Metachronous	9 (24%)
ECOG performance status	
0	22 (58%)
1	14 (37%)
2	2 (5%)
Previous chemotherapy lines	
0	0
1	14 (37%)
2	15 (40%)
>2	9 (23%)
Previous bevacizumab ¹	
Yes	22 (58%)
No	16 (42%)
Extrahepatic disease	
None	25 (66%)
Lymph node	7
Lung	2
Bone	3
Recurrence (colon)	3
Other	4
Liver tumor burden	
Mean % (range)	15 (1 - 50)
<25%	33 (87%)
26-50%	5 (13%)
>50	0

This table shows the baseline characteristics for the 38 included patients. The numbers represent number of patients (% of total) or mean (range). No percentage of total is given for the extrahepatic disease site categories, since patients can have multiple sites of extrahepatic disease.

¹Mostly given in combination with Capecitabine and Oxaliplatin (CAPOX-B).

Table 2: Treatment Characteristics (38 patients)

Reduction of prescribed activity ¹	
Yes	4 (11%)
No	34 (89%)
Net administered activity (MBq)	
Median (range)	1533 (670–2241)
Whole liver dose (Gy)	
Median (range)	44 (24–78)
Treatment strategy	
Whole liver treatment in one session	29 (76%)
Sequential whole liver treatment	7 (18%)
Lobar treatment	2 (5%)

This table shows the most important treatment characteristics for the 38 included patients. The numbers represent number of patients (% of total) or median (range). ¹Reduction of prescribed activity is in accordance with the manufacturer's recommendation if the liver-to-lung shunt exceeds 10%.

Image acquisition

Dynamic contrast enhanced (DCE) images were acquired with MRI scans of the liver on a 1.5 T scanner (Philips), using a SENSE body coil(12).

A time-of-flight PET/CT scanner with TrueV capacity (Biograph™ 40 mCT, Siemens Healthcare) was used for PET imaging. All patients were required to fast for at least 6 hours before the image acquisition. Subsequently, 2.0 MBq/kg of ¹⁸F-FDG was injected intravenously(13). A comprehensive description of the protocols and settings can be found in the supplementary information.

Response assessments

A comprehensive description of response assessment can be found in the supplementary information. In short, anatomic and metabolic tumor response assessments were performed independently by two different raters. Anatomic tumor response was assessed per RECIST 1.1 on liver MRI (3). The LTD of all metastases >1 cm was recorded at baseline and follow-up. The appearance of new liver metastases and extrahepatic lesions was recorded.

Metabolic tumor response on ¹⁸F-FDG-PET was assessed quantitatively with ROVER software (ABX GMBH, Radeberg, Germany) (14, 15). A partial volume corrected total lesion glycolysis measure was used in this analyses. TLG is calculated by multiplying SULmean (partial volume corrected SUVmean adjusted for lean body mass) with metabolic volume. Total liver TLG was determined by taking the sum of the TLG values. First, the response of two TLs and the two largest NTLs was compared on MRI (% decline LTD), to evaluate whether TL response is representative for response in other liver

lesions. Second, a per-lesion comparison of anatomic and metabolic tumor response was made at 1- and 3 months posttreatment separately. Only the response of metastases - identifiable on both ^{18}F -FDG-PET and MRI - was compared on a per-lesion basis. Third, the classification of liver response—as defined by RECIST and total liver TLG criteria (Table 3) — was compared for 1 and 3 months separately. Last, the association of liver response for RECIST and total liver TLG with overall survival (OS) was explored.

Table 3: Definitions of Response Evaluation Criteria in Solid Tumors (RECIST) and Total Liver - Total Lesion Glycolysis (total liver TLG) Classification

RECIST	
Complete Response (CR)	100% reduction in the sum of longest tumor diameter in all target lesions. ¹
Partial Response (PR)	$\geq 30\%$ – $< 100\%$ reduction in the sum of longest tumor diameter in all target lesions. ¹
Stable Disease (SD)	Between 20% increase and 30% reduction in the sum of longest tumor diameter in all target lesions. ¹
Progressive Disease (PD)	$\geq 20\%$ progression in the sum of longest tumor diameter in all target lesions.
Total liver TLG	
Complete Metabolic Response (CMR)	100% reduction in total liver TLG. ²
Partial Metabolic Response (PMR)	$\geq 50\%$ – $< 100\%$ reduction in total liver TLG. ²
Stable Metabolic Response (SMR)	Between 30% increase and 50% reduction in total liver TLG. ²
Progressive Metabolic Response (PMR)	$\geq 30\%$ increase in total liver TLG.

Total liver TLG is a self-defined response classification, based on reasonable assumption. Total liver TLG is the sum of partial volume corrected total lesion glycolysis (TLG) values for all tumors in the liver; TLG is the product of SULmean and metabolic volume. ¹Appearance of a new liver metastasis indicated PD, regardless of the reduction in the sum of target lesions of longest tumor diameter. ²TLG values of new metabolically active liver metastases were automatically included in the total liver TLG.

Statistical Analysis

Standard descriptive statistics were used to display patient demographics and response measures. All response measures were converted from absolute differences (in LTD or TLG) between baseline and follow-up to percentages decline. Linear relationships were explored by linear regression with Pearson's correlation coefficient (ρ) and R^2 , agreement was determined by Bland-Altman analysis with 95% limits of agreement.

Univariable survival analysis by the Kaplan-Meier method was used to estimate median OS, including 95% confidence intervals (CI). Associations between percentage decrease in sum of LTD and total liver TLG at 1 and 3 months and OS was explored by univariable Cox Regression. Subsequently, a log-rank test was used to test for differences between median OS estimates across the different response classes. Multivariable modeling was not deemed feasible due to the limited sample size.

All analyses were performed with R version 3.1.2. A two-sided p -value <0.05 was considered statistically significant.

Results

Comparison of TL and NTL response: sum of LTD

Accuracy of TL as an indicator for whole liver response was evaluated. Due to absence of NTLs on the baseline MRI, 6 patients were excluded. Mean (\pm range) percentage decrease in sum of LTD at 1 month was $13\pm 16\%$ (-13% – 61%) for TLs (Figure 2a), and $11\pm 24\%$ (-76% – 39%) for NTLs (Figure 2b). There was a positive correlation ($\rho=0.57$, $R^2=0.33$, $p<0.01$) (Figure 2c) between TL and NTL at 1 month posttreatment. NTL reduction was 2% lower than TL reduction (95% limits of agreement -41% – $+37\%$) (Figure E1a).

At 3 months posttreatment ($n=17$), mean (\pm range) percentage decrease was $12\pm 38\%$ (-95% – 66%) for TLs (Figure 2d), and $22\pm 33\%$ (-66% – 59%) for NTLs (Figure 2e). Again, a positive correlation ($\rho=0.84$, $R^2=0.78$, $p<0.01$) (Figure 2f) was found between TL and NTL LTD. NTL reduction was 10% higher than TL reduction (95% limits of agreement -31% – $+50\%$) (Figure E1b).

Next, LTD and TLG on lesion level for both time-points was compared. At 1 month, 44/106 metastases (41%) appeared ‘fused’ on PET, while being identified as individual metastases on MRI. Mean \pm standard deviation (range) percentage decrease relative to baseline was $13\pm 25\%$ (-141% – 65%) for LTD (Figure 3a), and $35\pm 84\%$ (-434% – 100%) for TLG (Figure 3b). There was a weak positive correlation ($\rho=0.44$, $R^2=0.19$, $p<0.01$) (Figure 3c) between LTD and TLG. However, TLG reduction was 22% higher than LTD (95% limits of agreement -128% – $+171\%$) (Figure E2a). Notice that the waterfall plots for LTD and TLG resemble each other in shape, but the response/progression signal is amplified for TLG.

At 3 months, 28/58 (48%) appeared ‘fused’ on PET. Mean \pm standard deviation (range) percentage decrease relative to baseline was $16\pm 29\%$ (-94% – 62%) for LTD (Figure 3d), and $17\pm 106\%$ (-290% – 100%) for TLG (Figure 3e). A positive correlation ($\rho=0.66$, $R^2=0.43$, $p<0.01$) (Figure 3f) was also found for LTD and TLG at 3 months posttreatment. The average difference was smaller than at 1 month, with TLG being 2% higher than LTD reduction (95% limits of agreement -174% – $+177\%$) (Figure E2b). Yet, again a different

outcome for both response measures was commonly observed. Last, both 1- and 3 month Bland-Altman plots showed increasing discrepancies between both measurements as response/progression got more extreme (Figure E2a-b).

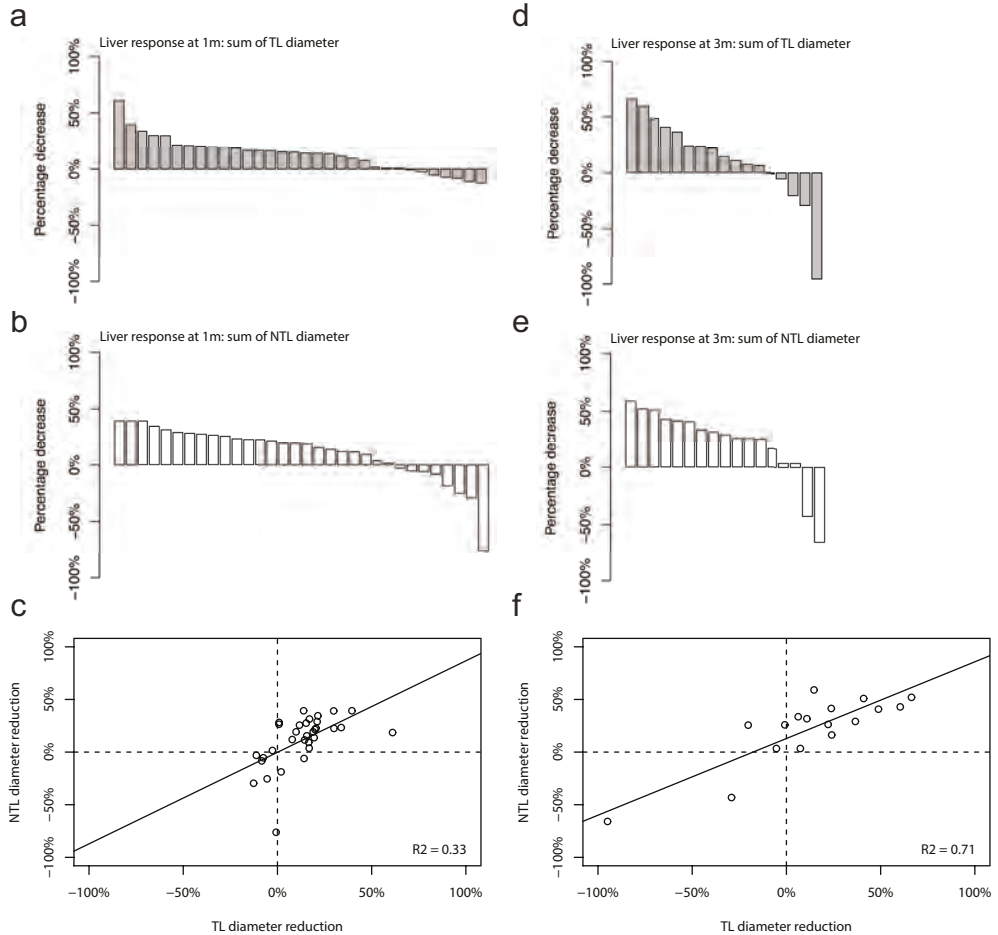


Figure 2. Comparison of LTD response for Target Lesions and Non-Target Lesions on a per-lesion basis. (a) Waterfall plot showing percentage decrease of TL at 1 month posttreatment. (b) Waterfall plot showing percentage decrease of NTL at 1 month posttreatment. (c) Linear regression for TL and NTL at 1 month posttreatment. (d) Waterfall plot showing percentage decrease of TL at 3 months posttreatment. (e) Waterfall plot showing percentage decrease of NTL at 3 months posttreatment. (f) Linear regression for TL and NTL at 3 months posttreatment. Outliers are not depicted in the waterfall plots (cropped axes in 1a and 1d) to increase readability. Ranges are described in in the results section.

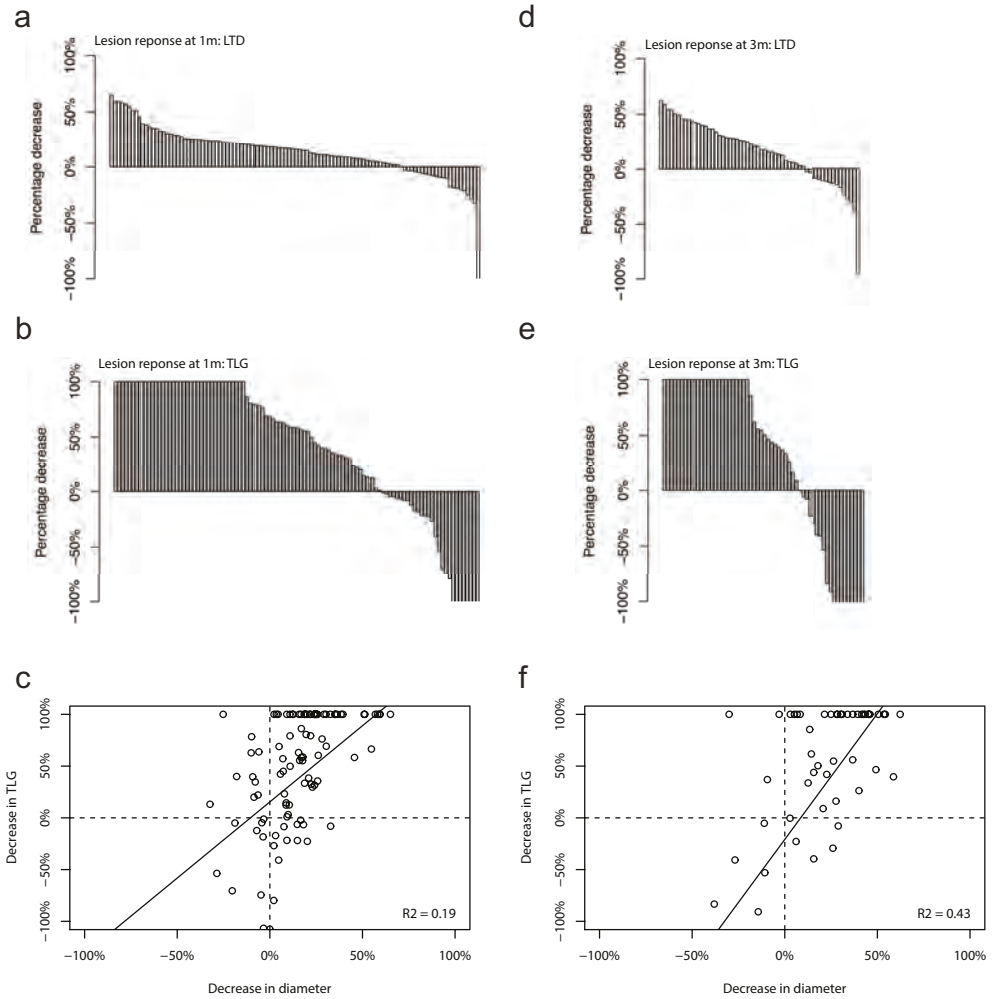


Figure 3. Comparison of response for target lesion LTD and TLG on a per-lesion basis. (a) Waterfall plot showing percentage decrease of target lesion LTD at 1 month posttreatment. (b) Waterfall plot showing percentage decrease of TLG at 1 month posttreatment. (c) Linear regression for target lesion LTD and TLG at 1 month posttreatment. (d) Waterfall plot showing percentage decrease of target lesion LTD at 3 months posttreatment. (e) Waterfall plot showing percentage decrease of TLG at 3 months posttreatment. (f) Linear regression for target lesion LTD and TLG at 3 months posttreatment. Outliers are not depicted in the waterfall plots (cropped axes in 2b and 2e) to increase readability. Ranges are described in the results section.

Comparison of lesion response: LTD vs. TLG*Comparison of liver response classification: LTD vs. total liver TLG*

The clinically used liver response based on LTD was compared with total liver TLG. Important differences in liver response classification were noted between LTD (based on liver lesion classification as described in RECIST) and total liver TLG (Table 4-5), with total liver TLG generally showing a higher response rate than LTD.

Table 4: Liver response classification at 1 month posttreatment

	CMR	PMR	SMD	PMD	Total
CR	0	0	0	0	0
PR	1	1	2	0	4 (11%)
SD	1	11	11	4	27 (71%)
PD	0	1	3	3	7 (18%)
Total	2 (5%)	13 (34%)	16 (42%)	7 (18%)	38

This table shows a comparison of the liver response classification per RECIST and total liver TLG at 1 months posttreatment. Numbers represent number of patients (% of total).

Table 5: Liver response classification at 3 months posttreatment

	CMR	PMR	SMD	PMD	Total
CR	0	0	0	0	0
PR	3	2	0	0	5 (24%)
SD	0	1	3	2	6 (29%)
PD	0	1	4	5	10 (48%)
Total	3 (14%)	4 (19%)	7 (33%)	7 (33%)	21

This table shows a comparison of the liver response classification per RECIST and total liver cTLG at 3 months posttreatment. Numbers represent number of patients (% of total).

At 1 month posttreatment, 6 patients (16%) showed new liver metastases on MRI. Local disease control rate was 82% (31/38) for both LTD and total liver TLG. Objective response rates were 11% for RECIST and 39% for total liver TLG. The specific proportion of agreement between the two was 39% (15/38). A total of 17 patients (45%) were found to have progressive disease per RECIST. Most patients showed progressive disease mainly in one domain (94%), of which 65% was extrahepatic disease (65%) (Figure 4a).

At 3 months, new liver metastases were found on MRI in 9 patients (43%). Local disease control rates were 52% (11/21) for LTD and 67% (14/21) for total liver TLG. Objective response rates were 24% (5/21) for RECIST and 33% (7/21) for total liver TLG. The specific proportion of agreement between the two was 48% (10/21). New hepatic lesions were present in 82% of the patients with progressive disease (Figure 4b).

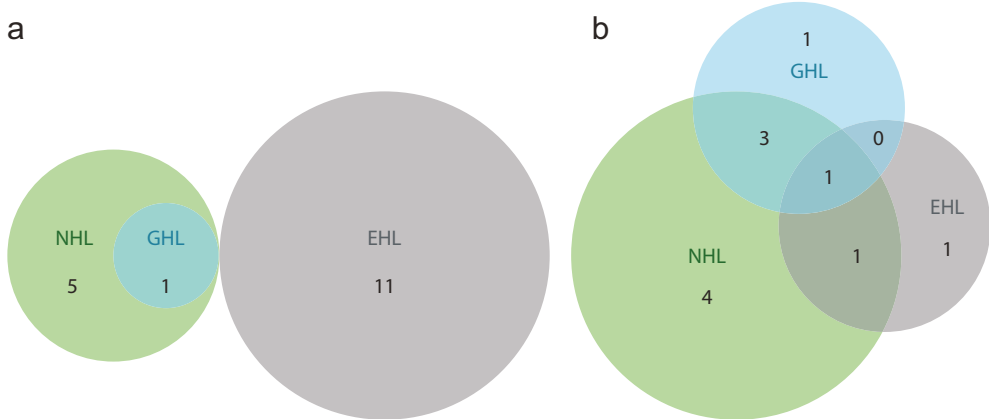


Figure 4. Cause of progression in progressive patients. Numbers indicate the number of patients in the indicated (overlapping) group. (a) Venn diagram for progressive patients at 1 month posttreatment. (n=16) (b) Venn diagram for progressive patients at 3 months posttreatment. (n=11) GHL = growth of hepatic lesions, NHL = new hepatic lesions, EHL = new extrahepatic lesions.

Prognostic value of disease control: LTD and total liver TLG

The association with OS was studied between percentage decline in the sum of LTD and total liver TLG. Reduction in total liver TLG at 1-month posttreatment was associated with significantly prolonged OS (Hazard Ratio [HR] 0.64, 95% CI 0.47–0.85, $p < 0.01$). This association was not found for percentage reduction in the sum of LTD (HR 0.14; 95% CI 0.01–1.43; $p = 0.10$). At 3 months posttreatment, both percentage reduction in sum of LTD (HR 0.10; 95% CI 0.02–0.50; $p < 0.01$) and total liver TLG (HR 0.43; 95% CI 0.24–0.76; $p < 0.01$) were associated with significantly prolonged OS.

Eventually, the prognostic value was compared between LTD and total liver TLG based on OS. Thirty-four of 38 patients were deceased at the time of analysis. Median OS for the entire cohort was 9.3 months (95% CI 6.6–11.8 months). Only total liver TLG at 1 month posttreatment showed a significant difference in median overall survival between the different response classes ($p = 0.02$) (Table 6). Survival curves stratified on liver response classes are displayed in Figure 5a-d.

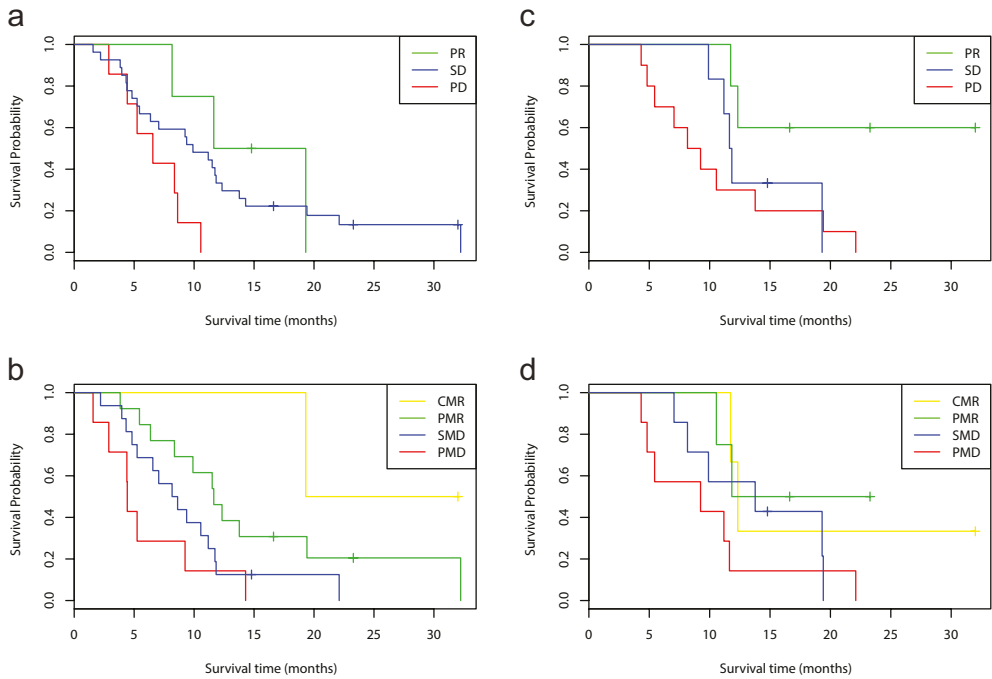


Figure 5. Kaplan-Meier survival curves, stratified per liver response classification. (a) Kaplan-Meier Survival curve for RECIST-based groups at 1-month posttreatment (b) Kaplan-Meier Survival curve for total liver TLG-based groups at 1-month posttreatment. (c) Kaplan-Meier Survival curve for RECIST-based groups at 3-months posttreatment. (d) Kaplan-Meier Survival curve for total liver TLG-based groups at 3-months posttreatment. Table 6 shows corresponding survival estimates and significance of the Log-rank test.



Discussion

In the present study, changes in TLG on ^{18}F -FDG-PET were compared with changes in LTD on MRI after ^{90}Y -RE treatment in 38 patients (106 lesions) with CRLM. This was driven by the hypothesis that (LTD based) RECIST is not ideal for tumor response assessment after RE in patients with CRLM, due to its subjectivity, the insufficient primary effect on tumor diameter and hypovascularity of CRLM.

Although there was a positive correlation between LTD reduction for TLs and NTLs, 67% and 22% of the variability in NTL reduction was left unexplained by TL reduction at 1 and 3 months respectively. Although reasons for variability in lesion response are described (16), the difference in response between TL and NTL emphasized the limitation of RECIST. The subjective choice of picking two target lesions out of the many – in patients typically exhibiting widespread liver disease – can actually determine patient response.

On a per-lesion basis, TLG was more sensitive to change after RE. This may be explained by the fact that TLG combines metabolic activity and three-dimensional volume, providing additional information on tumor biology and behavior. Studying total liver TLG value, liver response rates were generally higher than with RECIST which can be explained by the inclusion of all (hepatic) lesions in the total liver TLG. Importantly, it demonstrated that liver response classification with total liver TLG holds prognostic value. Percentage decrease in total liver TLG at both 1 and 3 months were significantly associated with prolonged OS in our cohort, in line with previous studies showing that both a decrease in TLG at early (4-6 weeks) (17, 18) and late follow-up (3 months) (10) are associated with prolonged OS.

Thus, semi-automated ^{18}F -FDG-PET derived total liver TLG analyses can potentially replace RECIST after RE in patients with CRLM. This may have the benefits that it diminishes the subjectivity of picking TLs, solves the problem of time-intensive and challenging RECIST assessments in patients with extensive liver metastases or heavily pretreated patients, and it allows the early detection of changes in tumor status. This can potentially facilitate more accurate and timely decisions and thereby improve patient outcome. This becomes increasingly important as ^{90}Y -RE treatment shifts to an earlier treatment modality in CRLM patients, e.g. concomitant with first line chemotherapy (19).

Response assessment with ^{18}F -FDG-PET after RE has been studied before, using different methods. However, the majority of these studies were small, retrospective in nature and did not use total liver TLG. The study of Wong *et al.* (n=8) found a significantly higher tumor response rate on ^{18}F -FDG-PET compared to CT/MRI which was correlated with decrease in CEA serum levels posttreatment (20). Two other small studies demonstrated that changes in tumor size did not correlate with changes in ^{18}F -FDG uptake and that ^{18}F -FDG-PET showed a significant decrease relative to baseline at 1- and 3 month follow-up compared to an absent or heterogeneous response on CT (21, 22). Lewandowski *et*

al. showed a response on ^{18}F -FDG-PET to bilobar, two-staged in 88% and 73% of the first and second treated lobes respectively, whereas this was only 35% and 36% for CT response (23). More recently, a study of Zerizer *et al.* (n=25) found that the ^{18}F -FDG-PET response assessment was superior to CT in predicting 2-year PFS and correlated with changes in carcinoembryonic antigen (CEA), cancer-antigen 19-9 (CA 19-9) and lactate dehydrogenase (LDH) (9). Unfortunately insufficient data on these markers is available in our study cohort to study potential correlations between total liver TLG and these markers.

There are also disadvantages to the use of ^{18}F -FDG-PET. This TLG-based method is not standardized yet and the quantitative results are hardware-, image acquisition-, reconstruction- and analyses dependent. Current software packages for ^{18}F -FDG-PET analyses still need further refinement and simplification to enable a widespread use. Although more expensive than CT/MRI, ^{18}F -FDG-PET imaging may benefit cost-effectiveness by improving therapeutic management in patients with CRLM (24). Although this phenomenon was not seen on matched MRI scans in our study, ^{18}F -FDG-PET can cause pseudo-lesions after RE due to radiation damage in the liver (25).

Our study has several limitations. The limited sample size prohibits extensive multivariable modeling to prove superiority of survival prediction by total liver TLG over RECIST. Furthermore, liver response information was unavailable in the majority of the patients 3 months after treatment. This was inherent to our IRB-approved study design, since liver response was not monitored any longer once extrahepatic disease progression was confirmed. This ensured that patients could still receive experimental systemic therapy. Third, since we use a new way of analyses, most are not clinically validated yet. For example, the cut-off values for total liver TLG response classification were chosen arbitrarily, striving for a reasonable and clinically meaningful treatment response and disease progression. Fourth, LTD response of individual metastases was clustered if they appeared fused on ^{18}F -FDG-PET/CT. This difference can be explained by the lower spatial resolution of ^{18}F -FDG-PET/CT, whereby adjacent tumors may appear connected. However, in genuine tumor progression or reduction this poses also a problem in RECIST-based evaluations; lesions may fuse or disintegrate. On the other hand, there might be an observation bias for lesions not visible on ^{18}F -FDG-PET/CT.

In conclusion, lesion based TLG response assessment by ^{18}F -FDG-PET/CT appears more sensitive and accurate, especially at early follow-up, than size-based, one-dimensional response assessment on MRI in patients with CRLM treated by RE. Objective, automated liver response assessment with total liver TLG is rapid, reproducible, and prognostic. Further research is needed for external validation of the described method, and to assess whether increased response assessment sensitivity will enable change of management or in some cases early re-intervention with RE. Finally, total liver TLG response assessment should be compared to other functional response assessment methods such as diffusion weighted MRI and pharmacokinetic analysis of dynamic contrast enhanced MRI (26, 27).



References

1. Buyse M, Thirion P, Carlson RW, Burzykowski T, Molenberghs G, Piedbois P. Relation between tumour response to first-line chemotherapy and survival in advanced colorectal cancer: a meta-analysis. *Meta-Analysis Group in Cancer. Lancet (London, England)*. 2000;356(9227):373-8.
2. Therasse P, Arbuck SG, Eisenhauer EA, Wanders J, Kaplan RS, Rubinstein L, et al. New Guidelines to Evaluate the Response to Treatment in Solid Tumors. *Journal of the National Cancer Institute*. 2000;92(3):205-16.
3. Eisenhauer EA, Therasse P, Bogaerts J, Schwartz LH, Sargent D, Ford R, et al. New response evaluation criteria in solid tumours: revised RECIST guideline (version 1.1). *European journal of cancer (Oxford, England : 1990)*. 2009;45(2):228-47.
4. Bruix J, Sherman M, Llovet JM, Beaugrand M, Lencioni R, Burroughs AK, et al. Clinical management of hepatocellular carcinoma. Conclusions of the Barcelona-2000 EASL conference. *European Association for the Study of the Liver. Journal of hepatology*. 2001;35(3):421-30.
5. Lencioni R, Llovet JM. Modified RECIST (mRECIST) assessment for hepatocellular carcinoma. *Seminars in liver disease*. 2010;30(1):52-60.
6. Choi H, Charnsangavej C, Faria SC, Macapinlac HA, Burgess MA, Patel SR, et al. Correlation of computed tomography and positron emission tomography in patients with metastatic gastrointestinal stromal tumor treated at a single institution with imatinib mesylate: proposal of new computed tomography response criteria. *Journal of clinical oncology : official journal of the American Society of Clinical Oncology*. 2007;25(13):1753-9.
7. Wolchok JD, Hoos A, O'Day S, Weber JS, Hamid O, Lebbe C, et al. Guidelines for the evaluation of immune therapy activity in solid tumors: immune-related response criteria. *Clinical cancer research : an official journal of the American Association for Cancer Research*. 2009;15(23):7412-20.
8. Nishino M, Gargano M, Suda M, Ramaiya NH, Hodi FS. Optimizing immune-related tumor response assessment: does reducing the number of lesions impact response assessment in melanoma patients treated with ipilimumab? *Journal for immunotherapy of cancer*. 2014;2:17.
9. Zerizer I, Al-Nahhas A, Towey D, Tait P, Ariff B, Wasan H, et al. The role of early (1)(8)F-FDG PET/CT in prediction of progression-free survival after (9)(o)Y radioembolization: comparison with RECIST and tumour density criteria. *European journal of nuclear medicine and molecular imaging*. 2012;39(9):1391-9.
10. Fendler WP, Philippe Tiega DB, Ilhan H, Paprottka PM, Heinemann V, Jakobs TF, et al. Validation of several SUV-based parameters derived from 18F-FDG PET for prediction of survival after SIRT of hepatic metastases from colorectal cancer. *Journal of nuclear medicine : official publication, Society of Nuclear Medicine*. 2013;54(8):1202-8.
11. Mahnken AH, Spreafico C, Maleux G, Helmberger T, Jakobs TF. Standards of practice in transarterial radioembolization. *Cardiovascular and interventional radiology*. 2013;36(3):613-22.

12. Schalkx HJ, van Stralen M, Coenegrachts K, van den Bosch MA, van Kessel CS, van Hillegersberg R, et al. Liver perfusion in dynamic contrast-enhanced magnetic resonance imaging (DCE-MRI): comparison of enhancement in Gd-BT-DO₃A and Gd-EOB-DTPA in normal liver parenchyma. *European radiology*. 2014;24(9):2146-56.
13. Rosenbaum CE, van den Bosch MA, Veldhuis WB, Huijbregts JE, Koopman M, Lam MG. Added value of FDG-PET imaging in the diagnostic workup for yttrium-90 radioembolisation in patients with colorectal cancer liver metastases. *European radiology*. 2013;23(4):931-7.
14. Wahl RL, Jacene H, Kasamon Y, Lodge MA. From RECIST to PERCIST: Evolving Considerations for PET response criteria in solid tumors. *Journal of nuclear medicine : official publication, Society of Nuclear Medicine*. 2009;50 Suppl 1:122s-50s.
15. Hofheinz F, Langner J, Petr J, Beuthien-Baumann B, Oehme L, Steinbach J, et al. A method for model-free partial volume correction in oncological PET. *EJNMMI research*. 2012;2(1):16.
16. van den Hoven AF, Rosenbaum CE, Elias SG, de Jong HW, Koopman M, Verkooijen HM, et al. Insights into the Dose-Response Relationship of Radioembolization with Resin 90Y-Microspheres: A Prospective Cohort Study in Patients with Colorectal Cancer Liver Metastases. *Journal of nuclear medicine : official publication, Society of Nuclear Medicine*. 2016;57(7):1014-9.
17. Gulec SA, Suthar RR, Barot TC, Pennington K. The prognostic value of functional tumor volume and total lesion glycolysis in patients with colorectal cancer liver metastases undergoing 90Y selective internal radiation therapy plus chemotherapy. *European journal of nuclear medicine and molecular imaging*. 2011;38(7):1289-95.
18. Soydal C, Kucuk ON, Gecim EI, Bilgic S, Elhan AH. The prognostic value of quantitative parameters of 18F-FDG PET/CT in the evaluation of response to internal radiation therapy with yttrium-90 in patients with liver metastases of colorectal cancer. *Nuclear medicine communications*. 2013;34(5):501-6.
19. van Hazel GA, Heinemann V, Sharma NK, Findlay MP, Ricke J, Peeters M, et al. SIRFLOX: Randomized Phase III Trial Comparing First-Line mFOLFOX6 (Plus or Minus Bevacizumab) Versus mFOLFOX6 (Plus or Minus Bevacizumab) Plus Selective Internal Radiation Therapy in Patients With Metastatic Colorectal Cancer. *Journal of clinical oncology : official journal of the American Society of Clinical Oncology*. 2016;34(15):1723-31.
20. Wong CY, Salem R, Raman S, Gates VL, Dworkin HJ. Evaluating 90Y-glass microsphere treatment response of unresectable colorectal liver metastases by [18F]FDG PET: a comparison with CT or MRI. *European journal of nuclear medicine and molecular imaging*. 2002;29(6):815-20.
21. Bienert M, McCook B, Carr BI, Geller DA, Sheetz M, Tutor C, et al. 90Y microsphere treatment of unresectable liver metastases: changes in 18F-FDG uptake and tumour size on PET/CT. *European journal of nuclear medicine and molecular imaging*. 2005;32(7):778-87.



22. Szyszko T, Al-Nahhas A, Canelo R, Habib N, Jiao L, Wasan H, et al. Assessment of response to treatment of unresectable liver tumours with 90Y microspheres: value of FDG PET versus computed tomography. *Nuclear medicine communications*. 2007;28(1):15-20.
23. Lewandowski RJ, Thurston KG, Goin JE, Wong CY, Gates VL, Van Buskirk M, et al. 90Y microsphere (TheraSphere) treatment for unresectable colorectal cancer metastases of the liver: response to treatment at targeted doses of 135-150 Gy as measured by [18F]fluorodeoxyglucose positron emission tomography and computed tomographic imaging. *Journal of vascular and interventional radiology : JVIR*. 2005;16(12):1641-51.
24. Lejeune C, Bismuth MJ, Conroy T, Zanni C, Bey P, Bedenne L, et al. Use of a decision analysis model to assess the cost-effectiveness of 18F-FDG PET in the management of metachronous liver metastases of colorectal cancer. *Journal of nuclear medicine : official publication, Society of Nuclear Medicine*. 2005;46(12):2020-8.
25. Grant MJ, Didier RA, Stevens JS, Beyder DD, Hunter JG, Thomas CR, et al. Radiation-induced liver disease as a mimic of liver metastases at serial PET/CT during neoadjuvant chemoradiation of distal esophageal cancer. *Abdominal imaging*. 2014;39(5):963-8.
26. Barabasch A, Kraemer NA, Ciritsis A, Hansen NL, Lierfeld M, Heinzl A, et al. Diagnostic accuracy of diffusion-weighted magnetic resonance imaging versus positron emission tomography/computed tomography for early response assessment of liver metastases to Y90-radioembolization. *Investigative radiology*. 2015;50(6):409-15.
27. Choyke PL, Dwyer AJ, Knopp MV. Functional tumor imaging with dynamic contrast-enhanced magnetic resonance imaging. *Journal of magnetic resonance imaging : JMRI*. 2003;17(5):509-20.

Supplementary information

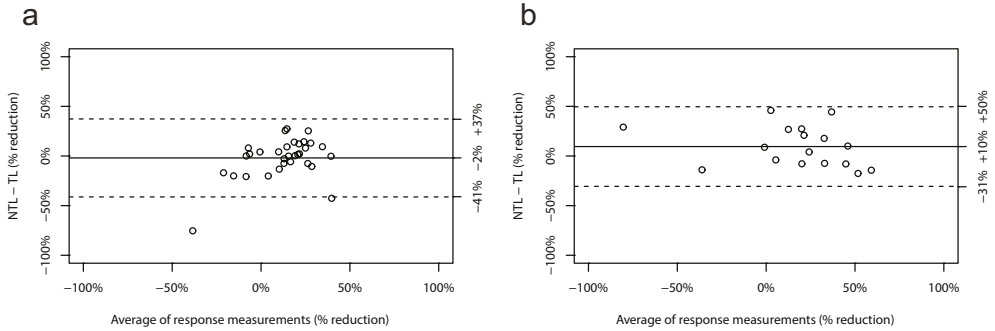


Figure E1. Bias and range of agreement for the comparison of TL and NTL reduction. (a) Bland-Altman plots on per-lesion basis for 1 month posttreatment. (b) Bland-Altman plots on per-lesion basis for 3 months posttreatment.

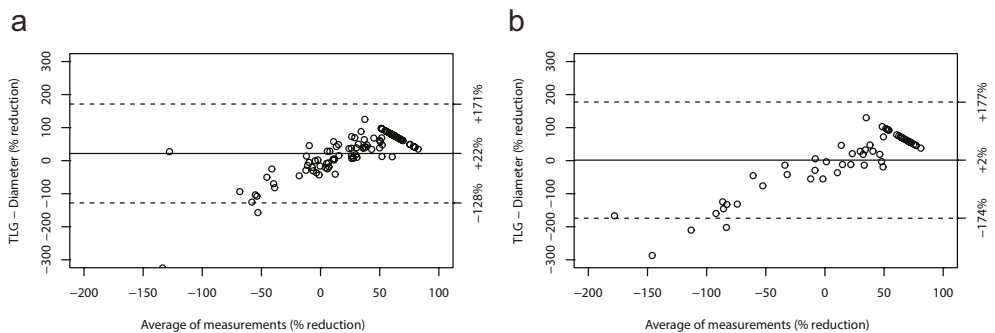


Figure E2. Bias and range of agreement for the comparison of LTD and TLG reduction. (a) Bland-Altman plots on per-lesion basis for 1 month posttreatment. (b) Bland-Altman plots on per-lesion basis for 3 months posttreatment.

PART III

Discussion and Summary

The background of the page is a light teal color. It is decorated with several abstract, circular shapes in a darker teal and a light orange color. These shapes are scattered across the page, some overlapping, and they resemble stylized cells or molecular structures. The overall aesthetic is clean and modern.

CHAPTER 7

General discussion and future perspectives

This thesis investigated disease progression and therapy-induced changes in patients with metastatic colorectal cancer. Despite the curative surgical option for these patients, colorectal cancer is still the third leading cause of cancer related deaths worldwide. Specific tumor characteristics were identified that might lead to novel (adjuvant) treatment modalities. Based on these insight novel adjuvant treatment strategies may be developed that limit recurrence following surgical interventions, thus improving life expectancy of patients with metastatic colorectal cancer.

Therapy-induced changes

Over the last decades, better model systems and tools for researching cancer have emerged. Improved imaging modalities and more extensive use of patient-derived material, such as three-dimensional organoid culture systems and organ-on-a-chip technology, are being employed [1-3]. Three-dimensional organoid culture systems not only recapitulate the genetic heterogeneity of the original tumor, but also remain genetically and phenotypically stable during prolonged culturing [4]. Whether organoids can be used to predict response to treatment is currently being evaluated. The first published studies show a remarkable positive correlation between the drug response of organoids and the tumors from which they were derived [4]. Organoid technology is a rapidly expanding field of research with model systems becoming available for many different diseases and organs. Further improving the system(s) will include optimizing matrix composition and adding cells from the tumor micro-environment. The timing of organoid derivation is important as therapy may alter the phenotype and genotype of the therapy-surviving tumor residue.

Chapter 2 reviews our current understanding of how surgical resection of primary tumors and liver metastases might accelerate outgrowth of remaining/residing micro-metastases in patients with mCRC. Despite overwhelming preclinical evidence, solid clinical proof for surgery-stimulated tumor growth in patients is lacking. This seems to be mainly attributed to culturing cells *in vitro* and experimental design. Experiments are generally set up to generate maximal effects, in immunocompromized mice, using early disease stage models and suffering from poor reproducibility. Hence, these systems cannot be relied on for trustworthy translation to the clinic. The novel methodologies described here (improved imaging modalities and organoid culture systems [5]) will help elucidate which of the observed preclinical phenomena bears clinical relevance. Consequently, individual cancer treatment plans can be made by targeting tumor cells at the right moment and location.

Specific tumor characteristics as therapeutic target

In CRC, gene expression-based tumor classification has identified 4 distinct molecular subtypes. These subtypes reflect differences in the activity of signaling pathways, tumor behavior, and clinical outcome. CMS4 is characterized by atypical expression of gene signatures reflecting a mesenchymal and a stem cell-like phenotype [5]. One of these signatures is increased oxidative signaling resulting in oxidative stress [6]. Oxidative stress is characterized by an imbalance between the production of reactive oxygen species (ROS) and their neutralization by antioxidants [7,8]. These mesenchymal-type primary colon tumors also express high levels of hypoxia-related genes [9]. This is in line with the observation that CMS4 is characterized by expression of angiogenesis-stimulating genes [6]. In addition, hypoxia is a driving force behind tumor recurrence following liver surgery: hypoxic tissue areas in the remnant liver form a niche for stem-like tumor cells that can subsequently drive recurrence [10,11]. Multiple approaches to targeting hypoxic tumor tissue are being explored, p.e. HIF modulators/inhibitors, HSP90 inhibitors, (V) EGFR inhibitor, RAF inhibitor, PI3K-AKT inhibitors [12,13]. However, problems with these drugs limited specificity or shortcomings in knowledge about their mechanism of action. Therefore, improvements need to be made for optimal clinical application. However, in addition to targeting the consequences of hypoxia it can also be used to activate prodrugs. Recently a study in multiple myeloma (MM) used this concept of using hypoxia to eliminate tumor cells. Bufalin, the used drug, induced DNA double strand breaks (DSBs), ROS induction and apoptosis under hypoxic condition resulting in cell death [14].

Chapter 3 focuses on hypoxia as a potential targetable tumor characteristic in CRLM. Reduced repair capacity in a subset of human colorectal cancers and in post-treatment tumor tissue provides a clear opportunity for therapeutic intervention. DNA repair defects and sensitivity to hypoxia-activated topoisomerase inhibitors are the basis for further developing combination therapies aimed at eradicating hypoxic tumor tissue. Hypoxic CRLM tissue with increased numbers of stem-like cells shows decreased expression of DNA repair proteins and increased DNA damage. This may be therapeutically exploited using hypoxia-activated prodrugs.

In line with this, **chapter 4** zooms in on oxidative stress as a targetable tumor feature. Oxidative stress is known to be a common characteristic of cancer cells that can be exploited therapeutically [7,8,15]. Both initial molecular classification, as well as therapy, influences the redox status. Sub-classification based on redox status may improve the prognostic value of colon cancer subtyping and the desired therapy. Therapeutics that interfere with redox status might be particularly effective in targeting metastases, therapy-surviving tumor cells, and mesenchymal-like tumors. They can be administered in combination with conventional oxidative stress-inducing radio- and chemotherapeutics. Treating patients with therapeutics that interfere with redox status after treatment with HAPs, might eliminate residual tumor cells.

A remaining challenge involves the delivery of drugs to these tumors. For many years researchers have been looking into a way to deliver drugs more efficiently into cancer cells, and to keep them in the target cell. One way in which drugs can leave cells is by being pumped out by drug efflux pumps. For instance, differentiated colorectal cancer cells express high levels of the drug efflux pumps ABCB1 and ABCG2. These pump the chemotherapeutic drug irinotecan into the lumen, thereby protecting nearby cancer stem cells [16]. In addition, lipid membrane-coated silica-carbon (LSC) hybrid nanoparticles were used to target the mitochondria of cancer cells to enhance ROS production. ROS could in its turn reduce the amount of ATP required for drug efflux in cancer cells. In this way, a larger window for drug treatment was created [17]. This ROS-elevating therapeutic approach may have value in targeting hypoxic (post-surgery) tumor residue and/or CMS4 CRC. Alternatively, local drug-releasing millirods, beads or nanoparticles can be used to embolize tumor-surrounding vessels, or can be placed in RFA needle tracts to help prevent or delay local recurrence [18]. Nanoparticles may also be applied in adjuvant hepatic arterial infusion pump (HAIP) chemotherapy. Recently, the PUMP trial, has been initiated in the Netherlands, evaluating the effect of HAIP in patients following resection of colorectal liver metastases. In this study, adjuvant chemotherapy is administered using a hepatic arterial infusion pump (HAIP). HAIP continuously delivers floxuridine directly into the hepatic artery aimed at achieving high local concentrations of the drug in the liver while reducing systemic exposure. Floxuridine is used since it has a 95% first-pass effect in the liver, which allows for a 400-fold increase in intratumoral concentration compared to systemic administration with only few systemic side effects. This approach has already led to improvement in overall survival (OS) of patients with CRLM in a recent phase 3 trial [19]. The concept of HAIP could be particularly interesting for patients with CRLM in combination with either hypoxia-activated prodrugs or therapeutics that interfere with redox status.

Novel imaging and (adjuvant) treatment modalities

Another newly developed local therapeutic alternative for liver malignancies involves radio embolization (RE), i.e. the intra-arterial delivery of radioactively labelled nanoparticles to hepatic tumors (such as HCC and CRLM). Technically feasible and hampered by surprisingly low morbidity rates, tumor-response rates to RE have been reported to vary widely [20]. Notwithstanding the fact that these results have been attained in end-stage disease only, RE in CRLM has produced mixed response rates in conjunction with rapid disease recurrence. In **chapter 5** of this thesis, an attempt was made to clarify the possible reasons for progression after treatment with radioembolization in patients with metastatic colorectal cancer. Patients with extrahepatic disease at baseline appeared to have a higher chance of early progression (3-month follow-up) after RE. Also, most patients with early progressive disease develop new intrahepatic as well as extrahepatic tumor-manifestations. This implies the need for a more restricted patient selection which excludes patients with extrahepatic disease. A reason for the high recurrence rate

and early progression after RE could be our current inability to detect micro-metastases and/or single tumor cells. Visualization of micrometastatic disease might create an opportunity to select only patients that might actually benefit from RE. Intra-operative fluorescence imaging might create this ability. Optical imaging with near infrared fluorescence is already starting to be implemented in several surgical oncological settings and can be used as a navigator during oncological surgical procedures to delineate normal from tumor tissue [21,22]. It can both be used for the just described patient selection, as well as for tumor cell targeting. Detection of micro-metastases in the liver makes targeting them possible and thereby preventing outgrowth of dormant or otherwise undetected tumor cells. Eventually this principle of optical imaging with near infrared fluorescence can also be used postoperative to detect residual disease.

In addition, RE is accompanied by surprisingly low morbidity rates. However, the fact that it is currently only used in end-stage disease, leaves room for improvement. It could for instance be used in earlier stage disease. The embolizing character triggers the thought of combining RE with hypoxia activated prodrugs. Using RE (and the resulting hypoxia) in combination with neoadjuvant HAP might be an elegant downsizing method before performing surgery.

PET/CT as possible alternative for Response-assessment following RE is addressed in **chapter 6** of this thesis. Metabolic based total liver glycolysis (TLG) response assessment on 18F-FDG-PET/CT appears more sensitive and accurate, especially at early follow-up, than size-based (anatomic) response assessment on MRI in patients with CRLM treated by radio embolization. Semi-automated liver response assessment with total liver TLG is objective, reproducible, rapid, and prognostic. Further research is needed for external validation of the described method and to assess whether increased response assessment sensitivity will enable change of management or in some cases early re-intervention with RE. Also, total liver TLG response assessment should be compared to other functional response assessment methods such as diffusion weighted MRI and pharmacokinetic analysis of dynamic contrast enhanced MRI [23,24]. In hepatocellular carcinoma (HCC), RE reportedly causes tumor down staging, serving as a bridge to transplantation. In addition, RE may induce overall survival benefit [25]. Prospective RCTs, such as Transarterial RADioembolisation versus ChemoEmbolisation for the treatment of hepatocellular carcinoma (TRACE), are currently ongoing. And following the SARAH trial in which sorafenib is compared to RE [26], several randomized studies are currently ongoing comparing RE with sorafenib in advanced disease setting. However, the role of RE in the treatment of CRLM remains to be further delineated. Possibly, RE will prove most valuable in early CRLM, or might serve for downsizing, and/or as a bridge to the application of other treatment modalities [27]. One example is the application of RE to induce hypertrophy in the future liver remnant while treating existing tumor(s) in the lobe to be resected. This concept known as radiation lobectomy has recently been shown to convert unresectable hepatic malignancy to a resectable state [28].



Considering the outcomes of this thesis a focus on early detection of (micro)metastases and on targeting these tumor cells by exploiting their characteristics could be a realistic way forward. The tumor specific characteristics could be identified by initiating 3D cultures from each patient, leading to patient-specific treatment protocols [29]. After debulking, metastatic residual disease could be detected with fluorescence-guided imaging, allowing additional 'targeted surgery'. Adjuvant treatment may subsequently consist of nanoparticles loaded with hypoxia-activated prodrugs or therapeutics interfering with redox status, via adjuvant hepatic arterial infusion pump.

References

1. Huh, D., G.A. Hamilton, and D.E. Ingber, From 3D cell culture to organs-on-chips. *Trends Cell Biol*, 2011. 21(12): p. 745-54.
2. Skardal, A., et al., A reductionist metastasis-on-a-chip platform for in vitro tumor progression modeling and drug screening. *Biotechnol Bioeng*, 2016. 113(9): p. 2020-32.
3. Bhatia, S.N. and D.E. Ingber, Microfluidic organs-on-chips. *Nat Biotechnol*, 2014. 32(8): p. 760-72
4. Drost J, Clevers H. Organoids in cancer research. *Nat Rev Cancer*. 2018 Jul;18(7):407-418
5. Fujii M, Clevers H, Sato T. Modeling Human Digestive Diseases with CRISPR-Cas9-modified Organoids. *Gastroenterology*. 2018 Nov 23. pii: S0016-5085(18)35296-X.
6. Guinney J, Dienstmann R, Wang X, de Reynies A, Schlicker A, Sonesson C, Marisa L, Roepman P, Nyamundanda G, Angelino P, Bot BM, Morris JS, Simon IM, et al. The consensus molecular subtypes of colorectal cancer. *Nat Med*. 2015; 21: 1350-6.
7. Trachootham D, Zhou Y, Zhang H, Demizu Y, Chen Z, Pelicano H, Chiao PJ, Achanta G, Arlinghaus RB, Liu J, Huang P: Selective killing of oncogenically transformed cells through a ROS-mediated mechanism by beta-phenylethyl isothiocyanate. *Cancer cell* 2006, 10:241-52.
8. Cairns RA, Harris IS, Mak TW: Regulation of cancer cell metabolism. *Nature reviews Cancer* 2011, 11:85-95
9. Fatrai S, van Schelven SJ, Ubink I, Govaert KM, Raats D, Koster J, Verheem A, Borel Rinkes IH, Kranenburg O. Maintenance of Clonogenic KIT(+) Human Colon Tumor Cells Requires Secretion of Stem Cell Factor by Differentiated Tumor Cells. *Gastroenterology*. 2015; 149: 692-704.
10. Nijkamp MW, van der Bilt JD, de Bruijn MT, Molenaar IQ, Voest EE, van Diest PJ, Kranenburg O, Borel Rinkes IH. Accelerated perinecrotic outgrowth of colorectal liver metastases following radiofrequency ablation is a hypoxia-driven phenomenon. *Ann Surg*. 2009; 249: 814-23.
11. Govaert KM, Emmink BL, Nijkamp MW, Cheung ZJ, Steller EJ, Fatrai S, de Bruijn MT, Kranenburg O, Borel Rinkes IH. Hypoxia after liver surgery imposes an aggressive cancer stem cell phenotype on residual tumor cells. *Ann Surg*. 2014; 259: 750-9.
12. LaGory EL, Giaccia AJ. The ever-expanding role of HIF in tumour and stromal biology. *Nat Cell Biol*. 2016 Apr;18(4):356-65
13. Jae-Young Kim and Joo-Yong Lee. Targeting Tumor Adaption to Chronic Hypoxia: Implications for Drug Resistance, and How It Can Be Overcome. *Int J Mol Sci*. 2017 Sep; 18(9): 1854
14. Fujii E, Inada Y, Kakoki M, Nishimura N, Endo S, Fujiwara S, Wada N, Kawano Y, Okuno Y, Sugimoto T, Hata H. Bufalin induces DNA damage response under hypoxic condition in myeloma cells. *Oncol Lett*. 2018 May;15(5):6443-6449



15. Wiseman H, Halliwell B: Damage to DNA by reactive oxygen and nitrogen species: role in inflammatory disease and progression to cancer. *The Biochemical journal* 1996, 313 (Pt 1):17-29. Gorrini C, Harris IS, Mak TW: Modulation of oxidative stress as an anticancer strategy. *Nature reviews Drug discovery* 2013, 12:931-47
16. Emmink, B.L., et al., Differentiated human colorectal cancer cells protect tumorigenic cells from irinotecan. *Gastroenterology*, 2011. 141(1): p. 269-78
17. Hai Wang, Zan Gao, Xuanyou Liu, Pranay Agarwal, Shuting Zhao, Daniel W. Conroy, Guang Ji, Jianhua Yu, Christopher P. Jaroniec, Zhenguo Liu, Xiongbin Lu, Xiaodong Li, Xiaoming He. Targeted production of reactive oxygen species in mitochondria to overcome cancer drug resistance. *Nature Communications*, 2018; 9 (1)
18. Jahanban-Esfahlan R, de la Guardia M, Ahmadi D, Yousefi. Modulating tumor hypoxia by nanomedicine for effective cancer therapy. *J Cell Physiol.* 2018 Mar;233(3):2019-2031
19. Chakedis J, Beal EW, Sun S, Galo J, Chafitz A, Davidson G, Reardon J, Dillhoff M, Pawlik TM, Abdel-Misih S, Bloomston M, Schmidt CR. Implementation and early outcomes for a surgeon-directed hepatic arterial infusion pump program for colorectal liver metastases. *J Surg Oncol.* 2018 Dec;118(7):1065-107
20. Kennedy, A., et al., Updated survival outcomes and analysis of long-term survivors from the MORE study on safety and efficacy of radioembolization in patients with unresectable colorectal cancer liver metastases. *J Gastrointest Oncol*, 2017. 8(4): p. 614-624
21. van der Vorst, J.R., et al., Near-infrared fluorescence-guided resection of colorectal liver metastases. *Cancer*, 2013. 119(18): p. 3411-8
22. van den Berg NS, Miwa M, KleinJan GH, et al. (Near-infrared) fluorescence-guided surgery under ambient light conditions: a next step to embedment of the technology in clinical routine. *Ann Surg Oncol.* 2016;23:2586-95
23. Barabasch A, Kraemer NA, Ciritsis A, Hansen NL, Lierfeld M, Heinzl A, et al. Diagnostic accuracy of diffusion-weighted magnetic resonance imaging versus positron emission tomography/computed tomography for early response assessment of liver metastases to Y90-radioembolization. *Investigative radiology.* 2015;50(6):409-15
24. Choyke PL, Dwyer AJ, Knopp MV. Functional tumor imaging with dynamic contrast-enhanced magnetic resonance imaging. *Journal of magnetic resonance imaging: JMRI.* 2003;17(5):509-20
25. Crocetti L, Bargellini I, Cioni R. Loco-regional treatment of HCC: current status. *Clin Radiol.* 2017 Aug;72(8):626-635
26. Vilgrain V, et al. Efficacy and safety of selective internal radiotherapy with yttrium-90 resin microspheres compared with sorafenib in locally advanced and inoperable hepatocellular carcinoma (SARAH): an open-label randomised controlled phase 3 trial. *Lancet Oncol.* 2017 Dec;18(12):1624-1636.
27. M.N.G.J.A. Braat, M. Samim, M.A.A.J. van den Bosch, and M.G.E.H. Lam. The role of 90Y-radioembolization in downstaging primary and secondary hepatic malignancies: a systematic review. *Clin Transl Imaging.* 2016; 4: 283-295

28. Shah JL, Zendejas-Ruiz IR, Thornton LM, Geller BS, Grajo JR, Collinsworth A, George TJ Jr, Toskich B. Neoadjuvant transarterial radiation lobectomy for colorectal hepatic metastases: a small cohort analysis on safety, efficacy, and radiopathologic correlation. *J. Gastrointest Oncol.* 2017 Jun;8(3):E43-E51
29. Artegiani B, Clevers H. Use and application of 3D-organoid technology. *Hum Mol Genet.* 2018 Aug 1;27(R2):R99-R107.



The background of the page is a light teal color. It is decorated with several abstract, circular shapes in shades of teal and orange. These shapes are scattered across the page, some overlapping, and they have a slightly irregular, hand-drawn appearance. The shapes vary in size and are positioned around the central text.

CHAPTER 8

Summary - Nederlandse samenvatting

Darmkanker is wereldwijd de op drie na meest voorkomende vorm van kanker. Het is een belangrijke oorzaak van kanker-gerelateerde sterfte met wereldwijd ongeveer 700.000 sterfgevallen per jaar [1]. De prognose van darmkankerpatiënten wordt grotendeels bepaald door de aanwezigheid van uitzaaiingen, voornamelijk in de lever. Ongeveer 45% van de darmkankerpatiënten ontwikkelt uiteindelijk uitzaaiingen, terwijl 15-20% zich reeds presenteert met uitzaaiingen op het moment dat de diagnose gesteld wordt (synchrone uitzaaiingen) [2]. Indien onbehandeld, is de gemiddelde overleving van patiënten met leveruitzaaiingen in de lever minder dan 1 jaar [3] en de 5-jaarsoverleving slechts 13% [4,5]. Dit maakt (uitgezaaide) darmkanker een van de meest dodelijke ziekten wereldwijd. Chirurgische verwijdering van de tumor is momenteel de eerste keuze voor behandeling van darmkanker. Echter, ongeveer 100 jaar geleden werd reeds beschreven hoe opereren ook juist tumorgroei en het ontstaan van uitzaaiingen kan bevorderen [6]. Niet alleen chirurgie, maar ook andere behandelingen kunnen tumorgroei beïnvloeden. Dit proefschrift onderzoekt toename van ziekte en de veranderingen door verschillende therapieën in tumoren van patiënten met uitgezaaide darmkanker. Specifieke tumoreigenschappen kunnen worden geïdentificeerd die ons naar nieuwe (aanvullende) behandelingen zouden kunnen leiden. Ook kunnen aanvullende strategieën worden ontwikkeld die terugkeer van kanker na opereren verminderen. Uiteindelijk kunnen aanbevelingen worden gedaan om de overleving in deze groep patiënten te verbeteren. Dit zal uiteindelijk resulteren in verbetering van gepersonaliseerde kankerzorg en toegenomen levensverwachting bij patiënten met uitgezaaide darmkanker.

Therapie geïnduceerde veranderingen in tumorcellen

In de afgelopen decennia zijn betere modelsystemen en hulpmiddelen voor het bestuderen van kanker ontwikkeld. Verbeterde beeldvorming wordt gebruikt, evenals een beter en uitgebreider gebruik van patiënt-afgeleid materiaal, zoals 3D organoïden en orgaan-op-een-chip technologie [7-9]. Organoïden zijn mini-orgaantjes die in het laboratorium door mensen gekweekt zijn vanuit tumoren van patiënten. Driedimensionale organoïden bootsen niet alleen de genetische heterogeniteit van de oorspronkelijke tumor na, maar blijven ook genetisch en fenotypisch (zoals je aan de buitenkant kan waarnemen) stabiel tijdens langdurig kweken [10]. Of organoïden kunnen worden gebruikt om respons op behandeling te voorspellen, wordt momenteel geëvalueerd. De eerste gepubliceerde studies laten een opmerkelijke positieve correlatie zien tussen de medicatierespons van organoïden en de tumoren waarvan ze zijn gekweekt [10]. Deze organoïden-technologie is een snelgroeiend onderzoeksgebied waarbij modelsystemen beschikbaar komen voor veel verschillende ziekten en organen. Door in het laboratorium cellen toe te voegen die in de natuurlijke situatie ook in de micro-omgeving van de tumor voorkomen, worden de bestaande systemen steeds beter. **Hoofdstuk 2** beschrijft ons huidige inzicht in de manier waarop opereren van darmkanker en leveruitzaaiingen, het uitgroeien van resterende of achtergebleven micro-uitzaaiingen bij patiënten met uitgezaaide darmkanker kan versnellen. Ondanks

overweldigend preklinisch bewijs, ontbreekt solide bewijs bij patiënten voor tumorgroei die door chirurgie veroorzaakt wordt. Dit lijkt vooral te liggen aan het kweken van cellen in het laboratorium en de manier waarop experimenten zijn opgezet. Experimenten zijn vaak speciaal ontworpen om maximale effecten te verkrijgen. Er worden muizen met een onderdrukt immuunsysteem gebruikt en gewerkt met modellen van ziekte in een vroeg stadium die slecht te reproduceren zijn. Om deze redenen kan er niet altijd een betrouwbare vertaling naar de kliniek worden gemaakt. De nieuwe modellen die hier worden beschreven (verbeterde beeldvorming en gebruik van organoïden [5]) zullen verklaren welke van de waargenomen preklinische verschijnselen, daadwerkelijk klinische relevantie hebben. Uiteindelijk kunnen individuele behandelplannen voor kankerpatiënten worden gemaakt. Dit door tumorcellen op het juiste moment en op de juiste locatie te behandelen.

Specifieke tumoreigenschappen als therapeutisch doelwit

Dooropgenniveaunaardarmkankertekijken, is een tumorclassificatie (CMS) gemaakt die gebaseerd is op vier verschillende moleculaire subtypen. Deze subtypen weerspiegelen verschillen in de activiteit van signaalroutes, tumorgedrag en overleving. CMS4 wordt gekenmerkt door afwijkende expressie van genen, met name genen die mesenchymaal en stamcelachtig zijn [11]. Een van deze kenmerken is verhoogde oxidatieve signalering die leidt tot oxidatieve stress [12]. Oxidatieve stress wordt gekenmerkt door een disbalans tussen de productie van reactieve zuurstofspecies (ROS) en hun neutralisatie door antioxidanten [13,14]. Deze darmtumoren van het mesenchymale type hebben ook veel genen die gerelateerd zijn aan hypoxie (lage zuurstofspanning) [15]. Dit komt overeen met de waarneming dat CMS4 ook veel genen heeft gerelateerd aan angiogenese (nieuwe bloedvatvorming) [12]. Daarnaast is hypoxie een drijvende kracht achter tumorterugkeer na leverchirurgie: hypoxische gebieden in de resterende lever vormen een niche voor kankerstemcellen die vervolgens weer kunnen uitgroeien tot kanker [16,17]. Meerdere behandelingen specifiek tegen hypoxisch tumorweefsel worden onderzocht, o.a. HIF-remmers, HSP90-remmers, (V)EGFR-remmers, RAF-remmers, PI3K-AKT-remmers [18,19]. Echter, het grootste probleem van deze geneesmiddelen is dat ze niet heel specifiek werken en dat kennis over hun werkingsmechanisme ontbreekt. Daarom hebben ze een beperkte klinische toepassing. Naast het focussen op de gevolgen van hypoxie, kan deze lage zuurstofspanning ook worden gebruikt om pro-drugs (drugs die alleen geactiveerd worden onder zuurstofspanning) te activeren. Onlangs gebruikte een studie in multipel myeloom (MM) dit concept van het gebruik maken van hypoxie om tumorcellen te elimineren. Het gebruikte geneesmiddel zorgde voor (dubbelstrengs) breuken in het DNA en productie van reactieve zuurstofspecies, uiteindelijk resulterend in celdood [20].

Hoofdstuk 3 richtte zich op hypoxie als een potentieel doelwit in uitgezaaide darmkanker. Verminderde reparatiecapaciteit in een bepaalde groep darmkankerpatiënten en in

kankercellen na een behandeling, biedt een duidelijke mogelijkheid voor behandeling. Gebrek aan het herstellen van (dubbelstrengs)breuken in het DNA en gevoeligheid voor hypoxie-geactiveerde chemotherapie die deze (dubbelstrengs)breuken veroorzaakt, vormen de basis voor deze behandeling. Dit zal leiden tot combinatietherapieën gericht op het uitroeien van hypoxisch tumorweefsel. Hypoxisch tumorweefsel van patiënten met uitgezaaide darmkanker met meer kankerstemcellen heeft minder DNA-reparatie-eiwitten (om de breuken te maken) en meer DNA-beschadiging. Dit kan therapeutisch worden gebruikt met chemotherapie die alleen geactiveerd wordt als er lage zuurstofspanning is.

Hoofdstuk 4 gaat in op oxidatieve stress als doelwit tegen uitgezaaide darmkanker. Van oxidatieve stress is bekend dat het een gemeenschappelijk kenmerk is van kankercellen [13,14,21]. Zowel de initiële moleculaire classificatie (CMS4) als verschillende behandelingen hebben invloed op deze redox-status (balans tussen de productie van ROS en hun neutralisatie door antioxidanten). Sub classificatie op basis van de redox-status kan de voorspellende waarde van deze subtypen voor de juiste behandeling van darmkanker verbeteren. Behandelingen die invloed hebben op de redox-status kunnen met name effectief zijn voor patiënten met uitzaaiingen, therapieresistente tumorcellen en mesenchymaal-achtige tumoren. Ze kunnen worden toegevend in combinatie met radiotherapie en chemotherapie omdat die al voor oxidatieve stress zorgen. Als patiënten al behandeld zijn met de chemotherapie die enkel geactiveerd wordt door hypoxie, kunnen geneesmiddelen die de redox-status beïnvloeden resterende tumorcellen doden.

Een resterende uitdaging is dan nog altijd de toediening van geneesmiddelen aan deze tumoren. Al vele jaren zoeken onderzoekers naar een manier om geneesmiddelen efficiënter in kankercellen af te leveren en ze in de tumorcel te houden. Een manier waarop geneesmiddelen cellen kunnen verlaten, is door een effluxpomp. Gedifferentieerde darmkankercellen hebben veel van deze effluxpompen. Deze pompen specifieke chemotherapie (irinotecan) uit de gedifferentieerde cel, waardoor nabijgelegen kankerstemcellen worden beschermd [22]. In een recente studie werd gekeken naar hybride nanodeeltjes met lipidemembraan-gecoate silica-koolstof (LSC) om de ROS-productie van kankercellen via hun mitochondria (kleine energiecentrales van een cel) te verbeteren. ROS zou op zijn beurt de hoeveelheid energie in de cel (ATP) kunnen verminderen die nodig is voor het naar buiten pompen van chemotherapie. Op deze manier werd 'window' gecreëerd waarin medicijnen kunnen worden gegeven [23]. Deze behandeling waarbij er meer ROS in de cel komt, kan interessant zijn bij de behandeling van overgebleven hypoxische tumorcellen en bij CMS4 darmkankerpatiënten. Als alternatief kunnen kleine nanodeeltjes gebruikt worden die lokaal vastlopen in de vaten rondom de tumor en daar hun medicijn loslaten. Op deze manier kan lokale terugkeer van kanker worden voorkomen of vertraagd [24]. Nanodeeltjes kunnen ook worden gebruikt in aanvullende chemotherapie die via de leverslagader gegeven wordt (HAIP). Onlangs is de PUMP-studie in Nederland geïnitieerd, waarbij het effect van

HAIP werd geëvalueerd bij patiënten na resectie van leveruitzaaiingen. In deze studie wordt aanvullende chemotherapie toegediend met behulp van een leverslagader pomp. HAIP levert chemotherapie (floxuridine) continu rechtstreeks aan de leverslagader. Het is gericht op het bereiken van hoge lokale concentraties van het geneesmiddel in de lever terwijl de systemische blootstelling wordt verminderd. Floxuridine wordt gebruikt omdat het een first-pass effect van 95% heeft in de lever, wat een 400-voudige toename van de intratumorale concentratie mogelijk maakt in vergelijking met systemische toediening. Daarnaast heeft het slechts enkele systemische bijwerkingen. Deze benadering heeft al geleid tot verbetering van de algehele overleving van patiënten met naar de lever uitgezaaid darmkanker in een recente fase 3-studie [25]. Het concept van HAIP zou in het bijzonder interessant kunnen zijn voor patiënten met naar de lever uitgezaaid darmkanker in combinatie met enerzijds door hypoxie geactiveerde prodrugs of anderzijds geneesmiddelen die interfereren met de redox-status.

Nieuwe beeldvorming en (aanvullende) behandelingen

Een ander nieuw ontwikkeld lokaal therapeutisch alternatief voor levertumoren betreft radio-embolisatie (RE), d.w.z. de intra-arteriële afgifte van radioactief gemerkte nanodeeltjes aan levertumoren (zoals primaire levertumoren of leveruitzaaiingen). RE is technisch haalbaar en kent weinig bijwerkingen. Het resultaat van de tumoren na RE varieert sterk [26]. Zeker in leveruitzaaiingen bij darmkanker heeft RE een gemengd responspercentage en komt de tumor vaak snel terug. Daarbij moet worden vermeld dat dit allemaal studies zijn in het eindstadium van kanker. In **hoofdstuk 5** van dit proefschrift is een poging gedaan om de mogelijke redenen voor de snelle terugkeer na behandeling met RE te bekijken bij patiënten met uitgezaaide darmkanker. Patiënten die ook uitzaaiingen buiten de lever hebben als ze de diagnose darmkanker krijgen, hebben ook een grotere kans dat het snel terugkomt na RE (na 3 maanden). Ook ontwikkelen de meeste patiënten met vroege terugkeer van ziekte nieuwe uitzaaiingen in én buiten de lever. Dit impliceert de behoefte aan betere patiëntselectie, waarbij patiënten met uitzaaiingen in de lever worden uitgesloten. Een reden voor de hoge mate van tumorterugkeer na RE zou ons huidige onvermogen kunnen zijn om micro-uitzaaiingen en/of 'single-cell' tumorcellen te detecteren. Het aantonen van micro-uitzaaiingen kan een mogelijkheid creëren om alleen patiënten te selecteren die waarschijnlijk profijt hebben van RE. Intra-operatieve fluorescentiebeeldvorming (lichtgevende cellen) kan deze mogelijkheid creëren. Optische beeldvorming met infraroodfluorescentie wordt nu al geïmplementeerd in verschillende ziekenhuizen die oncologische zorg leveren. Het kan worden gebruikt als navigatie tijdens kankeroperaties om normaal van tumorweefsel te onderscheiden [27,28]. Het kan zowel gebruikt worden om tumorcellen doelwit te maken voor therapie, als voor de zojuist beschreven patiëntselectie. Detectie van micro-uitzaaiingen in de lever maakt het mogelijk om de behandeling erop te richten en uitgroei van slapende en/of anders niet-gedetectedeerde tumorcellen te voorkomen.

Uiteindelijk kan dit principe van optische beeldvorming met infraroodfluorescentie ook postoperatief worden gebruikt om resterende ziekte te detecteren.

Daarnaast biedt het feit dat RE momenteel alleen gebruikt wordt bij patiënten die in een eindstadium van kanker zitten en nog steeds weinig bijwerkingen hebben, ruimte voor verbetering. Het kan bijvoorbeeld worden gebruikt in een vroeger ziektestadium. Het vastlopen van de nanodeeltjes in bloedvaten rondom de tumor kan interessant zijn als het gecombineerd wordt met hypoxie-geactiveerde prodrugs. Het gebruik van RE (en de resulterende hypoxie) in combinatie met preoperatieve HAP kan een elegante manier zijn om de tumor te verkleinen voordat een operatie wordt uitgevoerd.

Het gebruik van PET/CT als mogelijk alternatief voor het beoordelen van respons na RE is onderwerp van discussie in **hoofdstuk 6** van dit proefschrift. Het beoordelen van respons van tumorcellen kan door naar het metabolisme (energiehuishouding) van de tumor te kijken middels totale leverglycolyse (TLG). Kijken naar TLG met een 18F-FDG-PET/CT-scan, lijkt gevoeliger en nauwkeuriger bij patiënten met naar de lever uitgezaaide darmkanker die met RE zijn behandeld. Vooral bij vroege follow-up tot 3 maanden. Dit is vergeleken met MRI, waarbij naar grootte van de tumor wordt gekeken. Deels geautomatiseerde evaluatie van de leverrespons met TLG voor de totale lever is objectief, reproduceerbaar, snel en prognostisch. Verder onderzoek is nodig voor externe validatie van de beschreven methode en om te kijken of deze vroege manier van respons beoordeling leidt tot andere behandeling. Het kan zorgen voor sneller ingrijpen als er tumor terugkeer is na RE. Ook moet TLG worden vergeleken met andere beeldvorming die naar de energiehuishouding van tumoren kijkt, zoals diffusie-gewogen MRI en farmacokinetische analyse van dynamisch-contrast-versterkte MRI [29,30]. In hepatocellulair carcinoom (HCC; een vorm van leverkanker) zorgt RE voor verkleining van de tumor, waardoor het als overbrugging naar transplantatie leidt. Bovendien zorgt RE hierbij ook voor een langere levensverwachting [31]. Prospectieve randomized controlled trials, zoals Transarteriële RAdioembolisering versus Chemo-Embolisatie voor de behandeling van hepatocellulair carcinoom (TRACE), zijn momenteel in uitvoering. Ook, na de SARAH-studie, waarin sorafenib wordt vergeleken met RE [32], zijn er meer gerandomiseerde studies in uitvoering die RE evalueren in vergelijking met sorafenib bij een vergevorderde ziekte. De rol van RE in de behandeling van naar de lever uitgezaaide darmkanker moet echter nog worden opgehelderd. Mogelijk zal RE voor patiënten in een vroeg ziektestadium van naar de lever uitgezaaide darmkanker waardevol blijken te zijn. Daarnaast kan het dienen voor verkleining van de tumor of als een brug naar de toepassing van andere behandelingen [33]. Een voorbeeld is de toepassing van RE voor het induceren van hypertrofie in het toekomstige leverrestant terwijl de bestaande tumor(en) in de te reseceren helft worden behandeld. Van dit concept, dat bekend staat als stralingslobotomie, is onlangs aangetoond dat het inoperabele levertumoren omzet naar een reseceerbare toestand [34].

Gezien de uitkomsten van dit proefschrift kan een focus op vroege detectie van (micro) uitzaaiingen en tumorleigenschappen een realistische stap voorwaarts zijn. De tumor-specifieke kenmerken kunnen worden geïdentificeerd door het initiëren van 3D-kweken van elke patiënt, leidend tot patiënt-specifieke behandelprotocollen [35]. Na het verwijderen van de tumor kon uitgezaaide restziekte worden opgespoord met fluorescentie-geleide beeldvorming, waardoor aanvullende 'gerichte chirurgie' mogelijk was. De aanvullende behandeling kan vervolgens bestaan uit nanodeeltjes die verschillende medicijnen bevatten. Enerzijds kan dat chemotherapie zijn die geactiveerd wordt door hypoxie, anderzijds kan het een medicijn zijn dat interfereert met de redox-status. Een elegante manier om dit toe te dienen is via een leverslagaderpomp zijn.



References

1. Ferlay, et al. Cancer incidence and mortality worldwide: wources, methods, and major patterns in GLOBOCAN 2012. *Int. J. Cancer*, 2015. 136 (5):p E359-86.
2. Siegel R, Desantis C, Jemal A. Colorectal cancer statistics, 2014. *CA Cancer J Clin* 2014; 64: 104-117
3. Hackl C, Neumann P, Gerken M, Loss M, Klinkhammer-Schalke M, Schlitt HJ. Treatment of colorectal liver metastases in Germany: a ten-year population-based analysis of 5772 cases of primary colorectal adenocarcinoma. *BMC Cancer* 2014;14:810
4. Torre, L.A., et al., Global cancer statistics, 2012. *CA Cancer J Clin*, 2015. 65(2): p. 87-108
5. Siegel, R.L., K.D. Miller, and A. Jemal, Cancer statistics, 2016. *CA Cancer J Clin*, 2016. 66(1): p. 7-30
6. Clunet J. Recherches expérimentales sur les tumeurs malignes. Steinhil, Paris. 1910; Marie PC, J. . Fréquences des métastases viscérales chez les souris cancéreuses après ablation chirurgicale de leur tumeur. *Bull Assoc Franc L'Étude Cancér.* 1910;3:19-23
7. Huh, D., G.A. Hamilton, and D.E. Ingber, From 3D cell culture to organs-on-chips. *Trends Cell Biol*, 2011. 21(12): p. 745-54.
8. Skardal, A., et al., A reductionist metastasis-on-a-chip platform for in vitro tumor progression modeling and drug screening. *Biotechnol Bioeng*, 2016. 113(9): p. 2020-32.
9. Bhatia, S.N. and D.E. Ingber, Microfluidic organs-on-chips. *Nat Biotechnol*, 2014. 32(8): p. 760-72
10. Drost J, Clevers H. Organoids in cancer research. *Nat Rev Cancer.* 2018 Jul;18(7):407-418
11. Fujii M, Clevers H, Sato T. Modeling Human Digestive Diseases with CRISPR-Cas9-modified Organoids. *Gastroenterology.* 2018 Nov 23. pii: S0016-5085(18)35296-X.
12. Guinney J, Dienstmann R, Wang X, de Reynies A, Schlicker A, Soneson C, Marisa L, Roepman P, Nyamundanda G, Angelino P, Bot BM, Morris JS, Simon IM, et al. The consensus molecular subtypes of colorectal cancer. *Nat Med.* 2015; 21: 1350-6.
13. Trachootham D, Zhou Y, Zhang H, Demizu Y, Chen Z, Pelicano H, Chiao PJ, Achanta G, Arlinghaus RB, Liu J, Huang P: Selective killing of oncogenically transformed cells through a ROS-mediated mechanism by beta-phenylethyl isothiocyanate. *Cancer cell* 2006, 10:241-52.
14. Cairns RA, Harris IS, Mak TW: Regulation of cancer cell metabolism. *Nature reviews Cancer* 2011, 11:85-95
15. Fatrai S, van Schelven SJ, Ubink I, Govaert KM, Raats D, Koster J, Verheem A, Borel Rinkes IH, Kranenburg O. Maintenance of Clonogenic KIT(+) Human Colon Tumor Cells Requires Secretion of Stem Cell Factor by Differentiated Tumor Cells. *Gastroenterology.* 2015; 149: 692-704.

16. Nijkamp MW, van der Bilt JD, de Bruijn MT, Molenaar IQ, Voest EE, van Diest PJ, Kranenburg O, Borel Rinkes IH. Accelerated perinecrotic outgrowth of colorectal liver metastases following radiofrequency ablation is a hypoxia-driven phenomenon. *Ann Surg.* 2009; 249: 814-23.
17. Govaert KM, Emmink BL, Nijkamp MW, Cheung ZJ, Steller EJ, Fatrai S, de Bruijn MT, Kranenburg O, Borel Rinkes IH. Hypoxia after liver surgery imposes an aggressive cancer stem cell phenotype on residual tumor cells. *Ann Surg.* 2014; 259: 750-9.
18. LaGory EL, Giaccia AJ. The ever-expanding role of HIF in tumour and stromal biology. *Nat Cell Biol.* 2016 Apr;18(4):356-65
19. Jae-Young Kim and Joo-Yong Lee. Targeting Tumor Adaption to Chronic Hypoxia: Implications for Drug Resistance, and How It Can Be Overcome. *Int J Mol Sci.* 2017 Sep; 18(9): 1854
20. Fujii E, Inada Y, Kakoki M, Nishimura N, Endo S, Fujiwara S, Wada N, Kawano Y, Okuno Y, Sugimoto T, Hata H. Bufalin induces DNA damage response under hypoxic condition in myeloma cells. *Oncol Lett.* 2018 May;15(5):6443-6449
21. Wiseman H, Halliwell B: Damage to DNA by reactive oxygen and nitrogen species: role in inflammatory disease and progression to cancer. *The Biochemical journal* 1996, 313 (Pt 1):17-29. Gorrini C, Harris IS, Mak TW: Modulation of oxidative stress as an anticancer strategy. *Nature reviews Drug discovery* 2013, 12:931-47
22. Emmink, B.L., et al., Differentiated human colorectal cancer cells protect tumor-initiating cells from irinotecan. *Gastroenterology*, 2011. 141(1): p. 269-78
23. Hai Wang, Zan Gao, Xuanyou Liu, Pranay Agarwal, Shuting Zhao, Daniel W. Conroy, Guang Ji, Jianhua Yu, Christopher P. Jaroniec, Zhenguo Liu, Xiongbin Lu, Xiaodong Li, Xiaoming He. Targeted production of reactive oxygen species in mitochondria to overcome cancer drug resistance. *Nature Communications*, 2018; 9 (1)
24. Jahanban-Esfahlan R, de la Guardia M, Ahmadi D, Yousefi. Modulating tumor hypoxia by nanomedicine for effective cancer therapy. *J Cell Physiol.* 2018 Mar;233(3):2019-2031
25. Chakedis J, Beal EW, Sun S, Galo J, Chafitz A, Davidson G, Reardon J, Dillhoff M, Pawlik TM, Abdel-Misih S, Bloomston M, Schmidt CR. Implementation and early outcomes for a surgeon-directed hepatic arterial infusion pump program for colorectal liver metastases. *J Surg Oncol.* 2018 Dec;118(7):1065-107
26. Kennedy, A., et al., Updated survival outcomes and analysis of long-term survivors from the MORE study on safety and efficacy of radioembolization in patients with unresectable colorectal cancer liver metastases. *J Gastrointest Oncol*, 2017. 8(4): p. 614-624
27. van der Vorst, J.R., et al., Near-infrared fluorescence-guided resection of colorectal liver metastases. *Cancer*, 2013. 119(18): p. 3411-8
28. van den Berg NS, Miwa M, KleinJan GH, et al. (Near-infrared) fluorescence-guided surgery under ambient light conditions: a next step to embedment of the technology in clinical routine. *Ann Surg Oncol.* 2016;23:2586-95

29. Barabasch A, Kraemer NA, Ciritsis A, Hansen NL, Lierfeld M, Heinzl A, et al. Diagnostic accuracy of diffusion-weighted magnetic resonance imaging versus positron emission tomography/computed tomography for early response assessment of liver metastases to Y90-radioembolization. *Investigative radiology*. 2015;50(6):409-15
30. Choyke PL, Dwyer AJ, Knopp MV. Functional tumor imaging with dynamic contrast-enhanced magnetic resonance imaging. *Journal of magnetic resonance imaging: JMRI*. 2003;17(5):509-20
31. Crocetti L, Bargellini I, Cioni R. Loco-regional treatment of HCC: current status. *Clin Radiol*. 2017 Aug;72(8):626-635
32. Vilgrain V, et al. Efficacy and safety of selective internal radiotherapy with yttrium-90 resin microspheres compared with sorafenib in locally advanced and inoperable hepatocellular carcinoma (SARAH): an open-label randomised controlled phase 3 trial. *Lancet Oncol*. 2017 Dec;18(12):1624-1636.
33. M.N.G.J.A. Braat, M. Samim, M.A.A.J. van den Bosch, and M.G.E.H. Lam. The role of 90Y-radioembolization in downstaging primary and secondary hepatic malignancies: a systematic review. *Clin Transl Imaging*. 2016; 4: 283–295
34. Shah JL, Zendejas-Ruiz IR, Thornton LM, Geller BS, Grajo JR, Collinsworth A, George TJ Jr, Toskich B. Neoadjuvant transarterial radiation lobectomy for colorectal hepatic metastases: a small cohort analysis on safety, efficacy, and radiopathologic correlation. *J. Gastrointest Oncol*. 2017 Jun;8(3):E43-E51
35. Artegiani B, Clevers H. Use and application of 3D-organoid technology. *Hum Mol Genet*. 2018 Aug 1;27(R2):R99-R107.

PART IV

Appendices

The background of the page is a light teal color. It is decorated with several abstract, hand-drawn shapes in a darker teal and a light orange color. These shapes are irregular and resemble ink blots or organic forms, scattered across the page. The word 'APPENDICES' is centered in the upper half of the page in a large, black, sans-serif font.

APPENDICES

Review committee
Authors and affiliations
List of publications
Acknowledgements
Curriculum vitae auctoris

Review Committee

Prof. dr. M.G.E.H. Lam
Department of Radiology and Nuclear Medicine
University Medical Center Utrecht
The Netherlands

Prof. dr. R.A.E.M. Tollenaar
Department of Surgery, in particular Oncology
University of Leiden
The Netherlands

dr. P.W.B. Derksen
Department of Pathology
University Medical Center Utrecht
The Netherlands

Prof. dr. I.Q. Molenaar
Department of Surgical Oncology and Hepato-Pancreato-Biliary Surgery
University Medical Center Utrecht
The Netherlands

Prof. dr. P.J. van Diest
Department of Pathology
University Medical Center Utrecht
The Netherlands



Authors and affiliations

Andor F. van den Hoven, MD, PhD

Department of Radiology and Nuclear Medicine
University Medical Center Utrecht
Utrecht, The Netherlands

Anne Trinh, PhD

Department of Medical Oncology
Dana-Farber Cancer Institute
Boston, United States of America

Caren van Roekel, MD

Department of Radiology and Nuclear Medicine
University Medical Center Utrecht
Utrecht, The Netherlands

Charlotte E.N.M. Rosenbaum, MD, PhD

Department of Radiology and Nuclear Medicine
University Medical Center Utrecht
Utrecht, The Netherlands

Daniel Y. Sze, MD, PhD

Division of Interventional Radiology
Stanford University Medical Center
Stanford, CA, United States of America

Inge Ubink, MD

UMC Utrecht Cancer Center – Surgical Oncology
University Medical Center Utrecht
Utrecht, The Netherlands

Inne H.M. Borel Rinkes, MD, PhD

Department of surgical oncology and endocrine surgical oncology
University Medical Center Utrecht
Utrecht, The Netherlands

Jamila Laoukili, PhD

UMC Utrecht Cancer Center – Surgical Oncology
University Medical Center Utrecht
Utrecht, The Netherlands

Kateryna Veremiyenko, BSc

UMC Utrecht Cancer Center – Surgical Oncology
 University Medical Center Utrecht
 Utrecht, The Netherlands

Kari Trumpi, MD, PhD

UMC Utrecht Cancer Center – Surgical Oncology
 University Medical Center Utrecht
 Utrecht, The Netherlands

Klaas M. Govaert, MD, PhD

UMC Utrecht Cancer Center – Surgical Oncology
 University Medical Center Utrecht
 Utrecht, The Netherlands

Lizet M van der Waals, MSc

UMC Utrecht Cancer Center – Surgical Oncology
 University Medical Center Utrecht
 Utrecht, The Netherlands

Maarten L.J. Smits, MD, PhD

Department of Radiology and Nuclear Medicine
 University Medical Center Utrecht
 Utrecht, The Netherlands

Manon N.G.J.A. Braat, MD, PhD

Department of Radiology and Nuclear Medicine
 University Medical Center Utrecht
 Utrecht, The Netherlands

Marnix G.E.H. Lam, MD, PhD

Department of Radiology and Nuclear Medicine
 University Medical Center Utrecht
 Utrecht, The Netherlands

Miriam Koopman, MD, PhD

UMC Utrecht Cancer Center – Medical Oncology
 University Medical Center Utrecht
 Utrecht, The Netherlands



Niek Peters, MD

UMC Utrecht Cancer Center – Surgical Oncology
University Medical Center Utrecht
Utrecht, The Netherlands

Onno Kranenburg, MD, PhD

Division of Biomedical Genetics
University Medical Center Utrecht
Utrecht, The Netherlands

Paul J. van Diest, MD, PhD

UMC Utrecht Cancer Center – Medical Oncology
University Medical Center Utrecht
Utrecht, The Netherlands

Sjoerd G. Elias, PhD

Julius Center for Health Sciences and Primary Care – Department of Epidemiology
University Medical Center Utrecht
Utrecht, The Netherlands

Susanne J. Schenningen-van Schelven, BSc

UMC Utrecht Cancer Center – Surgical Oncology
University Medical Center Utrecht
Utrecht, The Netherlands

Maurice A.A.J. van den Bosch, MD, PhD

Department of Radiology and Nuclear Medicine
University Medical Center Utrecht
Utrecht, The Netherlands

List of publications

van der Waals LM, Laoukili J, **Jongen JM**, Raats D.A., Borel Rinkes IHM, Kranenburg O. Differential anti-tumour effects of MTH1 inhibitors in patient-derived 3D colorectal cancer cultures. *Scientific Reports*. 2019 Jan; 9 (819)

van der Waals LM, **Jongen JM**, Elias SG, Veremiyenko K, Trumpi K, Trinh A, Laoukili J, Ubink I, Schenning-van Schelven SJ, van Diest PJ, Borel Rinkes IHM, Kranenburg O. Increased Levels of Oxidative Damage in Liver Metastases Compared with Corresponding Primary Colorectal Tumors: Association with Molecular Subtype and Prior Treatment. *Am J Pathol*. 2018 Oct;188(10):2369-2377.

Trumpi K, Frenkel N, Peters T, Korthagen NM, **Jongen JM**, Raats D, van Grevenstein H, Backes Y, Moons LM, Lacle MM, Koster J, Zwijnenburg D, Borel Rinkes IHM, Kranenburg O. Macrophages induce “budding” in aggressive human colon cancer subtypes by protease-mediated disruption of tight junctions. *Oncotarget*. 2018 Apr 13;9(28):19490-19507.

Jongen JM, Rosenbaum CENM, Braat MNGJA, van den Bosch MAAJ, Sze DY, Kranenburg O, Borel Rinkes IHM, Lam MGEH, van den Hoven AF. Anatomic versus Metabolic Tumor Response Assessment after Radioembolization Treatment. *J Vasc Interv Radiol*. 2018 Feb;29(2):244-253.e2.

Jongen JM, van der Waals LM, Trumpi K, Laoukili J, Peters NA, Schenning-van Schelven SJ, Govaert KM, Borel Rinkes IHM, Kranenburg O. Downregulation of DNA repair proteins and increased DNA damage in hypoxic colon cancer cells is a therapeutically exploitable vulnerability. *Oncotarget*. 2017 Sep 21;8(49):86296-86311.

Jongen JM, Govaert KM, Kranenburg O, Borel Rinkes IHM. Surgery-induced tumor growth in (metastatic) colorectal cancer. *Surg Oncol*. 2017 Dec;26(4):535-543.

Trumpi K, Ubink I, Trinh A, Djafarihamedani M, **Jongen JM**, Govaert KM, Elias SG, van Hooff SR, Medema JP, Lacle MM, Vermeulen L, Borel Rinkes IHM, Kranenburg O. Neoadjuvant chemotherapy affects molecular classification of colorectal tumors. *Oncogenesis*. 2017 Jul 10;6(7):e357.

Ubink I, **Jongen JM**, Nijkamp MW, Meijer EFJ, Vellinga TT, van Hillegersberg R, Molenaar IQ, Borel Rinkes IHM, Hagendoorn J. Surgical and Oncologic Outcomes After Major Liver Surgery and Extended Hemihepatectomy for Colorectal Liver Metastases. *Clin Colorectal Cancer*. 2016 Dec;15(4):e193-e198.

Snel J, Vissers YM, Smit BA, **Jongen JM**, van der Meulen ET, Zwijsen R, Ruinemans-Koerts J, Jansen AP, Kleerebezem M, Savelkoul HF. Strain-specific immunomodulatory effects of *Lactobacillus plantarum* strains on birch-pollen-allergic subjects out of season. *Clin Exp Allergy*. 2011 Feb;41(2):232-42.

Acknowledgements – Dankwoord

Beste **Prof. dr. Borel Rinkes, Inne!** Ons contact begon met een email vanuit mij of ik kon komen praten over een promotietraject en heeft via een KWF-beurs en vele ups-and-downs (aka een promotietraject) geresulteerd in dit boek. Inne, ik vind je een fantastisch arts, wetenschapper maar bovenal fantastisch mens. Het is ontzettend mooi om te zien hoe jij en je prachtige vrouw Signe het beste in elkaar naar boven halen. Dankjewel Inne, zowel op professioneel als persoonlijk vlak!

Beste **Prof. dr. Kranenburg, Onno!** je begon als mijn copromotor, eindigt als mijn promotor. Wat hebben wij veel uren in jouw kantoor doorgebracht. Met een lach en een traan, met blijdschap en teleurstellingen en met werk en privé issues ;). Onno, meer dan ik vooraf had kunnen denken: bedankt voor je kritische noten en peptalks. Daarin kan ik de rol van Jamila natuurlijk niet vergeten, jouw steun en toeverlaat.

Beste **Prof. dr. Vriens, beste Menno,** jouw enorme toewijding, tomeloze enthousiasme en eindeloze energie maken je een fantastische opleider. Dank voor je vertrouwen! Ik hoop op nog vele mooie momenten samen tijdens mijn opleiding in Utrecht.

Beste **dr. Consten, beste Esther,** dank voor het vertrouwen dat je me hebt gegeven als ANIOS en de geweldige start die je me hebt gegeven als AIOS in het Meander. Ik kijk uit naar heel veel vliegreuen (o.a.) onder jouw hoede!

Beste **Prof. dr. Leenen,** uw gedrevenheid in het vak, uw hart voor de patiënt en uw passie voor hardlopen intrigeert mij. Dat tezamen met uw oprechte interesse maakt dat ik u wil bedanken voor uw wijze woorden op de juiste momenten. Dank!

Beste **dr. Derksen, Patrick!** Ik leerde je pas een beetje kennen als mijn AIO commissielid. Daarna hebben we vaak van gedachte gewisseld op allerlei vlakken. Wat heb ik enorm kunnen lachen met je, samen biertjes drinkend in Lunteren ;). Aim high Patrick, the sky is the limit! Heel veel geluk met S. en M. in jullie prachtige huis in Leiden.

Geachte leden van de beoordelingscommissie, veel dank voor de tijd en inspanning voor het beoordelen van mijn proefschrift. Dank **Prof. dr. M.G.E.H. Lam, Prof. dr. R.A.E.M. Tolenaar, dr. P.W.B. Derksen, Prof. dr. I.Q. Molenaar, Prof. dr. van Diest.**

Mijn lab, wij, met z'n allen, hoe anders we ook zijn, hoeveel we toch één zijn. Zoals dat gaat tijdens een PhD traject, heb ik mensen zien gaan en komen maar ik zou niet weten hoe ik het had moeten doen zonder jullie guys: **Jamila, Tijana, Szabi, Thomas, Kari, André, Daniëlle, Susanne, Susana, Kirsten, Inge, Lizet, Nicola, Petra, Anneta, Liza en Emre** bedankt voor de onvergetelijke momenten! In deze lijst mag ik mijn studenten: **Annelot, Robbert, Rebeca en Niek** zeker niet vergeten. De meeste passeerden, maar jij bleef hangen. Niek, rock this!

Daarnaast een woord van dank voor de **Derksen groep, Kops groep, Lens groep, pathologie, PhD council, ICT-mannen** en de **FACS facility (Pien en Jeroen ☺)**

De cola app! Een stuk minder actief maar nog altijd bestaand; **Lutsie, Kaar en Elfi**. Het eerste waar ik aan denk bij jou Luts, is onze zoektochten naar de juiste fashionpieces op internet. Even schrijfmoe; de nieuwste mode checken. Love it! Kaar, huppelende hinde in de weide (aka hockey) en het kiten natuurlijk. Mijn steun en toeverlaat in het lab en als dat écht even k*t is, gewoon gaan wakeboarden op een boot van een van je kennissen :D! Elfi, de internist in de chirurgenkamer. Je bracht balans is ons zootje ongeregeld. Ik heb respect voor hoe je alles hebt gedaan afgelopen jaren, je boek is af! Guys, wat mis ik de 'weekend' verhalen bij MiCafe op maandagochtend en het hitje (met dikke bass) om 16 uur inclusief het colatje.

Christine....de vreemde eend in de bijt in het heelkunde lab. Jij van de MDL, in ons lab. 2015 was echt ons jaar, een soort van samen een huis gekocht. Alleen dan ieder een eigen huis ;) Jij in Utrecht, ik in het Amsterdamse. Wat hebben we lol gehad; samen naar de woonbeurs, plattegronden maken én in spanning gezeten...mooie herinneringen Chris.

Kirsten, Kir, je kwam pas laat in ons lab maar er was weinig tijd nodig om te beseffen dat we met elkaar konden lezen en schrijven. Ik heb onbeschrijfelijk veel respect voor de beslissing die je gemaakt hebt mama Kir. Ik vind het jammer dat je hier niet bent om me te zien zweten en shinen maar dit neemt nooit iemand meer van jullie af.

Veertje, al zien we elkaar veel te weinig, als we samen zijn is het net of we elkaar gisteren nog hebben gezien. Onze dronken avonturen, onze vele 'eerste keren' en onze liefde voor 'even een hapje eten'. Op naar veel nieuwe eerste keren en hapjes eten Veer!

Barbara, Babs... so close, yet so far. It seems like yesterday that we met in the streets of NYC. However, 8 years later, things changed....you have two amazing little girls now! Some things however never change Babs, I can't even tell how special it is to have you at my defense. An oversea hug!

Fleur, all the way back to Wageningen. Samen als de eeuwige vrijgezellen op vakantie op jacht naar zeekeoien...inmiddels super serieus en volwassen. Zou willen dat we wat dichterbij elkaar woonde Fleur(tie)...

Hardloopmaatjes, teamKWF, mijn marathon in 2016 is niet vanzelf gegaan. Thanks! Na de marathon was het tijd voor iets nieuws: crossfit. Lieve partners in crime; **Pax, Kim, Myrte, Iloen en Marieke**. Wat zijn jullie een geweldige afleiding en uitlaatklep (geweest)!

Alle **onderzoekers in het UMCU**, jeetje wat zijn het er inmiddels veel.... en ik durf me er niet aan te wagen jullie allemaal bij naam te noemen, want ik vergeet gegarandeerd mensen. Je start alle als collega, maar als je geluk hebt zitten er mooie vriendschappen

verborgen in collega's. **Djurre**, in jou heb ik toch wel een (dans)maatje gevonden. Op naar jaren samen opereren. **Do'tje**, de passie voor natuur delen we, ooit gaan we samen hiken, toch?! **Leo**, kijk voor de grap eens in onze gedeelde fotogeschiedenis, haha... Op nog vele gezellige borrels en etentjes samen! **Mors en Mark**, helaas zien we elkaar veel minder, maar ons idee van een kookclubje was leuk ;) **F*cking vetste SkiCie ever: Marieke, Steven en Lucas** we are/were the best :D. Ik hoop tegen deze tijd te mogen zeggen dat ook wij samen gaan opereren!

Al mijn **danspartners in crime en festivalmaatjes**; Dit boek was er niet geweest zonder jullie! Over de jaren heen zijn er heel wat mensen geweest waarmee ik in het zonnetje heb gedanst op heerlijke muziek; dank jullie wel! En guys, what's 'NEXT'?

Maatschap heelkunde en A(N)IOSSEN Meander MC en UMCU, dank voor jullie geduld, leermomenten en vele onvergetelijke borrels! Op naar nog heel veel mooie jaren!

Tesse, zoals ik aan jouw zijde stond op 20 december, zo sta jij nu aan de mijne. Geen feestje te gek: zoektochten naar beste line-ups, op zoek naar zakjes in de bus en op jacht naar suiker voor hypo's. We hebben vele ellendige maar bovenal heel veel mooie momenten meegemaakt. Ik kijk uit naar alle volgende pieken die we gaan beleven!

Aan de andere zijde sta jij op 28 maart **Annique**. Niemand kent mij én dan in het bijzonder 'mij tijdens mijn promotietijd' zo goed als jij: van lachen naar huilen, via de motor naar de kano, van Ibiza tot Oostenrijk en weer naar de Bilt en Amsterdam....en zo kan ik nog uren doorgaan. Wât hebben wij nog niet samen meegemaakt Piep?! A trip down memory lane.... De eerste 7 zijn inmiddels ruim voorbij, op naar de volgende 7 jaar Piep!

Joyce, grote zus! Wat ben ik toch altijd ongelofelijk trots op jou. Geen uitdaging is voor jou te groot. Zo ver als we vroeger van elkaar af stonden en hoe irritant ik voor jou kon zijn, zo close zijn we nu. Door alle ups en downs van het leven. What doesn't kill you makes you stronger. Ik hou van je Joy!

Papa en mama, woorden kiezen is moeilijk omdat ik jullie niet genoeg kan bedanken voor jullie onvoorwaardelijke liefde, ongekende trots en blind vertrouwen in mij. Dank voor het warme nest dat jullie Joyce en mij geven paps en mams.

En toch verdien jij mijn laatste paar regels **Boy**. You make me smile, shine and sparkle! Op heel veel mooie momenten samen. #AlpacaSquad



Curriculum vitae auctoris

Jennifer Jongen was born on November 16th 1986, in Loon op Zand, The Netherlands. After graduating from the Cobbenhagen College Tilburg in 2009, she started her scientific career at Wageningen University (WU). During her study 'Nutrition & Health' at Wageningen University, her interest in scientific research arose and made her realize she wanted to continue working in scientific research. However, her master-thesis internship in collaboration with the Rijnstate hospital in Arnhem triggered her interest to work with patients as well. With starting the Selective Utrecht Medical MAster (SUMMA) at Utrecht University in 2009, both interests were answered. She finished her last Master year of 'Nutrition & Health' at the WU between 2009-2011, next to SUMMA. In 2011, she decided to go abroad for her scientific training program of SUMMA. Her scientific thesis at Columbia University NYC, was the starting point of her surgical career. Where Prof. Savelkoul showed her the beauty of science in general at the Wageningen University, Kenneth P. Olive, PhD showed her the beauty of science in surgical oncology in his lab in the United States, the Olive lab.



After finishing both her Master degree in Nutrition and Health and SUMMA, Jennifer started her PhD at Utrecht University in the lab of Prof. Borel Rinkes and Prof. Kranenburg. In October 2017, she started her clinical career as a surgical resident not in training (ANIOS) in the Meander Medical Center, Amersfoort, the Netherlands. In July 2018, she started her training in general surgery (AIOS) at the Meander Medical Center under supervision of dr. E.C.J. Consten. In November 2018, she continued at the University Medical Center Utrecht under supervision of prof. dr. M.R. Vriens where she will stay until July 2019 after which she will return to the Meander Medical Center.



